國立臺灣大學環境工程學研究所

碩士論文

Graduate Institute of Environmental Engineering

College of Engineering

National Taiwan University

Master Thesis

利用轉爐石與鋼鐵廢水在漿體反應槽中進行碳酸
化反應

Carbonation of Basic Oxygen-Furnace Slag with

Metalworking Wastewater in a Slurry Reactor

邱安家

An-Chia Chiu

指導教授：蔣本基 博士

Advisor: Pen-Chi Chiang, Ph.D.

中華民國 100 年 7 月
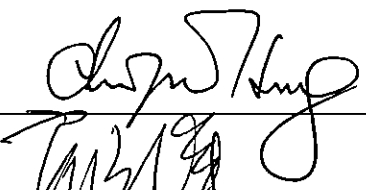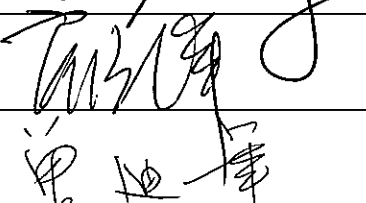
July, 2011

# 國立臺灣大學碩士學位論文
# 口試委員會審定書

## 利用轉爐石與鋼鐵廢水在漿體反應槽中進行碳酸化之研究

## Carbonation of Basic Oxygen-Furnace Slag with

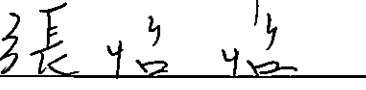## Metalworking Wastewater in a Slurry Reactor

本論文係邱安家君(學號 r98541102)在國立臺灣大學環境工程學研究所完成之碩士學位論文，於民國一百年七月二十九日承下列考試委員審查通過及口試及格，特此證明
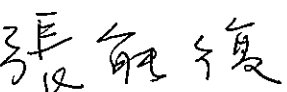
論文審查委員：

黃金寶博士
美國德拉瓦大學土木與環境工程系教授

顧　洋博士
國立台灣科技大學化學工程學系教授

曾迪華博士
國立中央大學環境工程研究所教授

張怡怡博士
台北醫學大學醫學系生化學科教授

指導教授：

所　　長：

# 謝誌

**Abstract**

$CO_2$ sequestration by basic oxygen slag in a slurry reactor containing metalworking wastewater was investigated in this study. There were two types of metalworking wastewater used in this study including effluent from metalworking wastewater treatment plant and cold-rolling wastewater.

The effect of operational conditions on the $CO_2$ sequestration process were evaluated including the type of metalworking wastewater, reaction time, liquid to solid ratio and $CO_2$ flow rate. The results indicated that basic oxygen slag in cold-rolling wastewater provided a better carbonation conversion approximate 89.18% at reaction time of 2 h, liquid to solid ratio of 20 and $CO_2$ flow rate of 1 L/min. The developed surface coverage model for $CO_2$ sequestration was used in this study to evaluate the carbonation conversion process. Although there were insignificant differences between wastewater and tap water in carbonation conversion, reuse of metalworking wastewater as feedstock recycles the water resource and reduces operational cost. It is a promising alternative for carbon sequestration.

On assessment aspect, the commercial value of $CO_2$ sequestration technology by technical assessment was confirmed. LCA software, i.e., Umberto 5.5 is a useful tool for environment analysis and quantifying the different environmental impact categories by combining international database, i.e., CML with interior statistics. The

results indicate that the sequestration of aqueous carbonation by slurry reactor is more efficient than literature. Although it still has room to reduce $CO_2$ emissions from experiment, this study is a feasible technique due to the highest conversion rate (89.18%) without extra consumption of energy and resources.

**Key words**: $CO_2$ sequestration, slag, metalworking wastewater, surface coverage model, carbonation conversion, slurry reactor, LCA

## 中文摘要

本研究針對中鋼鹼性固體廢棄物搭配中鋼廢水進行溼式碳酸化進行二氧化碳封存。鹼性固體廢棄物選用中鋼轉爐石，其成分含有大量的氧化鈣；中鋼廢水則是選用冷軋製程所產生的廢水和廢水處理場處理過後的放流水。

用泥漿反應器針對各種不同的操作參數進行實驗。為了不再額外增加能源消耗，不另外再針對實驗進行升溫或升壓。操作參數包含反應時間、不同水樣比較、液固比、氣體流量和反應體積。

實驗結果發現，在常溫常壓下反應時間 2 小時，氣體流量控制在 1LPM 且粒徑小於 44$\mu$m 時，相較於放流水和自然水等其他水樣，冷軋水擁有較佳的轉化率約為 89.19%。其反應過後的產物接附著在轉爐石表，故其整個反應的動力模式可以用「表面反應模式」進行推估，且其具有良好的廻歸，其 $R^2$ 值都可以達到 0.90 以上。

以 3E(環境、工程、經濟)三種不同面相，針對五種不同情境與本土數據結合，進行不同衝擊類別下的量化工作。評估結果發現，本研究對於二氧化碳封存具有較為正面的效應，每封存 1 公斤二氧化碳產生 2.48 公斤二氧化碳，相較於文獻已經大幅下降，是一個新的里程碑。因使用的能源少資源少，對於環境衝擊降到最低，最經濟。故本研究確為可行的二氧化碳的減量技術。


關鍵字：二氧化碳封存、濕式碳酸化、流體化床、生命週期評估

# Contents

# Figure Captions

XIII

# List of Table

# Chapter 1 Introduction

## 1-1    Background

According to the report by Intergovernmental Panel on Climate Change (IPCC), the global greenhouse gas (GHG) emissions due to human activities have increased globally by 70% from 1970 to 2004, (IPCC, 2007).  The global $CO_2$ concentration in the atmosphere was from a range of 275 to 285 ppm before the industrial evolution, and that increased by about 100 ppm (36%) over the last 250 years (IPCC, 2007).  Currently, the globally average $CO_2$ concentration was 386.27 ppm in 2009 and has been increased steadily in the past thirty years (USNOAA, 2010). The increase in GHG concentrations through anthropogenic activities would cause further warming and induce many changes in the global climate system (IPCC, 2007). There are some options for mitigating climate change such as improving energy efficiency, renewable energy, coal to gas substitution and carbon capture and storage technologies (IPCC, 2005).

The carbon capture and storage (CCS) technologies consists of capturing and separating of $CO_2$ from emission source, transport and storage as shown in Figure 1-1. In general, the CCS technologies include chemical and physical absorption, low-temperature distillation, gas-separating membranes, mineralization, and chemical looping processes as shown in Table 1-1.    The potential $CO_2$ storage methods are: (1) geological sequestration including oil and gas fields, deep saline formations and unmineable coal beds etc; (2) ocean storage; (3) mineral carbonation; (4) reuse in industrial processes.

Table 1-1 Characteristics of different $CO_2$ capture techniques    (Chen, 2009)

| Technology | Methods\Feedstock | Cost | Advantages | Disadvantages |
|---|---|---|---|---|
| **Chemical and physical absorption** | ● Recticoll<br>● Selexol<br>● MEA<br>● MDEA<br>● Sulfinol | ● Medium | ● High selectivity<br>● High-purity product<br>● High capacity of carbon capture<br>● Mature technology | ● High energy consumption on solvent regeneration<br>● NOx, SOx and $O_2$ cause solvent poisoned |
| **Chemical and physical adsorption** | ● Activated carbon<br>● Zeolite | ● High | ● Easy to operate | ● Low selectivity<br>● High energy consumption on solvent regeneration |
| **Low-temperature distillation** | | ● Very high | ● Easy to transport | ● Very high energy consumption on operation |
| **Mineralization** | ● Mineral<br>● Solid waste | ● Low | ● Long term stability<br>● Economically viable | ● Fewer study<br>● Immature technology<br>● High transportation cost |
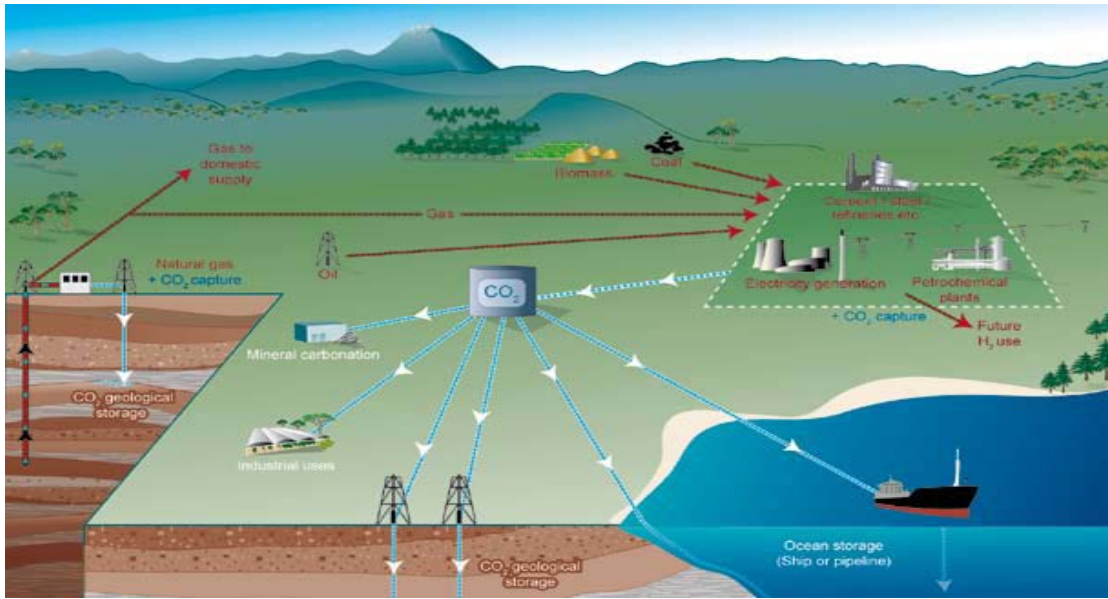
Figure 1-1 Schematic diagram of CCS

The capacity of $CO_2$ geological sequestration is approximately 2.8 billion tons of $CO_2$ in Taiwan, and it is equivalent to 10 times of Taiwan yearly $CO_2$ emission in 2000 (Exploration & Development Research Institute, Taiwan). Chinese Petroleum Corporation (CPC) of Taiwan is planning a $CO_2$ sequestration pilot project. The short term goal of CPC is using gas reservoirs for $CO_2$ sequestration, and the long term goal is using deep saline reservoirs and unmineable coal seams for sequestration. The CPC pilot plant sites were evaluated and selected as shown in Figure1-2.

Since the CCS pilot geological sequestration project in Taiwan is on hold, the $CO_2$ mineralization becomes a potential alternative. Mineral sequestration is a method that accelerates natural weathering processes (Lackner et al., 2003) and the products of mineralization are thermodynamically stable and common in nature (Huijgen and Comans, 2005; Lackner et al., 1995).
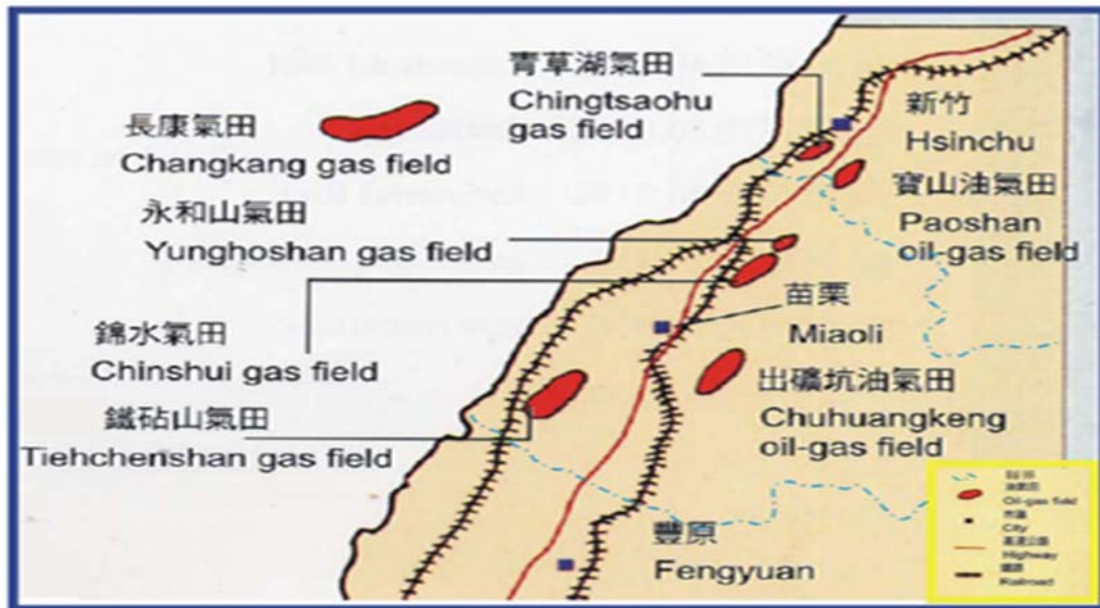
Figure 1-2 Sites of CPC testing pilot plant selected

The choices of feedstocks will affect the efficiency of CO2 mineralization. The alkaline waste solid tends to be more reactive for carbonation than primary minerals due to their chemical instability (Huijgen, 2004).   As for the choice of the reactor; slurry reactor is a very attractive one since it can provide high contact opportunity between $CO_2$ and feedstock, and it can be operated in a continuous state.

In order to evaluate the impact of $CO_2$ sequestration to the environment, life cycle assessment (LCA) was performed to classify and quantify the environment impact of each process using the software – Umberto5.5.

## 1-2　Objectives

The objectives of this research include:

1. Finding the optimum operating conditions for $CO_2$ sequestration using waste alkaline solid mixed with waste water from China Steel Corporation in a slurry reactor

2. Determining the chemical reaction and mechanism for the carbon sequestration

3. Analyzing the physic-chemical characteristics of the alkaline solid wastes and its carbonated products

4. Evaluating the environmental impact of laboratory-scale $CO_2$ sequestration using LCA

# Chapter 2 Literature Review

## 2-1 Mineralization Carbonation

The concept of mineral carbonation was introduced by Seifritz (Seifritz, 1990) and developed by Lackner (Lackner et al., 1995). Mineral carbonation is based on the reaction of $CO_2$ with metal oxide bearing materials to form insoluble carbonates, with calcium and magnesium being the most attractive metals. In nature such a reaction is called silicate weathering and takes place on a geological time scale. It involves naturally occurring silicates as the source of alkaline and alkaline-earth metals and consumes atmospheric $CO_2$ (Abanades et al., 2007). Carbonation is a method that accelerates natural weathering processes (Lackner et al., 2003). $CO_2$ is rarely released from the carbonation products after mineralization, because they are thermodynamically stable after carbonation and require significant amount of energy to regenerate $CO_2$ from the carbonate minerals (Huijgen and Comans, 2005; Lackner et al., 1995). Comparing with unclear, wind, and solar energy, carbonation is cheaper, safer and more permanent. The carbonation is a promising technology for $CO_2$ sequestration (Lackner, 2002).

## 2-2 Suitable Feedstock for Mineralization of Carbon Capture

There are a few metals can be carbonated such as Mn, Fe, Co, Ni, Cu and Zn but these metals are costly(Huijgen and Comans, 2003). The carbonation product formed from Na or K is not suitable for carbonation because they are too soluble (Sanni Eloneva, 2010). Materials with high calcium and magnesium contents are suitable feedstocks for mineral $CO_2$ sequestration because they are abundant in the world. Minerals that contain calcium or magnesium but do not contain carbonate, such as

magnesium and calcium silicates are suitable for carbonation. Carbonate-containing materials (such as limestone) cannot be used for mineral carbonation as they have already been carbonated and thus have no capacity to fix more $CO_2$ (Eloneva et al., 2008). The Ca-silicates tend to be more reactive towards carbonation than Mg-silicates (Huijgen and Comans, 2003; Lackner et al., 1997; IPCC, 2005).

The suitable carbonate materials were selected based on following criteria：(1) solid which would be advantageous in storage, (2) inorganics, (3) alkali material which would be higher reactivity with acidic $CO_2$ solution, (4) uncarbonated Ca and Mg contents thus no capacity to fix more $CO_2$ (Cho et al., 2011).

Most of literature recommended using mineral rock as feedstock for $CO_2$ sequestration. In recent years, steelmaking slag such as alkaline waste solid became an attractive material to capture carbon dioxide. The alkaline waste solid, which is inorganic and rich in Ca/Mg, could be an alternative source for $CO_2$ sequestration (Huijgen, 2003). The alkaline waste solid has several advantages such as low cost of sequestration, close to the energy and industrial sites which are the source of $CO_2$, readily accessible in fine particle size (Fauth, 2002). In addition, metal stabilization in alkaline waste through fast carbonation reduces the hazardous metal extraction that carbonation enables engineering application, safe disposal of waste and pH-neutralisation (Huijgen, 2003). The alkaline waste solid tends to be more reactive for carbonation than primary minerals due to their chemical instability. Their chemically unstable characteristics make the pre-treatment process simple and require less energy. Sequestration by alkaline waste solid is a promising option in the future (Huijgen, 2004).

Soong et al.,(2004) suggested wet mineral carbonation using coal fly and brine solution for $CO_2$ capture. This process was found to generate a fairly pure $CaCO_3$

product. The other combustion waste, which can be used for carbonation, is the fly ash and bottom ash from the municipal solid waste incinerators (MSWI). These ashes are alkaline in nature, with pH values ranging from 9.5 to 11.5, and contain alkaline and alkaline earth elements and metal oxides, which would form hydroxides during hydrolysis. The elemental composition of MSWI bottom ash depends primarily on the composition of the feed stock and on the type, capacity and operational temperature of the incinerator. Using MSWI bottom ash for carbonation might result in mineralogical changes similar to those occurring as a result of natural weathering and to induce a related reduction in trace metal mobility (Cho et al., 2011).

Steelmaking slag is the by-product of iron and steel production such as ultra fine slag (UF), fly ash slag (FA), blended hydraulic cement slag (BHC), basic oxygen furnace slag (BOF) etc. BOFs are used during steel production to melt the impurities of iron or steel and they are primarily comprised of fluxing agents (mainly lime). The major component of BOF included $SiO_2$, $Al_2O_3$, $Fe_2O_3$, $CaO$ and $MgO$. (Proctor et al., 2000). The production of basic oxygen furnace slag in China Hi-ment was approximately 1.77 million tons in 2009. The compositions of mineral and waste residues are shown in Table 2-1.

There is free CaO that is not completely combined in steel slag. The CaO in contact with moisture hydrates rapidly to hydroxide (Emery, 1982). Due to weathering, X-ray diffraction showed that there is $CaCO_3$ in BOF (Mahieux, 2009). In order to decrease the error of experiment, the slag will be pre-heat to 850℃ to decompose calcium hydroxide ($Ca(OH)_2$) and calcium carbonate ($CaCO_3$).

Table 2-1. Compositions Of Mineral And Waste Residues (WT%)

| Feedstock | | CaO | MgO | $SiO_2$ | $Al_2O_3$ | $Fe_2O_3$ | FeO | $Na_2O$ | $K_2O$ | $Cr_2O_3$ | MnO | Others | REF. |
|---|---|---|---|---|---|---|---|---|---|---|---|---|---|
| Mineral | Wollastonite | 45.53 | 0.03 | 52.91 | 0.07 | ----- | 0.38 | | ----- | | 0.56 | ------ | W.K. O=Connor |
| | Olivine | 0.070 | 49.677 | 41.357 | 0.208 | 2.558 | 5.966 | 0.099 | 0.007 | 0.044 | ----- | 0.722 | |
| | Serpentine | 0.077 | 40.623 | 36.155 | 0.167 | 3.274 | 3.499 | 0.010 | 0.003 | NA | ----- | 14.87 | |
| Alkaline Solid Waste | Coal Ash | 2.97 | 1.62 | 62.9 | 16.9 | 5.71 | ----- | 0.23 | 20 | ----- | 0.15 | 8.64 | Jong Soo Cho,.. 2011 |
| | MSWI Ash | 16.3 | 2.6 | 49.3 | 7.5 | 7.6 | ----- | 6.0 | 1.1 | ----- | 0.1 | 9.5 | |
| | Blast converter1 | 41 | 10 | 35 | 9.2 | ----- | 0.8 | ----- | ----- | ----- | 0.5 | | Dott. Ing. Giulia CostaA.A. 2008/2009 |
| | GGBS3 | 41.4 | 6.8 | 34.6 | 14 | ----- | 0.7 | ----- | ----- | ----- | n.a. | n.a. | |
| | Steel converter1 | 46 | 2.1 | 13 | 1.7 | ----- | 23.2 | ----- | ----- | ----- | 3.2 | 0.2 | |
| | BOF2 | 30-55 | 5-15 | 8-20 | 1-6 | ----- | 10-35 | ----- | ----- | ----- | 2-8 | 0.1-0.5 | |
| | EAF (carbon steel) | 35-60 | 5-15 | 9-20 | 2-9 | ----- | 15-30 | ----- | ----- | ----- | 3-8 | 0.1-1 | |
| | EAF(alloy/stainless) | 39-45 | 8-15 | 24-34 | 3-7.5 | ----- | 1-6 | ----- | ----- | ----- | 0.4-2 | 0.1-20 | |
| | AOD1 | 56 | 8.3 | 30 | 1.2 | ----- | 0.8 | ----- | ----- | ----- | 0.4 | 0.3 | |
| | Ladle2 | 30-60 | 1-10 | 2-35 | 5-35 | ----- | 0.1-15 | ----- | ----- | ----- | 0-5 | 0-0.5 | |
| | Chrome converter1 | 39 | 17 | 36 | 3.5 | ----- | 0.4 | ----- | ----- | ----- | 0.3 | 1 | |
| | Ferrochrome1 | 1.4 | 23 | 28 | 28 | ----- | 5.9 | ----- | ----- | ----- | n.a. | 8.5 | |

## 2-3 Characteristic of Cold-Rolling Waste Water

Cold-rolling waste water includes many different types such as acid waste water from pickling line, waste water from activated steel's surface containing salt and metal inos, wastewater contained emulsified oil used to remove hot deformation of cold-rolling and alkaline solution of degreasing, etc.

Emulsified oil is a cutting fluids, which is used as a coolant and lubricant for metalworking. There are minerals or plant oils, anion or non-ionic surfactant and water in emulsified oil. The wastewater containing emulsified oil is the most difficult to treat in metalworking (Wang, 2005).

The criteria for selecting waste water used in this study include waste alkaline, containing cation such as $Ca^{2+}$ and surfactant, and no toxic material content. This study chooses alkaline solution of degreasing as the liquid phase of the slurry.

## 2-4 Principles of Mineral Carbonation Reaction

Carbonate minerals can be formed in natural or artificial environments by three different pathways and/or conditions: (1) aqueous nucleation-growth in homogeneous or heterogeneous systems (aqueous conditions), e.g. the chemical or biogenic formation of carbonates in lakes, oceans, $CO_2$ storage sites, natural caves, etc.; (2) solid – gas carbonation of alkaline minerals in presence of adsorbed water (water humidity conditions, $0 <$ water activity $< 1$), e.g. the carbonates formation in unsaturated soils, in terrestrial or extraterrestrial aerosols, etc.; (3) dry solid – gas carbonation of granular/porous ultrabasic materials (dry conditions, water activity = 0), e.g. the industrial mineralization, recovery or capture of $CO_2$ under high temperature using binary oxides or metastable alkaline silicates (nanoparticles) (Hernandez et al., 2011)

As show in Figure 2-1, the carbonate minerals are the lowest energy-state of carbon. The $CO_2$ mineral carbonation is an exothermic reaction (Lackner et al., 1995) as show in eq. (2-1) and (2-2).

$$CaO(s)+CO_2(g) \Leftrightarrow CaCO_3(s) \quad (\Delta H = -179 \ kJ/mole) \hspace{2cm} (2\text{-}1)$$

$$MgO(s)+CO_2(g) \Leftrightarrow MgCO_3(s) \quad (\Delta H = -118 \ kJ/mole) \hspace{2cm} (2\text{-}2)$$
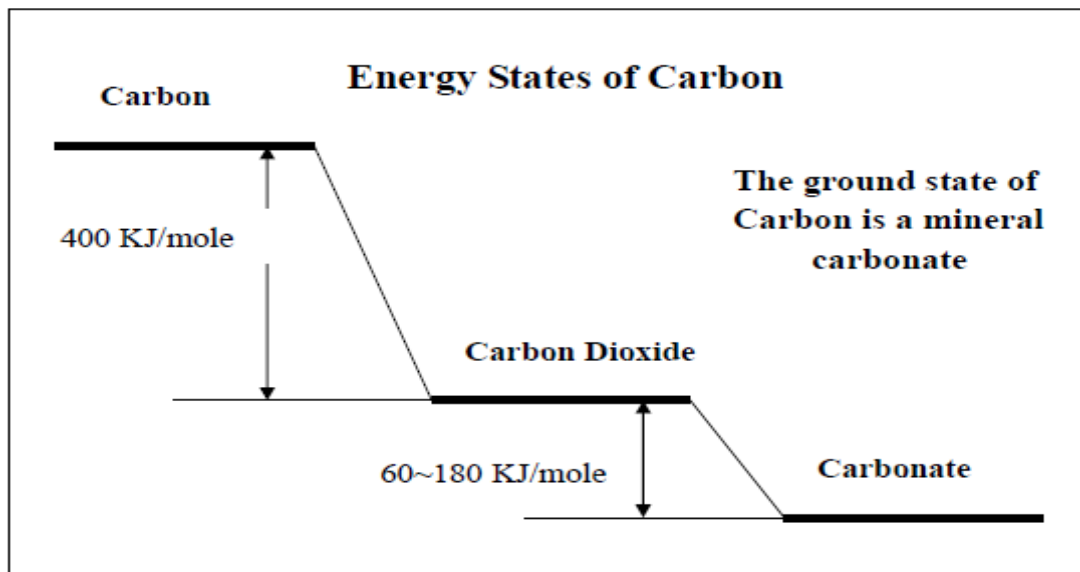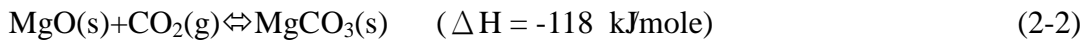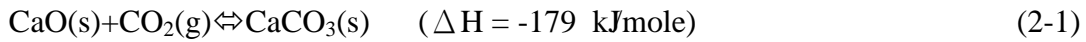


Figure 2-1 Qualitative illustration of thermodynamic stability of carbonated minerals (U.S. DOE, 1999)

There are two routes for the carbonation process routes: (1) indirect carbonation which the calcium ion extracted from the slag and carbonated in second step (2) direct carbonation under which the carbonation process is completed in one step (Huijgen and Comans, 2005). Huijgen et al. (2005) compiled the variety of mineral carbonation processes as following (Figure 2-2).
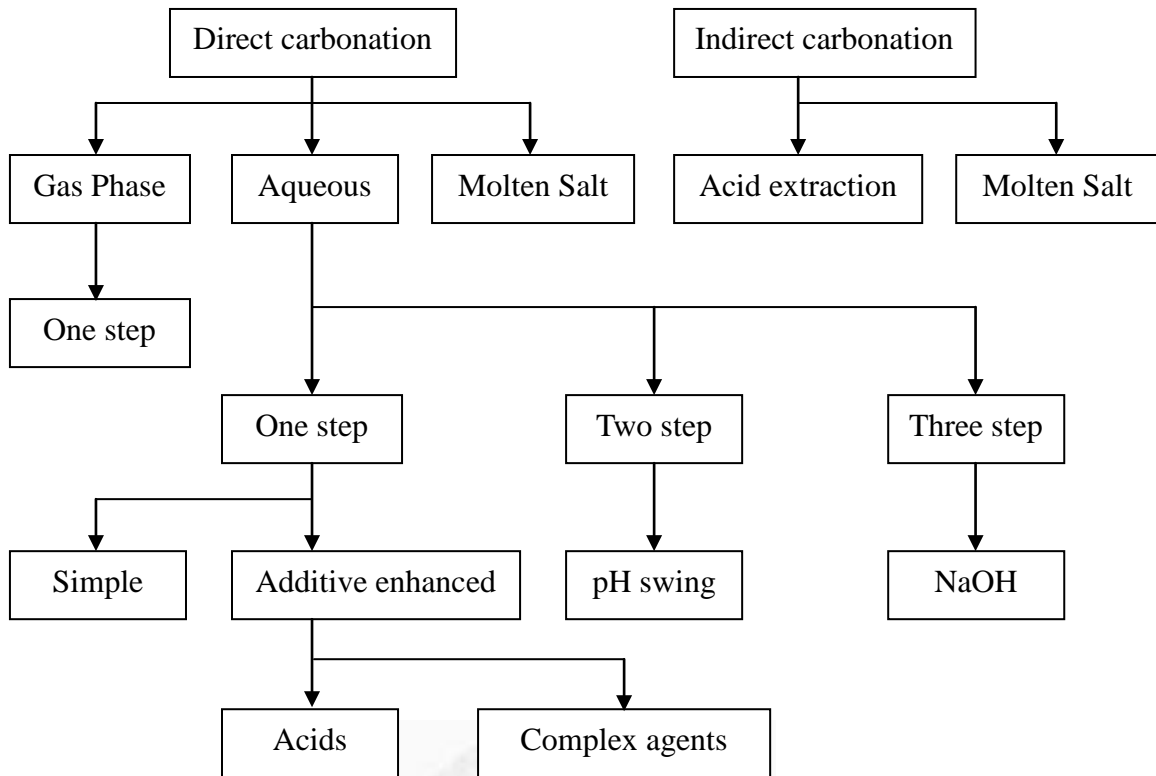
Figure 2-2 Main process routes for mineral carbonation (Huijgen and Comans, 2005)

The direct carbonation is much slower than the indirect carbonation. The rate of direct carbonation is difficult to determine. It is not a suitable process for carbonation in practical purpose (Huijgen and Comans, 2003).

$CO_2$ mineralization involves the carbonation of natural silicate minerals that contain alkaline-earth oxides like magnesium oxide (MgO) and calcium oxide (CaO), which can be available as in situ rock material. Carbonation of these environmentally stable solid carbonates, including serpentine (R1), forsterite/olivine (R2) and wollastonite (R3) minerals can be described by the reactions shown in table 2-2 Overall exothermic chemistry of mineral carbonation (Fagerlund et al., 2010).

As shown in Table2-3, equations (1)-(6) below present a direct carbonation route. The equations (1) and (4) are processes in which wollastonite ($CaSiO_3$) and olivine ($Mg_2SiO_4$) directly react with $CO_2$, and the equations (2)-(3)-(5)- (6) show the reactions

of $CO_2$ with CaO, $Ca(OH)_2$, MgO, and $Mg(OH)_2$ which are converted from those minerals. The carbonation of CaO and $Ca(OH)_2$ are fast reactions and are completed within a few minutes, whereas the carbonation of $Mg(OH)_2$ under dry conditions is very slow for sequestrating $CO_2$ (Cho et al., 2011).

Table2-2 Overall exothermic chemistry of mineral carbonation

| Feedstock | Process | Reaction | | |
|-----------|---------|----------|---|---|
| Serpentine | Direct Aqueous Process | Mg3Si2O5(OH)4 (s) + 3CO2 (g) →3MgCO3 (s) + 2SiO2 (s) + 2H2O (l) | $\Delta H$ = - 64 kJ/mol | |
| Forsterite/olivine | | Mg2Si2O4(s) + 2CO2 (g) →2MgCO3 (s) + SiO2 (s) | $\Delta H$ = - 89 kJ/mol | |
| Wollastonite | | CaSiO3 (s) + CO2 (g) →CaCO3 (s) + SiO2 (s) | $\Delta H$ = -90 kJ/mol | |
| Wollastonite | Direct carbonation route | CaSiO3(s) + CO2(g) + 2H2O(l) → CaCO3(s) + H4SiO4(aq) | $\Delta H$ = -75 kJ/mol CO2 | （1） |
| | | Ca(OH)2(s) + CO2(g) → CaCO3(s) + H2O(l/g) | $\Delta H$ = -113 kJ/mol CO2 | （2） |
| | | CaO(s) + CO2(g) → CaCO3(s) | $\Delta H$= -178 kJ/mol CO2 | （3） |
| Olivine | | 2Mg2SiO4(s) + CO2(g) + 2H2O(l) → Mg3Si2O5(OH)4(s) + MgCO3(s) | $\Delta H$ = - 157kJ/molCO2 | (4) |
| | | Mg(OH)2(s) + CO2(g) → MgCO3(s) + H2O(l/g) | $\Delta H$ = -81 kJ/mol CO2 | （5） |
| | | MgO(s) + CO2(g) → MgCO3(s) | $\Delta H$ = -118 kJ/mol CO2 | （6） |

The mechanisms involved in the carbonation of MSWI bottom ash are not yet fully known, due to the material's complex chemistry and mineralogy. However, it is likely that more than one alkaline oxide-containing mineral (including Ca and Mg silicates) reacts with $CO_2$ in addition to calcium hydroxide. Most of the previous studies have considered a simplified approach for the carbonation of $Ca(OH)_2$ via the aqueous route. The rate limiting steps of the carbonation reaction involve the dissolution of calcium from the solid matrix into the liquid phase and the diffusion of $CO_2$ into the pore system. The kinetics of $CO_2$ uptake is generally characterized by two reaction steps: (1) a first steep increase in the rate of $CO_2$ uptake with time, followed by (2) a decrease in the rate until an approximately constant value of $CO_2$ uptake is attained (Cho et al., 2011).

Table 2-3. Carbonation reaction of industrial waste solid

| Feedstock | Reaction |
|---|---|
| fly-ash | The irreversible hydration of calcium oxide or lime<br>$CaO(s) + H_2O \rightarrow Ca(OH)_2$ $\Delta H = -65$ kJ/mol |
| | The spontaneous carbonation of calcium hydroxide suspension.<br>$Ca(OH)_2 + CO_2 \rightarrow CaCO_3 + H_2O$ $\Delta H = -116$ kJ/mol |
| | The global reaction becomes<br>$CaO + CO_2 \rightarrow CaCO_3$ $\Delta H = -181$ kJ/mol |
| Coal combustion by-product, fly ash | $CaSiO_3(s) + CO_2(g) \rightarrow CaCO_3(s) + H_2O(l)$ |
| Oil residue | $3CaO \cdot Al_2O_3 3CaSO_4 \cdot 32H_2O$ (ettringite) + $3CO_2 \rightarrow 3CaCO_3$ (calcite) + $3CaSO_4 \cdot 2H2O$ (gypsum) + $Al2O_3 \cdot xH_2O$ (alumina gel) + $(26-x)H_2O$ |

## 2-4-1 Pre-treatment

Many pre-treatment options are available before carbonation. The major method include size reduction, magnetic separation, thermal treatment, chemical and mechanical method. The purpose of pre-treatment is to increase reactive surface for

carbonation. The average pre-treatment options mention below:

1. Size reduction:

In order to achieve a reasonable reaction rate the minerals have to be grinded. The reaction rate increases with the surface area. Among others, O'Connor et al. examined the influence of the particle size on the conversion. These authors found that a reduction from 106-150μm to <37μm increased the conversion in their experiments from 10% to 90% (O'Connor et al., 2000b). High-energy attrition grinding12 induces imperfections into the crystal lattice (Gerdemann et al., 2002). This results in a higher conversion than size reduction to the same diameter using 'normal' grinding. Attrition grinding, however, is energy intensive and difficult to conduct on a large scale.

2. Thermal treatment

The purpose of thermal treatment is to remove chemically bonded water and impurities. Serpentine contains up to 13wt% chemically-bound water. By heating the serpentine to 600- 650°C the water is removed and an open structure is created (O'Connor et al., 2000b). This significantly improves the reaction kinetics owing to the increase reactive surface. For example heat-treatment of antigorite increased the surface areas from 8.5m2/g to 18.7m2/g (NETL, 2001). The heating process can be further extended to higher temperatures in order to separate, for example, MgO from its matrix. Temperatures above 900°C are needed for serpentine and even higher values for olivine (Zevenhoven et al., 2002):

$$xMgO \cdot ySiO_2 \cdot zH_2O \ (s) \ T \ xMgO \ (s) + ySiO_2 \ (s) + zH_2O \ (g) \ (eq. \ 15)$$
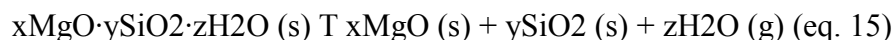
The mineral porosity can also be increased by treatment with steam (NETL, 2001) or supercritical water (T=385°C, p=272atm) (O'Connor et al., 2000b).

3. Magnetic separation

The oxidation of iron (magnetite) slows down the carbonation of serpentine due

to the formation of a layer of hematite on the mineral surface (Fauth et al., 2000). To execute the process in a non-oxidising atmosphere complicates the process and increases the costs significantly. Magnetic separation of the iron compounds prior to the carbonation process resolves this complication (NETL, 2001). Furthermore, a potentially marketable iron ore byproduct is formed (O'Connor et al., 2001a). When a combination of magnetic separation and thermal treatment is used, it is more effective first to conduct the magnetic treatment step (O'Connor et al., 2000a).

  4.  Surface activation technique

Surface activation technique including physical activation by steam treatment and chemical activation by acid have been investigated. The specific surface area of serpentine could be increased from 8 to 330 $m^2$/g. Drawback of the chemical activation are the increased sequestration costs and a reduction of Mg-content of the feedstocks due to leaching from it. Evaluation of the cost-effectiveness of this method by life cycle analysis (LCA) is necessary.

  5.  Other pre-treatment options

O'Connor et al. have tried ultrasonic pre-treatment of olivine, but it failed to activate the mineral (O'Connor et al., 2001a). Furthermore, these authors have used chemical pre-treatment steps combined with size reduction. Wet grinding in a caustic solution (1M NaOH, 1M NaCl) was found to be most effective, but still insufficient to achieve a reasonable reaction rate (O'Connor et al., 2001a).

**2-4-2 Kinetics of Calcium Leaching**

There are operational factors that will affect the calcium leaching including particle size, temperature of solution, pH value and characteristic of slag. The particle size dominates the amount of calcium leaching in mineral carbonation (Lekakh et al.,

2008). Increasing the temperatures enhances the quantity of dissolve calcium (Lekakh et al., 2008; Lin., 2001). On the other hand, calcium solubility increases slightly with pH decrease (Montes-Hernandez et al., 2007)

Since calcium solubility is affected by pH value, multi-steps process, such as pH-swing process, has been proposed with the benefit of increasing calcium extraction rate and producing purer carbonate products (Park et al., 2004; Kawizawa et al., 2004).

Two main reaction steps are involved: (1) extractions of natural calcium and magnesium silicate mineral by acid shown in (Eq. (2-1) and (2-2)) (Stumm et al.,1992), and (2) precipitations of calcium and magnesium carbonate shown in (Eq. (2-3) and (2-4)).

$$CaSiO_3 + 2CH_3COOH \rightarrow Ca^{2+} + 2CH_3COO^- + SiO_2 + H_2O \tag{2-1}$$

$$Mg_3Si_2O_5(OH)_4 + 6H^+ \rightarrow 3Mg^{2+} + 2Si(OH)_4 + H_2O \tag{2-2}$$

$$Ca^{2+} + 2CH_3COO^- + CO_2 + H_2O \rightarrow CaCO_3 + CH_3COOH \tag{2-3}$$

$$Mg^{2+} + CO_3^{2-} \rightarrow MgCO_3 \tag{2-4}$$
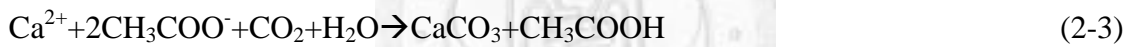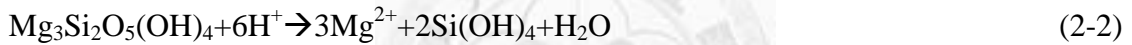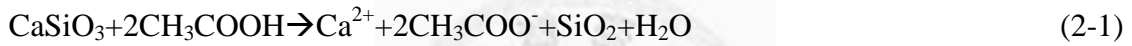
### 2-4-3 Kinetic of Carbon Dioxide Dissolution

In aqueous carbonation, $CO_2$ is dissolved in pure water and reacts with the leached calcium or magnesium from slag to form carbonated species. Dissolution of $CO_2$ in water resulting in the conversion of $CO_2$ into $H^+$ and $HCO_3^-$ in aqueous carbonation (Dreybrodt et al., 1996). Two parallel reactions control this process (Kern, 1960; Usdowski, 1982; Stumm and Morgan, 1981),

$$CO_2 + H_2O \leftrightarrow H_2CO_3 \leftrightarrow H^+ + HCO_3^- \tag{2-5}$$

$$CO_2 + H_2O \leftrightarrow CO_2 + H^+ + OH^- \leftrightarrow H^+ + HCO_3^- \tag{2-6}$$
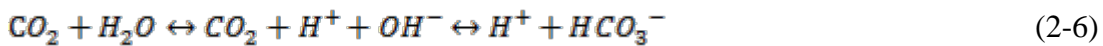
The hydration of $CO_2$ in reaction (2-5) is slower than that of reaction (2-6). However, the reaction of (2-6) becomes dominant at high pH (>9).

According to Henry's law, the limit of $CO_2$ solubility "$[CO_2]$" in the pure water is directly related to its partial pressure "$(CO_2)$" in the surrounding gaseous phase.

$$[CO_2] = k_{CO_2} * p(CO_2) \tag{2-7}$$

where $k_{CO_2}$ is Henry's constant. Henry's constant decreases as temperature increases.

Figure 2-3 shows the fraction of each carbonate species present, which is dependent on the pH of solution. The dominant of carbonate species is $HCO_3^-$ when pH is close to 8.5, and $CO_3^{2-}$ when pH is greater than 11.
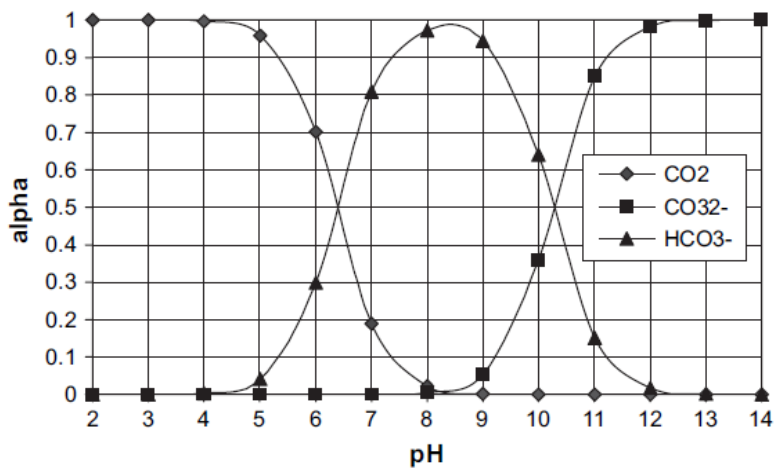
Figure 2-3 Distribution of dissolved carbonate species at equilibrium as a function of

pH

### 2-4-4 Kinetic of Aqueous Carbonation

### (a) Surface Reaction

There are three steps in aqueous carbonation: the dissolution of carbon dioxide, calcium leaching and the calcium carbonate precipitation. The factors affecting the conversion of carbonation are listed in Table 2-4. In aqueous carbonation, the slag carbonation proceeds slower than Ca leaching. The carbonation product forms a coating layer on the surface of the slag and inhibits the dissolution of Ca (Lekakh, 2008).

The kinetic model of carbonation reaction was determined by surface reaction which only takes place on the surface of the feedstocks (Shih et al., 1999). The reaction rate of per unit surface area can be expressed as

$$r_s = k_s \Phi \tag{2}$$

where $k_s$ is the rate constant [min$^{-1}$], $\Phi$ is the fraction surface area which is not covered by product.

The rate of conversion δCa can be expressed as

$$\frac{d\delta_{Ca}}{dt} = S_g M \cdot r_s = S_g M \cdot k_s \Phi \qquad (3)$$

where $S_g$ [m$^2$/g] is the initial specific surface area of the solid waste, and $M$ [g/mole] is the molecular weight. $\Phi$ [mole/m$^2$] is a function of time and the manner in which the product is deposited on the surface. Hence, $\Phi$ changes with reaction time depended on the reaction rate, and it can be expressed by the following equation:

$$-\frac{d\Phi}{dt} = k_p \cdot r_s = k_p \cdot k_s \Phi \qquad (4)$$

where $k_p$ is a function of temperature, concentrations of reacting species, and relative humidity, is a proportional constant reflecting $\Phi$ [mole/m$^2$].

By integrating equation (4), $\Phi$ can be expressed in a function of time shown as equation (5)

$$\Phi = \exp(-k_1 k_2 t) \qquad (5)$$

where $k_1 = k_s S_g M$, and $k_2 = k_p /( S_g M )$.

By substituting equation (5) into equation (3), the integration of equation (3) can obtain the relationship between conversion and reaction time can be obtained.

$$\delta_{Ca} = [1 - \exp(-k_1 k_2 t)] / k_2$$

Table 2-4 The influence of different paths and its attribute regarding carbonation

| Pathway | Property | Property |
|---|---|---|
| Chemical properties required for effective carbonation | Solid composition | Ferrite/$C_3A$ |
| | pH | Organics and anions |
| | Ca content | Certain heavy metals (Pb, Cd, and Ni) |
| | Ca/Si ratio | Free water content |
| | Microstructure | Specific surface area |
| Physical characteristics of the solid that influence carbonation | Size | Porosity |
| | Surface area | Permeability |
| Effect of the exposure conditions on the carbonation process | $CO_2$ partial pressure | Temperature |
| | Relative humidity | Pressure |

(Ref: Fernandez Bertos et al., 2004)

**(b) BOD of Thomas method**

The conversion rate of carbonation was fast in the beginning and then it slowed down in the end of reaction time.   Because the carbonation product attached on the surface of feedstock will inhibit the dissolution of calcium.   The trend of the conversion was similar with BOD of Thomas method. In this study, we used the BOD model fitted the experimental data.

The BOD of Thomas method in the carbonation model could be expressed as follows (A. R. Bowers et al., 1987) :

$$\left(\frac{t}{y}\right)^{1/3} = (L_0 k)^{-1/3} + \left(k^{\frac{2}{3}} L_0^{-\frac{1}{3}}\right) t/6$$

## 2-5 Slurry Foam-bed Reactors

The first application of two phase fluidization system was made by Winkler in 1922, and then the three phase systems were developed (Ostergaard, 1968; Shah, 1979; and Fan et al., 1988). Gas-liquid-particle three phase systems is a more efficient tool for chemical reactor (0stergaard, 1968). Aqueous carbonation by slurry reactor is a viable alternative for carbonation due to its higher mass transfer rate (Chang et al., 2011).

When a reactor contains fine solid particles suspended in a liquid, this reactor is called slurry reactor which is frequently used in chemical and biochemical industry (Alper, 1980). The foam-bed reactor which is a shallow pool of liquid above a gas distributor with a tall column of foam above it (Jackson et al.,1963, Asolekar et al., 1988). The surfactant creates foam and the foam will rise to the water surface. A foam-bed system offers enormous gas - liquid interfacial area and provides a longer contact time. The carbonation conversion efficiency of a foam-bed slurry system was 6-40% greater than that of a slurry system (Jana et al., 2010).

## 2-6 Life Cycle Assessment (LCA) on Carbon Sequestration

## 2-6-1 LCA

To evaluate if the slag slurry carbonation process is a sustainable alternative, the environmental impacts of this process from beginning to the end involved in transportation, manufacture, use and waste of product or services must be assessed. One of the assessment methods is the Life Cycle Assessment (LCA) in order to find the best solution (Guinée, J.B et al., 2002).

There is a fixed protocol for the LCA method because of the complexity of LCA.

The protocol of LCA study is established from ISO standard consist of four steps as show in Figure 2-4:

1. Goal and scope definition:

   The goal and scope definition is the first step of an LCA. It defines the service (aim or objective of the intended study), comparison basis (function unit), processes (system boundary), and types of environmental impacts being considered at the same time.

   There is no calculation made and no data collected in this step. It is only a place to define the initial objective.

2. Inventory analysis:

   The purpose of the inventory analysis is to analyze the relationship between the unit process and the process flow. All the data of the unit process in the system including raw material acquisition, transportation, manufacture, use and waste management should be collected. The relationship between four categories of flow and unit process is shown in Figure 2-5.

   1. Economic inflows

   2. Environmental inflows

   3. Economic outflows

   4. Environmental outflows

      The amount of resource use and the pollutant emission of the system are calculated relating to the functional unit. When the data background information is unclear, an assumption has to be made and its influence has to be investigated via a sensitivity analysis for the discussion of the results.

3. Impact assessment:

   According to ISO 14040, impact assessment is a "phase of LCA aimed at

understanding and evaluating the magnitude and significance of the potential environmental impacts of the product system". The inventory parameters were investigated for determining what environmental impact (classification) it attributes to. The relative contributions of the emissions and resource consumptions to each type of environmental impact were calculated (characterization). After calculating the environmental effects in these different categories, optional steps were normalized and weighted.

4. Interpretation:

The interpretation is a place for results to be summarized and discussed. The goal and scope definition of the first step sets the focus, and inventory analysis and impact assessment comprise of data collection and calculations.

Two key elements of LCA are the assessment of the entire life cycle of the investigated system and the assessment of a variety of environmental impacts (ISO14040 and 14044).
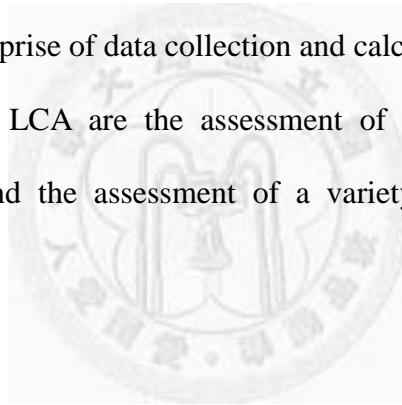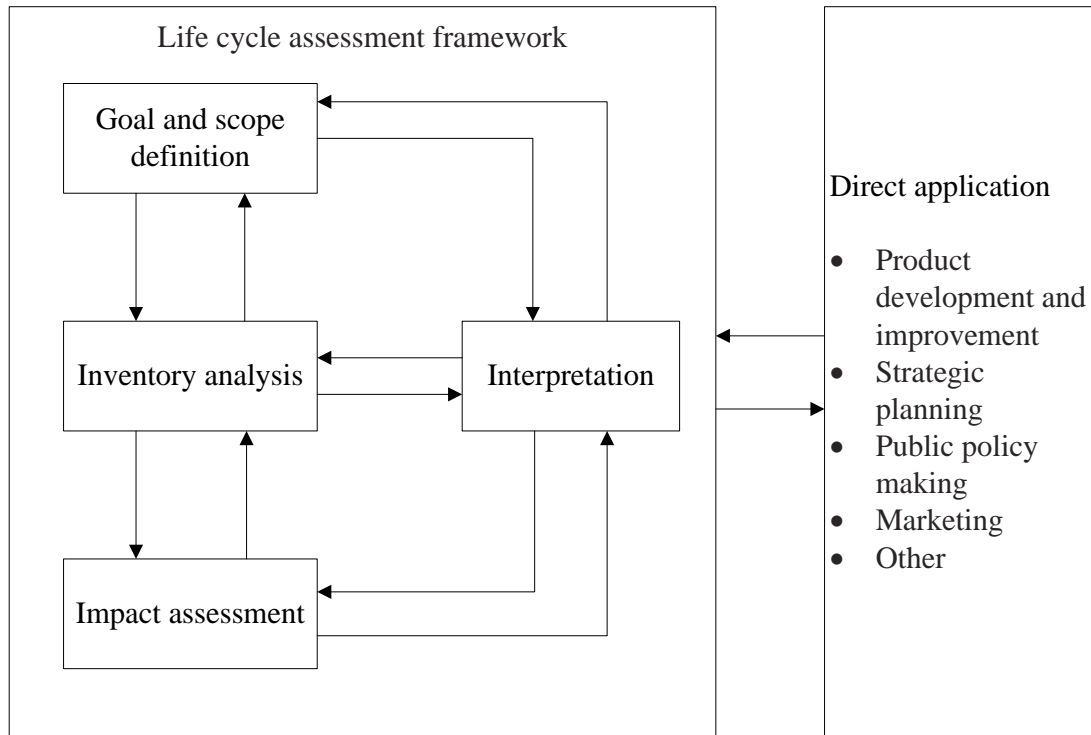
Figure 2-4 Methodological framework of LCA: phases of an LCA (CNS 14040)
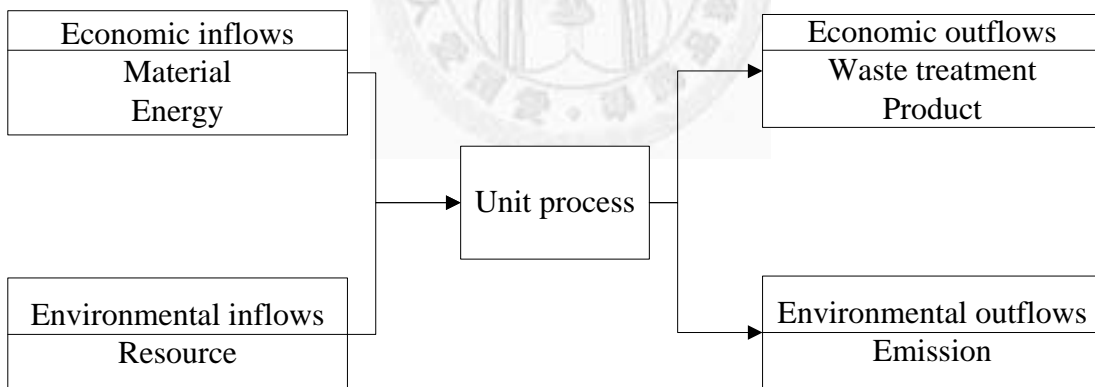


Figure 2-5 Methodological framework of LCA: phases of an LCA (CNS 14040)

**2-6-2 LCA of Energy System**

There are three analytical steps which enable LCA to determine a comprehensive factor of environmental impact (Hertwich et al., 2008):

1. Quantification of activities and flows associated with a product system:

   There are two types of quantification. One is the technical quantification including mass and energy flows. The other is economic input-output included resource, and disposal.

2. Quantification of environmental or economic interventions:

   Every activity that is part of the product system needs to be assessed for these interventions.

3. Evaluation of the environmental impacts caused by different interventions: There are two different approaches to perform the impact assessment: (a) the environmental themes approach aggregates impacts by environmental mechanism such as climate change, acidification, human toxicity, etc. (b) the damage function approach aggregates impacts by endpoints such as human health and ecosystems.

Carbon capture and storage (CCS) is an energy-intensive process which lowers the efficiency of the power plant. There will be additional emissions due to use of more fossil fuel per unit electrical output for the carbonation process (Odeh et al.,2008).

Viebahn et al. (2007) use Umberto which is the LCA software. As show in Figure 2-6, there are three elements in the material flow networks: transitions, places and arrows. Transitions stand for the locations of material and energy processes, which play a vital role in material flow networks because material and energy transformations are the source of material and energy flows.
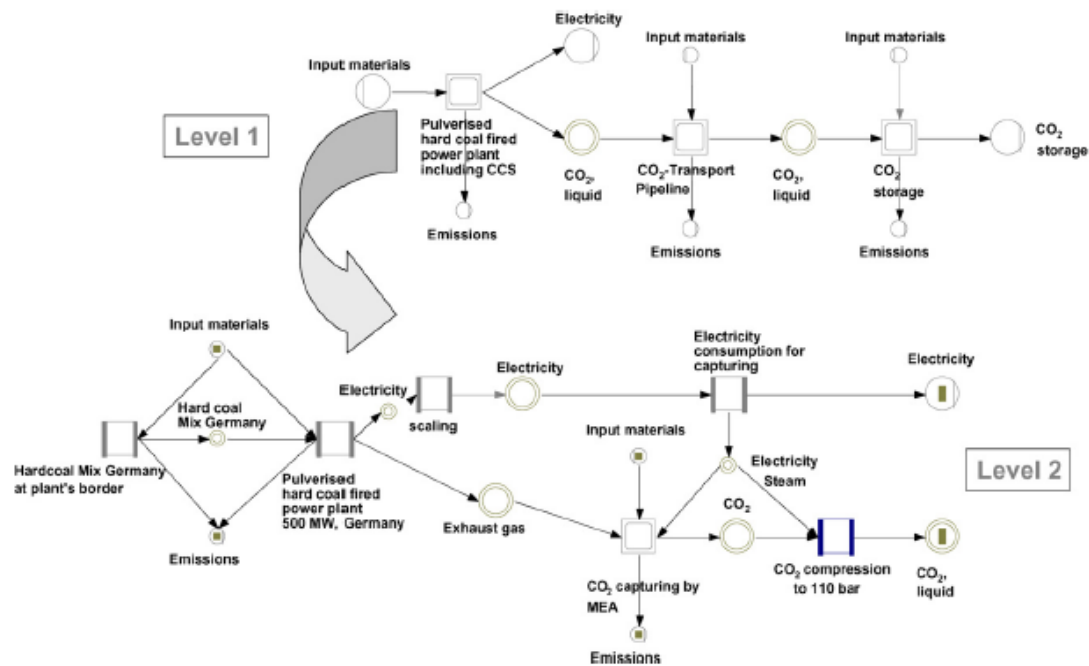
Figure 2-6 Material and energy flow network of a coal-fired power plant including $CO_2$ capture and storage (Viebahn et al., 2007)

In the Netherlands experience, environmental impact of carbon sequestration includeds the following field: land use, archaeological, cultural heritage, biodiversity, raw materials resources and water use, visual impact, energy requirement, gaseous emissions, waste management, socio-economic, noise, light and odor nuisance, soil disruption, soil disruption, soil contamination, safety, groundwater and surface water disturbance/contamination (Koornneef et al., 2008).

In the life cycle impact assessment (LCIA), environmental interventions are characterized. The CML 2 baseline 2000 V2.03 impact assessment method was used to estimate the potential environmental impacts of these interventions (Guinee et al., 2002). The environment impacts were categorized into the following 10 environmental themes (Koornneef et al., 2008): abiotic depletion potential (ADP), global warming potential (GWP), ozone layer depletion potential (ODP), human toxicity potential (HTP), fresh

water aquatic eco-toxicity potential (MAETP), terrestrial eco-toxicity potential (TEP), photochemical oxidation potential (POP), acidification potential (AP) and eutrophication potential (EP).

Khoo et al. (2006) used LCA software Simapro 6.0 with Eco-ondicator 99 method on mineral sequestration for impact assessment. This method was used to determine the following five environmental impact categories: climate change, fossil fuels, acidification, eco-toxicity, and carcinogens. Pehnt et al. (2009) summarized the considered and evaluated the impact categories shown in Table 2-5.

Table 2-5 Impact categories considered in the LCIA

| Impact category | Relevant parameters | Characterization factor |
| --- | --- | --- |
| Cumulative energy demand (CED) | Consumption of energetic resources | CED (fossil and nuclear) |
| Global warming | $CO_2$, $CH_4$, $N_2O$, halocarbons | GWP100, $CO_2$-equivalent |
| Summer smog | $NO_x$, NMHC, $CH_4$ | Ethene-equivalent |
| Eutrophication | $NO_x$, NH3 | $PO_4^{3-}$-equivalent |
| Acidification | $SO_2$, $NO_x$, $NH_3$, HCl, HF, $H_2S$ | $SO_2$- equivalent |
| Health impacts | $PM_{10}$, $PM_{2.5}$, soot, $SO_2$, $NO_x$, $CH_4$, formaldehyde, benzene, B(a)P, PAH, arsenic, cadmium, dioxin, furan | Year of life lost (YOLL) |

**2-6-3 LCA Software - Umberto 5.5**

Umberto is the software used for modeling the material and energy flow systems. Data are taken from external information systems or are newly modeled and calculated. With its graphic interface even complex structures can be modeled including the production facilities in a company, process and value chains, or product life cycles. Flows and stocks can be evaluated using standard or individual performance indicators.

Based on the material and energy flows and the costs of process activities, as well as of materials being used or waste materials that have to be disposed of, the material end energy flow systems can be analyzed and displayed. The internal cost allocation carried out during the calculation allows the model to identify improvement potentials on a consistent basis taking into account the ecological and economic aspects,
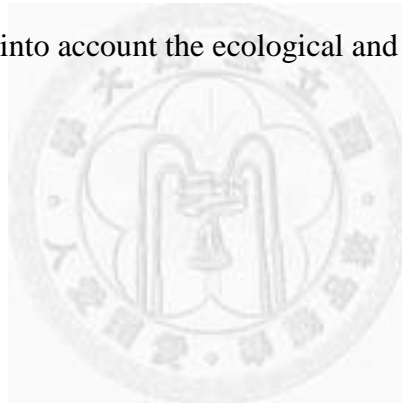
# Chapter 3 Materials and Methods

## 3-1 Research Flowchart

| Objectives |
|---|
| ➤ Finding the optimum operating conditions for $CO_2$ sequestration using steelmaking slag in steelmaking wastewater from China Steel Corporation by slurry reactor |
| ➤ Determining the chemical and mechanism for carbon sequestration |
| ➤ Analyzing the physic-chemical characteristics of the alkaline solid wastes and its carbonated products |
| ➤ Evaluating the environmental impact of laboratory-scale $CO_2$ sequestration using LCA |

| Literature review |
|---|
| ➤ The physic-chemical characteristics of surfactant used in waste water from China Steel Corporation |
| ➤ Aqueous carbonation mechanism and reaction pathway |
| ➤ Carbon sequestration and energy assessment technology by LCA methods |

| Material preparation |
|---|
| ➤ Physic-chemical characteristics |
| ➤ Pretreatment technology |

| Technical refinement |
|---|
| ➤ Operating conditions optimizing |
| ➤ Product analyses |

| Technical assessment |
|---|
| ➤ Laboratory-scale LCA methodology |
| ➤ The Analysis and Evaluation of 3E system |

| Expected performance |
|---|
| ➤ Determining the optimized carbonation operating parameters |
| ➤ Figuring out the reaction kinetics and mechanism |
| ➤ Integrating LCA technique and database on lab-scale carbon sequestration |

Figure 3-1 Research flowchart

## 3-2 Materials

### 3-2-1 Source of Agents

In this study, the agents used and their sources are listed below:

1. Basic oxygen furnace slag:

   China Hi-ment Corporation, cement and concrete laboratory

2. Wastewater :

   Cold-rolling waste water and effluent from metalworking wastewater treatment

   plant, China Steel Corporation

3. Tap water:

   Taipei Water Department

4. High pressure carbon dioxide:

   Taipei Ch'ing-Feng Gas, 99%

5. CTAB ( Cetyl trimethyl ammonium bromide) :

6. SDS (Sodium dodecyl sulphate) :

7. Triton X-100 (Octyl phenoxy polyethoxyethanol) :

## 3-2-2 Procedure of Preparing Steelmaking Slags
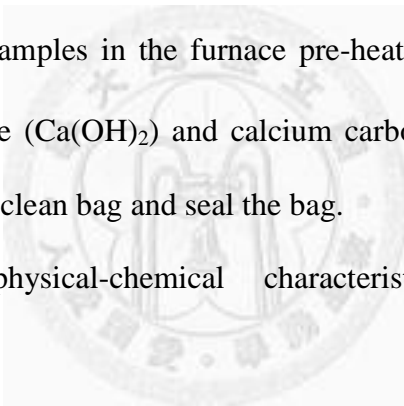
1. Method

  As shown in Figure 3-2

2. Apparatus

  As shown in Figure 3-3

3. Procedure

   a.  Put the BOF slags in an oven pre-heated to 105℃ to dry the moisture. This
       step will make particles easy to be sieved.

   b.  In order to get powders less than 44 μm, the BOF slags were sieved to get
       the desired diameter.

   c.  Put the cleaned samples in the furnace pre-heated to 850℃ to decompose
       calcium hydroxide ($Ca(OH)_2$) and calcium carbonate ($CaCO_3$). Collect the
       dried powder in a clean bag and seal the bag.

   d.  Analyze the physical-chemical characteristics before carbonation
       experiments.

| Material |
|---|
| ● Basic oxygen furnace slag |
| ● Cold-rolling waste water |
| ● Tap water |

| Pre-treatment |
|---|
| ● Pre-heated 105°C |
| ● Sieving |
| ● Diameter $< 44\mu$ m(mesh #325) |
| ● Heating (850°C) |

| Reserving |
|---|
| ● Seal in the clean bag |

| Analyzing and Experimenting |
|---|
| ● Physical-chemical analyses |
| ● Carbonation |
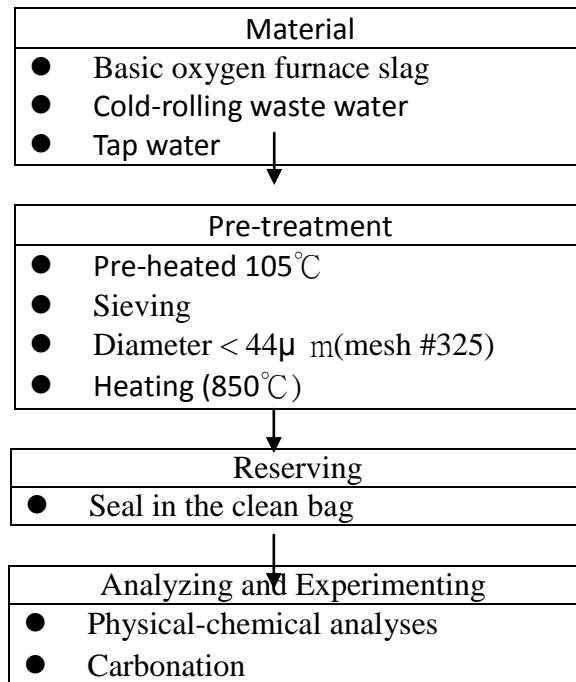
Figure 3-2 Flowchart of material preparation.

Sieve Opening and Cracking/ Grinding machine



Oven



Furnace

Figure 3-3 Photographs of preparing materials apparatus

## 3-3 Physico-Chemical Analysis

### 3-3-1 Scanning Electron Microscope (SEM)

SEM (JEOL JSM-7600F) is a type of electron microscope capable of producing high-resolution two dimensional images of sample surfaces, which is useful for observing the surface structure of the sample.



Figure 3-4 SEM equipment

### 3-3-2 X-Ray Diffractometry (XRD)

XRD (X' Pert Pro, PANalytical) is an efficient analytical technique to identify and characterize crystalline materials. Monochromatic X-rays are used to determine the interplanar spacings of the unknown materials. Samples are analyzed as powders with grains in random orientations to insure that all crystallographic directions are "sampled" by the X-ray beam. When reaching the constructive interference, a strong signal will be reflected, and the relative peak height is generally proportional to the number of grains in a preferred orientation.

The generated X-ray spectra thus, provide a structural fingerprint of the unknowns. Mixtures of crystalline materials can also be analyzed and relative peak heights of multiple materials may be used to obtain semi-quantitative estimates of abundances.



Figure 3-5 X-Ray Diffractometry

### 3-3-3 Composition Analysis

The analysis method was adopted by the chemistry analysis laboratory in China Hi-ment Corporation. Use aqua agent to dissolve most ingredients a sample but $SiO_2$, which needs be dissolved using hydrofluoric acid. If it still wasn't dissolved thoroughly, micro digestion method with increasing temperature and pressure can be used. Then, measure the content of metals in the extraction solution by ICP method, and compute the metal oxide percentage.

### 3-3-4 Thermogravimetric Analysis (TGA)

Thermogravimetric analyzer (TGA-51, Shimadzu) measures relation between weight changes and temperature in samples. The moisture is dried at $105℃$ as a known result. In the most literatures pronounced that the dehydration of calcium hydroxide was before $500℃$. There was continuous weight loss from $105℃$ to $1000$ $℃$ due to the dehydration of calcium silicate hydrate, calcium aluminate and other

minor hydrate. The rapid loss in weight is due to the decomposition of calcium carbonate. The weight loss due to the decomposition of calcium carbonation was determined by graphical technique used previously as shown in Figure 3-7(BK Marsh, 1984; BK Marsh, 1986; BK Marsh 1987).



Figure 3-6 Thermogravimetric analysis
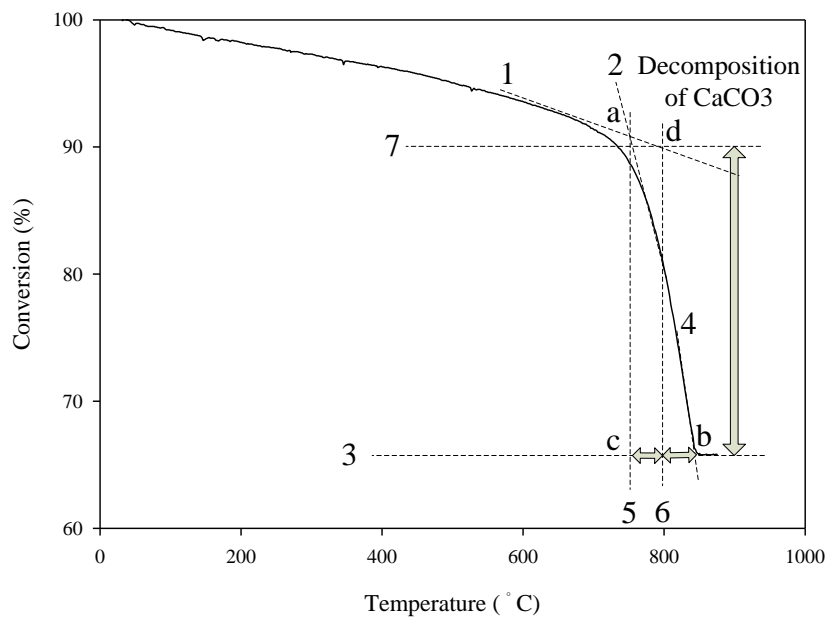


Figure 3-7 Method used to calculate calcium carbonation from weight loss curve during thermal analysis

## 3-4 Carbonation Experiment

### 3-4-1 Aqueous Carbonation Process by Slurry Reactor

1. Apparatus

   As shown in Figure 3-8

2. Method

   Experimental flowchart shown in Figure 3-9

3. Procedure

   a. Put 350mL cold-rolling waste water in the slurry reactor, and flow $CO_2$ for 5 minutes

   b. According to the setting L/S ratio 20, basic oxygen furnace slag was prepared

   c. Let $CO_2$ enter the slurry reactor and then set the flow rate to the setting value(0.5L/min, 1.0L/min, 2.0L/min, 2.5L/min, 3.0L/min)

   d. The reaction time was set to 0mins, 5mins, 10mins, 15mins, 20mins, 30mins, 40mins, 50mins, 60mins, 90mins, 120mins

   e. Filtrate the reacted slurry with 0.45 μm filter and put into oven (105℃) for 1 hour

   f. Cool down to room temperature, then weigh the sample

   g. Heat the sample up to 550℃, then heat the sample up to 850℃

   h. Compute the conversion rate

   i. Use TGA, SEM, TEM, XRD to analyze the samples

8 cm

50 cm

4 cm

(1)

(2)

(3)

(4)

(1) CO$_2$ cylinder
(2) Mass flow controller
(3) Slurry foam-bed reactor
(4) Vent to hood
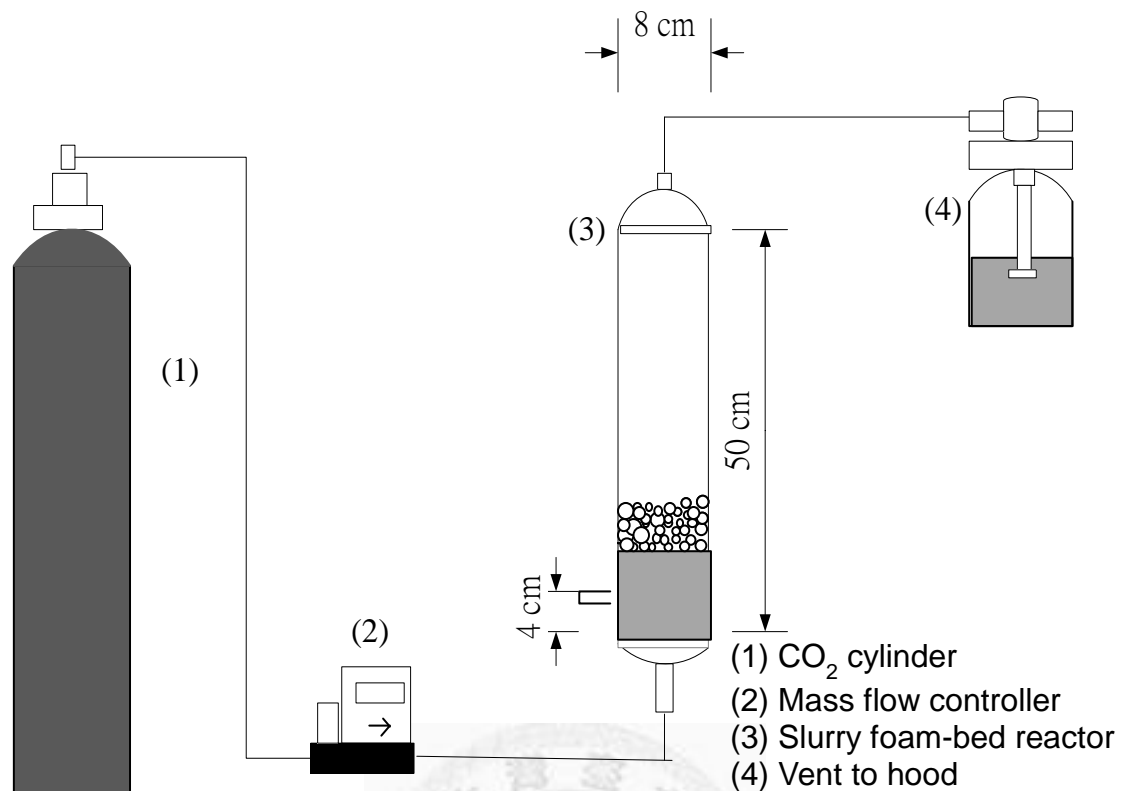
Figure 3-8 The schema of experimental apparatus of the experiment

Samples (15~20 mg) were heated in platinic cup under a nitrogen atmosphere. Weight loss was measured using TGA at two weight fractions: (1) 25℃~105$^o$C; (2) 105~850$^o$. The moisture is dried at 105℃ as a known result. In the most literatures pronounced that the dehydration of calcium hydroxide was before 500℃. There was continuous weight loss from 105℃ to 1000℃ due to the dehydration of calcium silicate hydrate, calcium aluminate and other minor hydrate. The rapid loss in weight is due to the decomposition of calcium carbonate. The weight loss due to the decomposition of calcium carbonation was determined by graphical technique used previously as shown in Figure 3-7(BK Marsh, 1984; BK Marsh, 1986; BK Marsh 1987). According to the thermal analysis the weight loss is $\Delta m_{CO_2}$, expressed in terms of CO$_2$ (wt%) :

$$CO_2(wt\%) = \frac{\Delta m_{CO_2}}{m_{105℃}} \times 100 \qquad \text{(eq 3-1)}$$

3-10

The carbonation degree ($\delta$) can be determined from the total Ca content of the fresh sample, the molar weights of Ca and $CO_2$ and the carbonate content measured with TGA. In Eq. 3-2, it is assumed that Ca is carbonated during the carbonation process and no significant amount of mass is lost due to leaching in the reactor:

$$\delta_{Ca}(\%) = \frac{\dfrac{CO_2(wt\%)}{100-CO_2(wt\%)} \times \dfrac{MW_{Ca}(kg/mol)}{MW_{CO_2}(kg/mol)}}{Ca_{total}(kg/kg)} \times 100 \qquad \text{(eq 3-2)}$$

$\delta$ : $CO_2$ conversion [%]

$MW_{Ca}$: molar weights of Ca [40 kg/mol]

$MW_{CO2}$: molar weights of $CO_2$ [44 kg/mol]

$Ca_{total}$: Total Ca content of the fresh sample

**Fixed Parameter**

- Reaction temperature = 25 ℃
- Reaction pressure = 101.3 kPa
- Particle size < 44 μm
- Basic oxygen furnace slag

**Synthetic Water**

**Cold-rolling wastewater**

**Surfactant**

- SDS (400 ppm)
- CTAB (500 ppm)
- Triton X-100 (500 ppm)

**CTAB**

- 500 ppm
- 200 ppm
- 175 ppm
- 150 ppm
- 100 ppm

**CO2 gas flow**

- 0.5 L/min
- 1.0 L/min
- 2.0 L/min
- 3.0 L/min
- 5.0 L/min

**L/S ratio**

- 5
- 10
- 20
- 40
- 50

**Reactor volume**

- 300
- 350
- 400
- 450

Reaction time = 5, 10, 15, 20, 30, 40, 50, 60, 90,120 mins

Solid product
- TGA
- SEM
- XRD

Liquid product
- pH meter
- AAS
- IC

Figure 3-9 Flowchart of carbonation experiments

## 3-5 Technical Assessment

### 3-5-1LCA

To consider the feasibility of carbonation slurry reactor, the environment impacts should be assessed including material flow and energy flow by using LCA software-, Umberto. Set the system boundary, and then collect the experimental data and domestic database. The unit of energy and material are expressed as kilowatt per hour (kJ) and kilogram (kg), respectively.

1. Method

   Use International Organization for Standardization (ISO) standards 14040 series and LCA software-Umberto 5.5

2. Procedure

   a. Goal and scope definition. System boundary is presented in Figure 3-10.

   b. Life cycle inventory. Inventory list is presented in Table 3-1.

   c. Life cycle impact assessment.

   d. Interpretation.
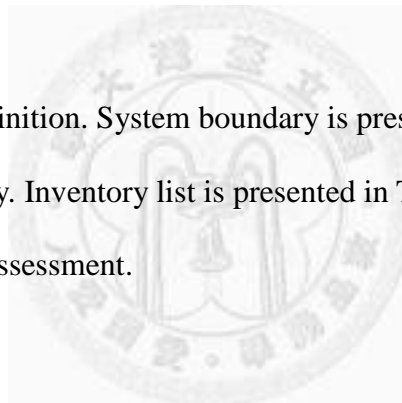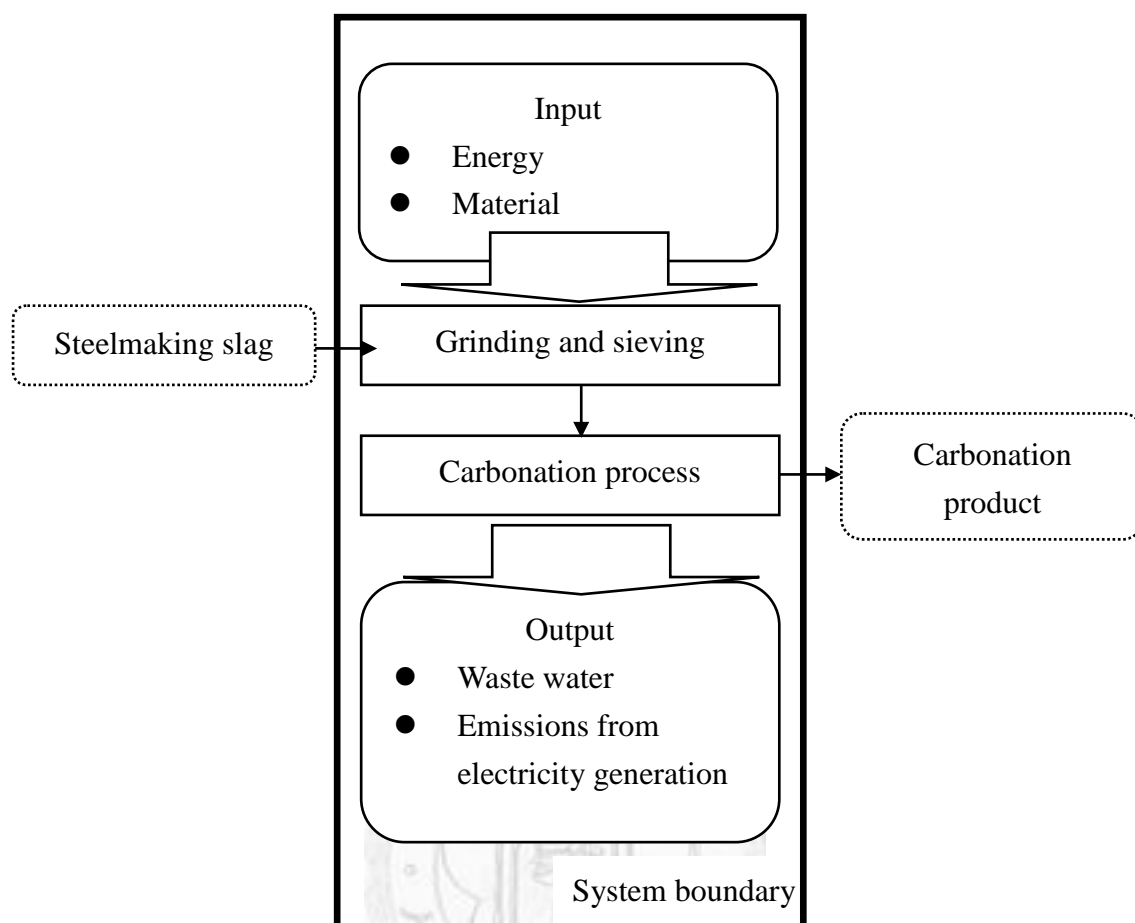
Figure 3-10 System boundary of aqueous carbonation experiment.

Table 3-1 Inventory list of aqueous carbonation using slurry reactor.

| Process | Inputs | | Outputs | |
| --- | --- | --- | --- | --- |
| Grinding and sieving | Electricity: | kJ | Emission: | kg |
| Carbonation process | Electricity: | kJ | Waste water: | kg |
| | Water used: | kg | Emission: | kg |
| | Chemical used: | kg | Product: | kg |

**3-5-2 3E Assessment**

     To consider the feasibility of $CO_2$ sequestration by carbonation in this study, the performance indicator and its benchmark can be expressed by Table 3-2. It contains engineering, economic and environment aspects in 3E assessment. Determine the value of this technology by comparison of experiment data and the other technologies in literature.

Table 3-2 The 3E assessment indicators for $CO_2$ sequestration technology

| Aspect | Indicator | Reference |
|---|---|---|
| **Engineering** | **Suitable geological media for $CO_2$ storage (1) Capacity; (2) Injectivity; and (3) Confinement** <br> The percentage of the $CO_2$ remaining in the storage location after 100 years will with high probability still amount to 99 percent. <br> The maximum annual leakage rate not to exceed 0.01 percent | Stefan Bsvhu, 2008 IPCC, 2005 German Environment Agency |
| | **Efficiency** <br> 8-12 percentage points loss vs. power plants with no CCS (potential decline to 4%) | IEA, 2006 |
| | **$CO_2$ emission reduction and storage potential** <br> > 85% in power plants <br> Sequester at least 90 percent of $CO_2$ emissions from the plant with the future potential to capture and sequester nearly 100 percent | IEA, 2006 USDOE, 2003 |
| **Economic** | **Cost** <br> The whole process chain (i.e. including transport and storage) not exceeding 20 EUR/tCO2 <br> Total CCS cost expected to fall below $25/tCO_2$ by 2030, depending on technology learning/advances, with incremental electricity cost of $10-20/MWh | Wuppertal Institute; IEA, 2006 |

| | | Capture of Cost<br>10% increase in cost of energy proven for direct capture concept | USDOE, 2003 |
|---|---|---|---|
| | | Measurement Monitoring & Verification of Cost<br>MMV represents no more than 10% of total sequestration cost | USDOE, 2003 |
| | | Incremental product cost<br>$$COE = [(TCR)(FCF)+(FOM)]/[(CF)(8760)(kW)]+VOM+(HR)(FC)$$<br>COE = levelized cost of electricity (NTD/kWh)<br>TCR = Total capital requirement (NTD)<br>FCF = Fixed charge factor (%/year)<br>FOM = Fixed operating costs (NTD/kWh)<br>CF = Capacity factor (%)<br>VOM = Variable operating costs (NTD/kWh)<br>HR = net plant heat rate (kJ/kWh)<br>FC = Unit fuel cost (NTD/kJ) | IPCC, 2005 |
| | | Cost of $CO_2$ avoided (NTD/$tCO_2$)=<br>$$[(COE)_{capture}-(COE)_{ref}]/[(CO_2/kWh)_{ref}-(CO_2/kWh)_{capture}]$$<br>$(COE)_{capture}$ = levelized cost of electricity generation with CCS(NTD/kWh)<br>$(COE)_{ref}$ = levelized cost of electricity generation without CCS(NTD/kWh)<br>$(CO_2/kWh)_{ref}$ = $CO_2$ mass emission rate per kWh generated without CCS<br>$(CO_2/kWh)_{capture}$ = $CO_2$ mass emission rate per kWh generated with CCS | IPCC, 2005 |
| | | Cost of $CO_2$ captured (NTD/$tCO_2$)=<br>$$[(COE)_{capture}-(COE)_{ref}]/ (CO_2/kWh)_{capture}$$ | IPCC, 2005 |

| | | |
|---|---|---|
| **Environment** | **Global warming**<br>kg $CO_2$-eq/function unit | Khoo et al., 2006<br>Viebahn et al., 2007<br>Koornneef et al., 2008<br>Odeh et al., 2008<br>Pehnt et al., 2008 |
| | **Photo-oxidant formation**<br>kg Ethen-eq/function unit | Viebahn et al., 2007 Koornneef et al., 2008<br>Pehnt et al., 2008 |
| | **Eutrophication**<br>kg $PO_4^{3-}$-eq/function unit | Viebahn et al., 2007<br>Koornneef et al., 2008<br>Pehnt et al., 2008 |
| | **Acidification**<br>kg $SO_2$-eq/function unit | Khoo et al., 2006<br>Viebahn et al., 2007<br>Koornneef et al., 2008<br>Pehnt et al., 2008 |
| | **Human toxicity**<br>kg 1,4-DCB/ kg $CO_2$ captured | Guinée, J.B., et al., 2002 |
| **Energy** | **Cumulative Energy demand**<br>kJ/function unit | Khoo et al., 2006<br>Viebahn et al., 2007<br>Pehnt et al., 2008 |

# Chapter 4 Results and Discussion

## 4-1 Physico-Chemical Characteristics of Steelmaking Slag and Wastewater

### 4-1-1 Physical and chemical properties of steelmaking slag

The physico-chemical composition of the basic oxygen furnace slag (BOF) used in this study was analyzed after the grinding and sieving. Table 4-1 presents results of the analysis which indicates that the volume-mean diameter was 27.2 μm and the BET surface area was 3.24 $m^2g^{-1}$.

The elemental composition of the fresh slag was analyzed using inductively coupled plasma atomic emission spectroscopy (ICP-AES) after total digestion of the slag. The major components of the BOF included $SiO_2$, $Al_2O_3$, $Fe_2O_3$, CaO and MgO. The $CO_2$ capture capacity of the slag material was attributed mainly to two components: CaO and MgO. Knowing the chemical composition, the theoretical capture capacity of the slag can be calculated. Assuming all of the calcium oxides was carbonated to calcium carbonate, the carbon capture capacity of the BOF slag was calculated as 0.32 kg $CO_2$/ kg BOF slag due to CaO.

The higher CaO content would present a higher carbonation reactivity of the slags. The desulphurization (De-S) regent which was added to basic oxygen furnace was mainly made of limestone. The BOF so generated the CaO as it major component. Therefore, the BOF rich in CaO is a suitable feedstock for carbonation.

Table 4-1 Physico-chemical properties of basic oxygen furnace (BOF) slags (China Hi-cement Corporation).

| | Composition | BOF |
|---|---|---|
| Physical characteristic | True destiny($gcm^{-3}$) | 2.8 |
| | Mean diameter (μm) | 27.2 |
| | BET surface area ($m^2g^{-1}$) | 3.2 |
| Chemical characteristic | $SiO_2$(%) | 6.99 |
| | $Al_2O_3$(%) | 1.83 |
| | $Fe_2O_3$(%) | 24.41 |
| | CaO(%) | 41.15 |
| | MgO(%) | 9.21 |
| | Total | 83.59 |

Basic oxygen furnace slag (BOF) was used as an absorbent for carbonation in this study. Scanning electronic microscope (SEM) with energy dispersive spectrometer (EDX) was used to determine the morphological characteristics of the slag and to quantify the chemical elements incorporated in the minerals.

Figure 4-1 (a) shows the SEM image of the basic oxygen furnace slag which was magnified at 15000X of the actual size. Figure 4-1 (b) shows the SEM image of the basic oxygen furnace slag at 35000X of the actual object. The surfaces of all fresh particles appeared to be un-uniform, needle in shape before carbonation experiments.

Figure 4-2 shows the SEM-EDS results of the fresh basic oxygen furnace slag. Based on the SEM-EDX data showed that the BOF was composed of 61.2, 31.8, 4.2 and 2.8% of oxygen, calcium, silicon and iron, respectively.

The EDS detector was capable of detecting elements with atomic number equal to or greater than six. Because the element was not distributed homogeneously in the slag, there was significant difference in element of contents at different location observed by the EDS analysis. Although the element contents varied at different points of the BOF surface, most results showed that oxygen and calcium were the major elements in the BOF slag. Therefore, the BOF would be a good material for carbonation because of the contents of calcium.

(a)
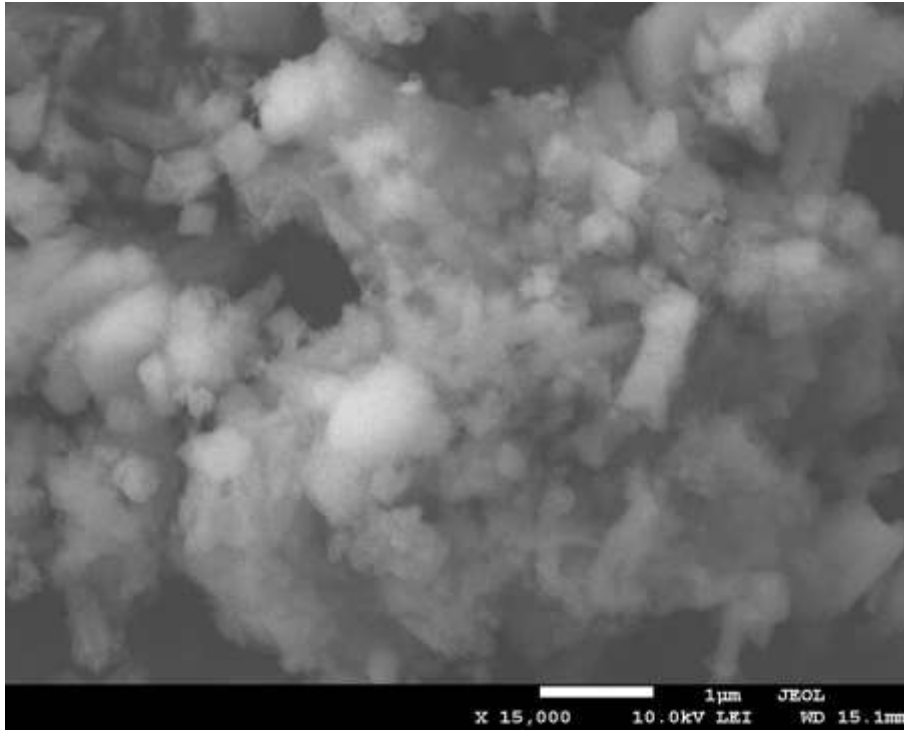


(b)
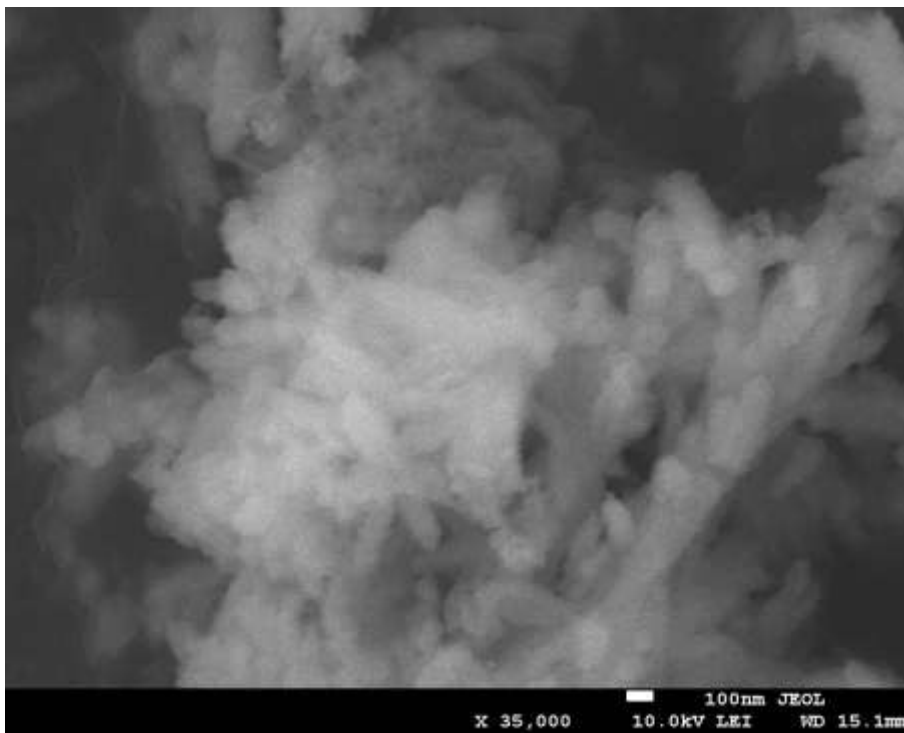


Figure 4-1 Scanning electronic micrographs of the BOF (a) 15000X of actuality and (b) 35000X of actuality
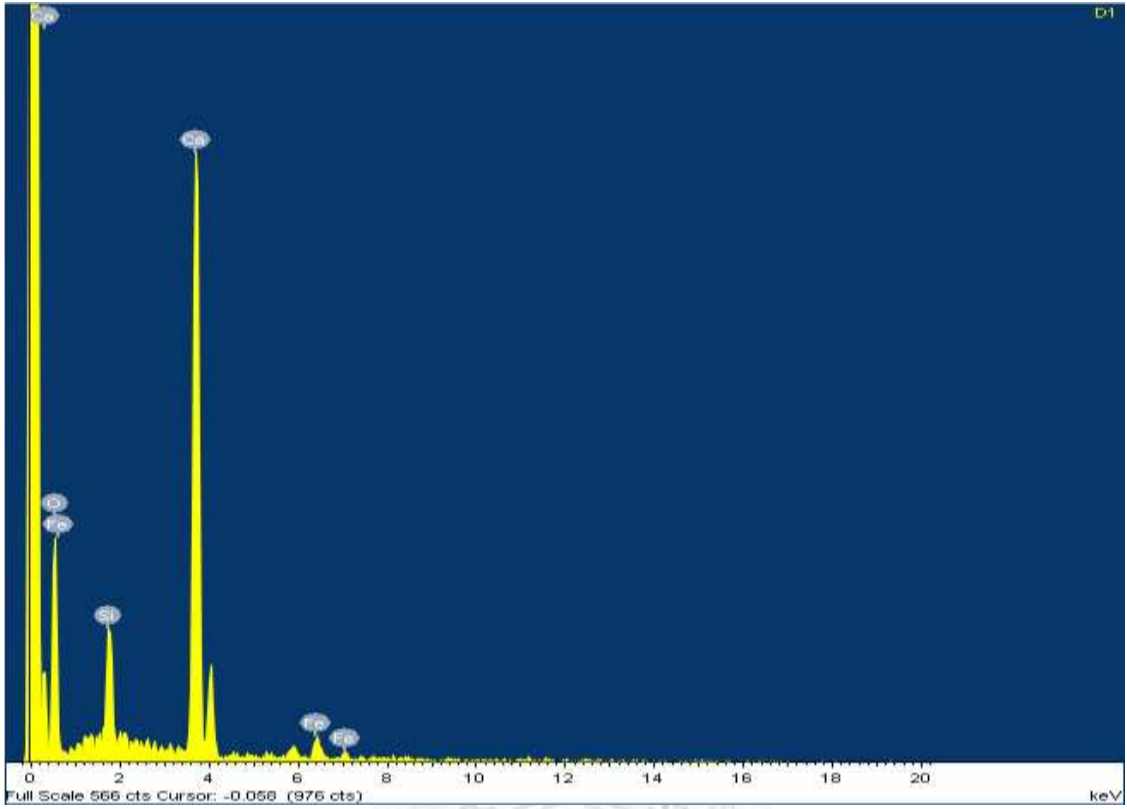
Figure 4-2 EDX spectra of fresh basic oxygen furnace slag

The fresh basic oxygen furnace (BOF) slag was examined using XRD.    Figure 4-2 shows the XRD images of the fresh basic oxygen furnace slag, which was preheated in an oven from ambient to 850℃.    Figure 4-3 showed the presence of many elements in the fresh BOF as evident by the various peaks.
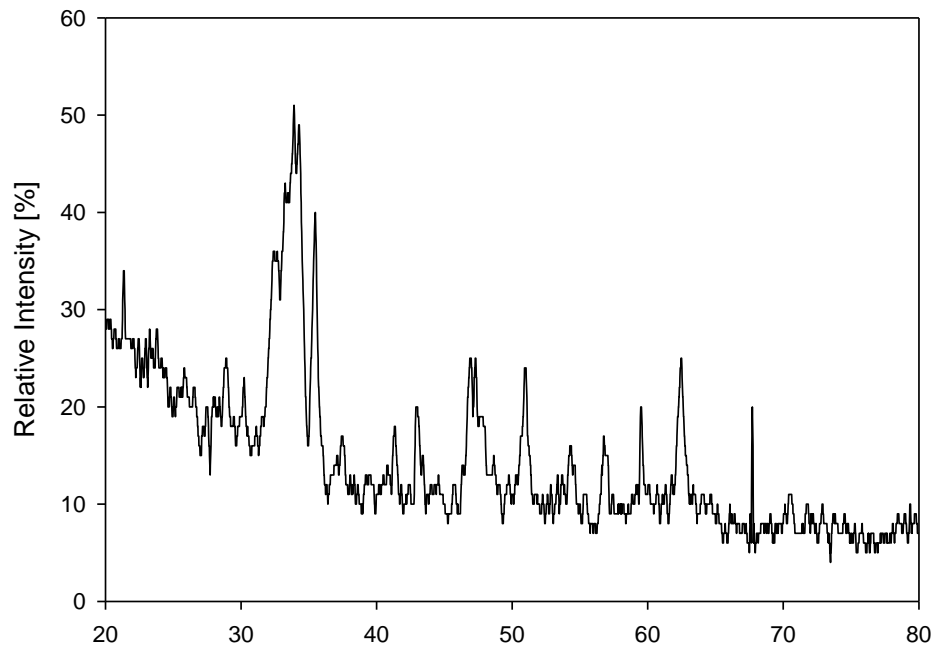


Figure 4-3 XRD spectra of fresh of basic oxygen furnace slag

## 4-1-2 Composition of Steelmaking Wastewater

In Taiwan, each ton of tap water contributes 0.193 kg of $CO_2$ (Taiwan Water Corporation, 2010). This is a significant consumption of energy for tap water production. Therefore it main proposed to use wastewater instead of tap water in this study for purpose of energy saving. This study selected the steelmaking wastewater as feedstock. Using steelmaking wastewater to prepare carbonation slurry will be a suitable and energy saving choice.

The criteria for selecting steelmaking wastewater as feedstock are high alkaline, content high $Ca^{2+}$ concentration and no toxic chemicals. The alkaline cold-rolling wastewater and effluent from steelmaking wastewater treatment plant were chosen for this study. The cations were analyzed using atomic absorption spectroscopy (AA) and the anions were analyzed using ion chromatography (IC). The water quality of the cold-rolling wastewater and effluent were analyzed as shown in Table 4-1.

The pH value may affect the dissolution of calcium and the rate of carbonation. The initial pH value is one of the important factors affecting carbonation. The pH value of cold-rolling wastewater was much higher than the effluent from steelmaking wastewater treatment plant.

The conductivity and total dissolved solid of cold-rolling wastewater were high due to the presence of various anions and cations. In theory, the electroneutrality of the wastewater be maintained. Results showed that there was discrepancy between the observed and the theoretical neutrals. Sodium and chloride ions were among the ions with highest concentration in the cold-rolling wastewater.

Table 4-2 Water quality of cold-rolling waste water and effluent

| Parameters | | Cold-rolling Wastewater | Effluent |
|---|---|---|---|
| pH | | 11.4 | 7.28 |
| Cond | | 5690 μS/cm | 2550 μS/cm |
| TDS | | 3000 mg/L | 1297 mg/L |
| $SiO_2$ | | 23.14 mg/L | 4.01 mg/L |
| $NH_3$-N | | 2.8 mg/L | 15.65 mg/L |
| Cations mg/L (meq/L) | Ca | 113.9 ( 5.69 ) | 105.5 ( 5.28 ) |
| | Mg | N.D | 14.99 ( 1.25 ) |
| | Na | 602 ( 26.17 ) | - |
| | K | 190 ( 4.87 ) | - |
| | Fe | 2.117 ( 0.08 ) | N.D |
| Anions mg/L (meq/L) | $F^-$ | 1.19 ( 0.06 ) | 26.9 ( 1.42 ) |
| | $Cl^-$ | 1420 ( 40.00 ) | 434 ( 12.23 ) |
| | $NO_2^-$ | 2.27 ( 0.05 ) | - |
| | $NO_3^-$ | 8.74 ( 0.14 ) | 33.5 ( 0.54 ) |
| | $PO_4^{3-}$ | 1.35 ( 0.03 ) | 0.56 ( 0.01 ) |
| | $SO_4^{2-}$ | 329 ( 6.85 ) | 878 ( 18.29 ) |

## 4-2 Aqueous Carbonation Processes

### 4-2-1 Determination of $CO_2$ conversion by the TGA method

Figure 4-4 compares the TGA results of the fresh and the carbonated basic oxygen furnace slag at various temperatures. The weight loss of the fresh slag about 5% due to the increase of temperature is not significant. On the other hand, the weight loss of the carbonated slag was about 35%. According to the Zeman (2008), calcium carbonate can be decomposed in the temperature range of 550 and 850℃. However, there is dehydration of calcium silicate hydrate, calcium aluminate and other minor hydrates in the temperature range studies. In this study the graphical method used by previously investigators were used to determine the weight loss due to the decomposition of calcium carbonate as shown in Figure 4-5 (BK Marsh, 1984; BK Marsh, 1986; BK Marsh 1987).
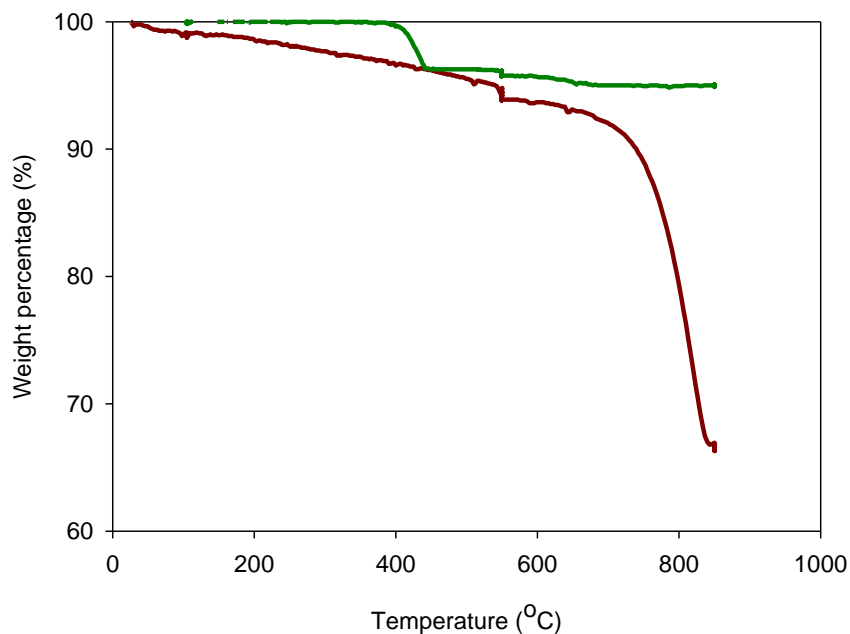


Figure 4-4 TGA curve of fresh and carbonated basic oxygen furnace slag.
(Carbonation conditions: pressure = 14.7 psig $CO_2$; temperature = 25 $^o$C; particle size < 44μm; L/S ratio = 20; flow rate = 1.0 L/min; reaction volume = 350mL)

The procedures for determining the weight loss during the decomposition of calcium carbonate are shown below

1. Draw a line tangent to the TGA curve at 550 ℃, line 1.

2. Draw another line tangent to the TGA curve in the upper branch of the rapid - weight loss zone, line 2.   Line 1 and line 2 meet at intersection point "a".

3. Draw a line tangent to the TGA curve at 850 ℃, line 3.

4. Draw a line tangent to the TGA curve in the lower branch of the rapid − weight loss zone, line 4.   Line 3 and line 4 meet at point "b".

5. Draw a vertical line passing point "a" and crosses line 3 at point "c", line 5.

6. Draw a vertical line bisect of point "b" and "c"; extends the vertical line until meet line 1 at point "d", line 6.

7. Draw a horizon line passing point "d", line 7.

8. The weight loss due to decomposition of calcium carbonation in the distance between line 4 and line 7.
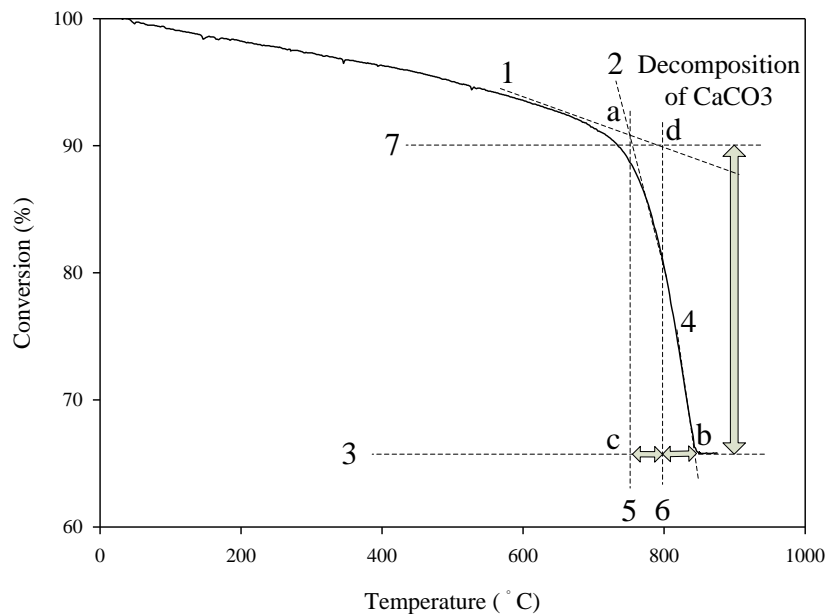


Figure 4-5 Method used to calculate calcium carbonation from weight loss curve during thermal analysis

**4-2-2 Aqueous Carbonation by Synthetic Water and Wastewater**

The experimental procedures include the following three steps: aqueous carbon dioxide dissolution, calcium leaching, and calcium carbonate precipitation. The operational conditions of the carbonation experiment were: $T = 25^{o}$C, $P_{CO2} = 101. 3$ kPa, particle size < 44 μm, $Q = 1.0$ L min$^{-1}$, L/S = 20, and t = 120 min.

This study used different surfactants including cationic, anionic and nonionic. The result is shown in Figure 4-6. The highest conversion of carbonation was observed for the tap water. This result showed that the surfactant was not positively influencing the carbonation. This result did not agree with the literature. Although there was no significant difference between three surfactants, the cationic surfactant - Cetyl trimethylammonium bromide (CTAB) appeared to exhibit the greatest conversion among all of three surfactants. It is highly likely that the concentration of the surfactant was the key factor affecting the carbonation conversion.
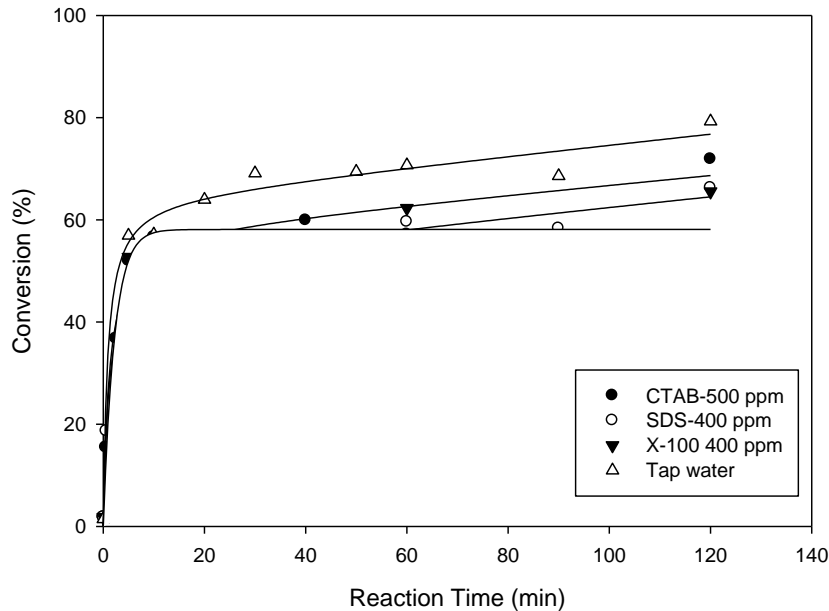


Figure 4-6. Influence of different kinds of surfactant on the carbonation conversion of the BOF slags (Carbonation conditions: pressure = 14.7 psig CO2; temperature = 25 ℃; particle size < 44 μm; L/S ratio = 20; CO$_2$ flow rate = 1.0 LPM).

The cationic surfactant - Cetyl trimethylammonium bromide (CTAB) was used to prepare the synthetic water for investigate on the effect of surfactant concentration on carbonation. The experimental conditions were ambient temperature, atmosphere pressure, L/S of 20, flow rate of 1 LPM and reaction volume of 350 mL. The result is shown in Figure 4-7. The surfactant concentration did not display significant effect on the carbonation process. Figure 4-8 shows the carbonation during the first 10 min of the experiment seem the degree of conversion was much slow in the presence CTAB. It can be seen that CTAB had no significant effect on the degree of conversion.
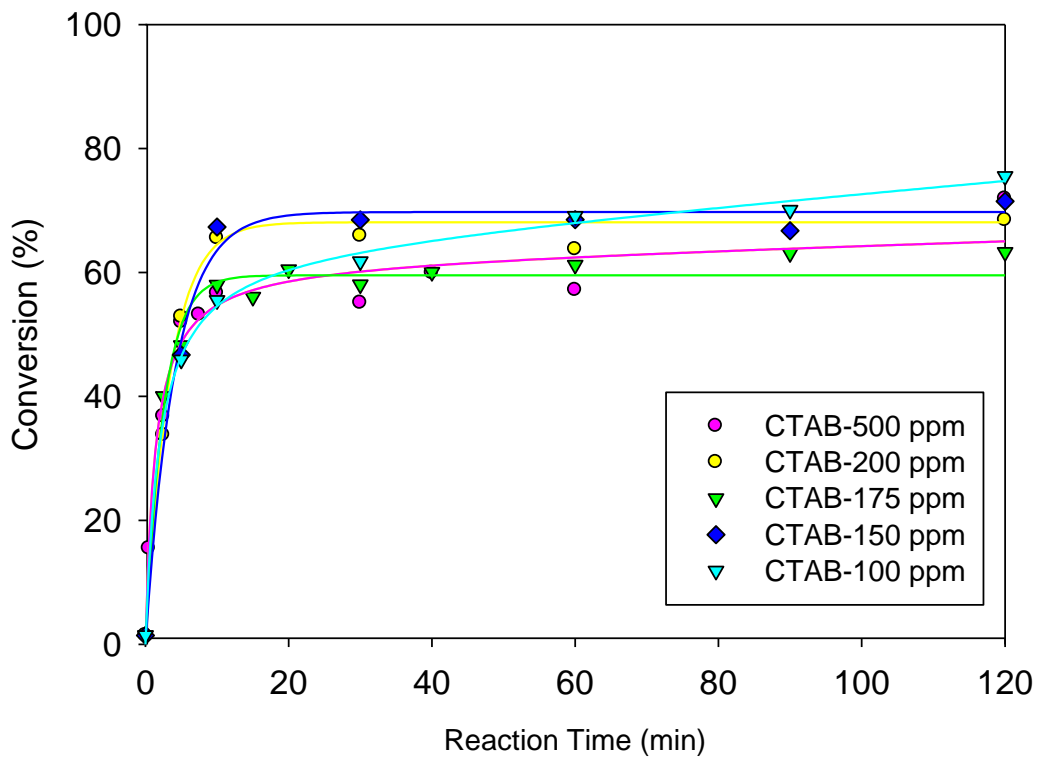


Figure 4-7. Influence of different concentration of CTAB on the carbonation conversion of the BOF slags (Carbonation conditions : pressure = 14.7 psig $CO_2$; temperature = 25 ℃; particle size < 44 μm; L/S ratio = 20; $CO_2$ flow rate = 1.0 LPM).

Figure 4-8.    Influence of different concentration of CTAB on the carbonation conversion of the BOF slags (Carbonation conditions: pressure = 14.7 psig $CO_2$; temperature = 25 ℃; particle size < 44 μm; L/S ratio = 20; $CO_2$ flow rate = 1.0 LPM).

The effects of reaction time on the conversion ratio for the BOF in three types of water sources are shown in Fig. 4-9.  Theoretically, the extent of carbonation would increases as the reaction time increases.  The carbonation reaction had a limited conversion because of the barrier forming during the carbonation reaction (Huijgen et al., 2005).  The carbonated product was adhered on the surface of feedstock which restricted the dissolution of calcium iron.  It was found that the carbonation rate decreased as the reaction time increased.  Carbonation reaction was fast at the beginning and then slowed down after 2 h (Chu et al., 2007).  The result shows that cold-rolling wastewater (89.18%) is more effective in carbonation conversion than that in effluent (76.69%) and tap water (79.27%) in carbonation conversion.

A possible explanation was due to the effect of pH.    The higher pH value the more carbon dioxide dissolved in the wastewater which enhanced the carbonation process.

The surfactant on the surface of feedstock would inhibit the dissolution of calcium iron.  The conversions were not always higher in wastewater than that of tap water which did not contain surfactant.  The surfactant wasn't homogeneous attached on the surface so that the curve of carbonation conversion was not smooth.

Figure 4-9 Influence of reaction time on the carbonation conversion of the BOF (Carbonation conditions: pressure = 14.7 psig $CO_2$; temperature =25 $^{\circ}$C ; particle size < 44 μm; L/S ratio = 20; flow rate = 1.0 L/min).

**4-2-3 Variation of Cold-Rolling Wastewater**

Figure 4-15 shows the changes of pH value, concentration of calcium ion and conversion at various reaction time. The pH value was higher than 12 at the beginning and it was decreased to about 6 at the end of the reaction time. The conversion maintained constant when the pH value remained at about 6. The dominant species is carbon dioxide under acidic condition (pH < 6. 3) and the activity of carbonate ions was not sufficient to react with calcium ions.

The concentration of calcium ion was about 900 ppm at the beginning and it was rapidly decreased then slower increased with the reaction time. The reaction of aqueous carbonation was fast and it consumed a lot of calcium ions. After the reaction became slowly, the calcium ion dissolved from the unreacted basic oxygen furnace slag (BOF) resulting in the increase of the concentration of the calcium ion increased at the end of the reaction time.
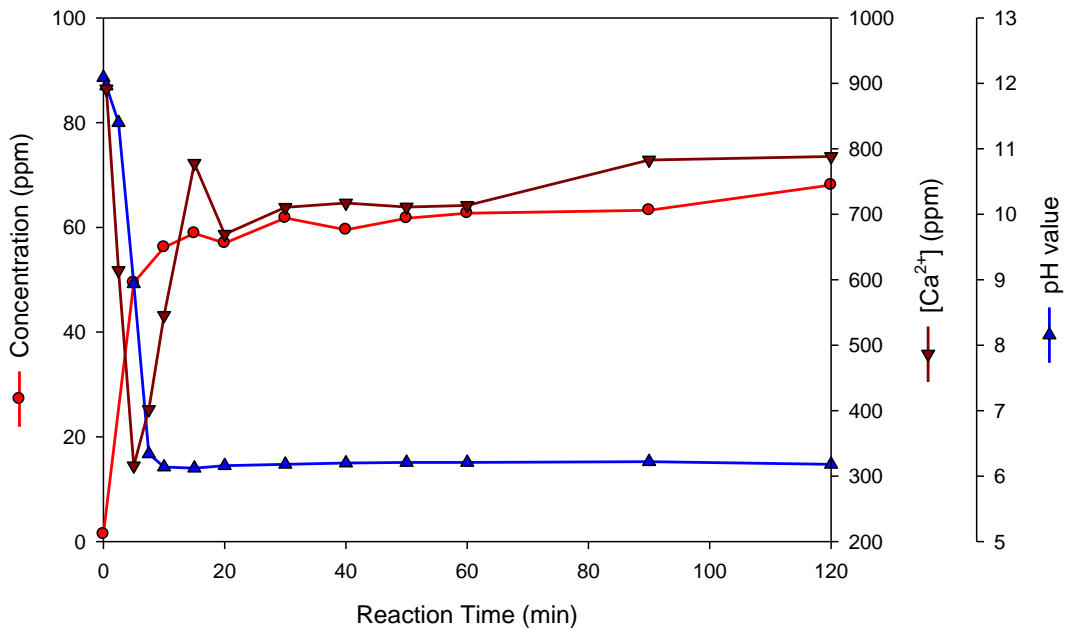
Figure 4-10.   The change of pH values, concentration of calcium ion and conversion during reaction time.   (Carbonation conditions: pressure = 14.7 psig $CO_2$; temperature = 25 ℃; particle size < 44 μm; L/S ratio = 20; $CO_2$ flow rate = 1.0 LPM; reaction volume =350mL).

Figure 4-16 shows the variation of water quality in the course of reaction which indicates that could be explained by the fact that the chloride ion decreased at the beginning and then increased afterwards.   If the presence of chloride was in the BOF that the concentration of chloride increased after the BOF added.   The chloride was adsorbed on the BOF and the BOF was attached on the foam and raised to the surface with foam.   The foam and the solid were rest on the surface of the liquid.   Then the foam broke up and the solid was returned back to the slurry.   The concentration of chloride was affected by the life cycle of the foam.

The $NO_2^-$ and $NO_3^-$ and the nitrate ion were maintained constant during the reaction because they were relatively stable chemicals.   However, the sulfate ion was decreased after adding the BOF because the sulfate ion reached with the calcium ion from the BOF to form the calcium sulfate precipitation.
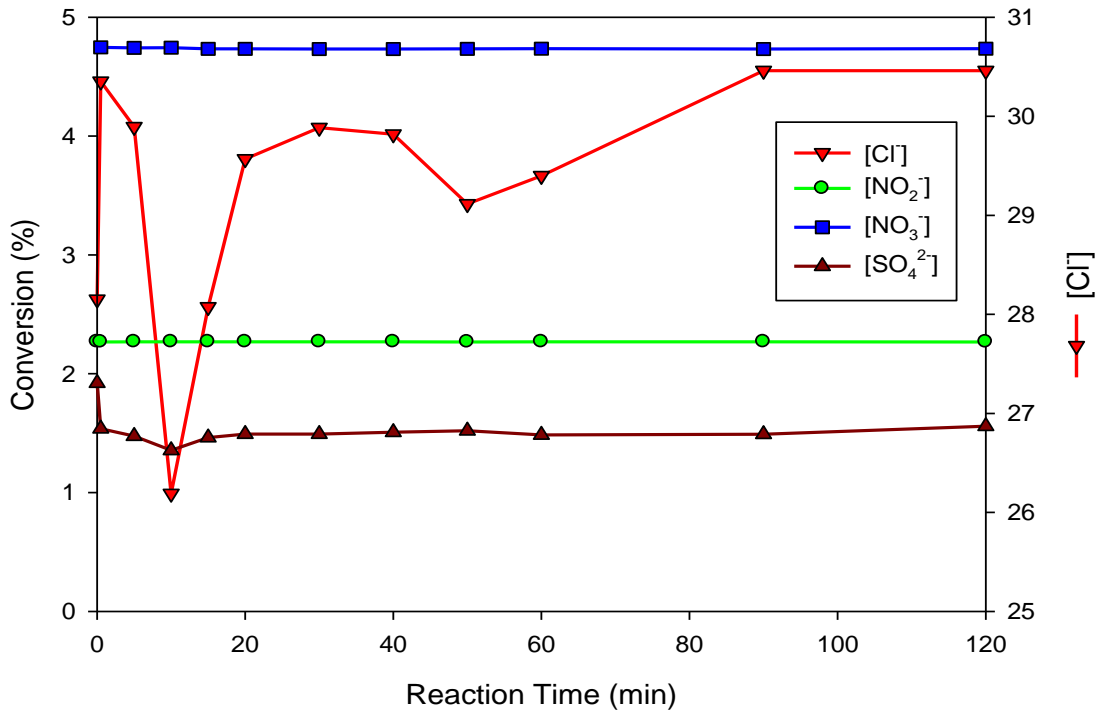
Figure 4-11. The changed of water quality during reaction time (Carbonation conditions: pressure = 14. 7 psig CO2; temperature = 25 ℃; particle size < 44 μm; L/S ratio = 20; CO2 flow rate = 1. 0 LPM; reaction volume = 350mL).
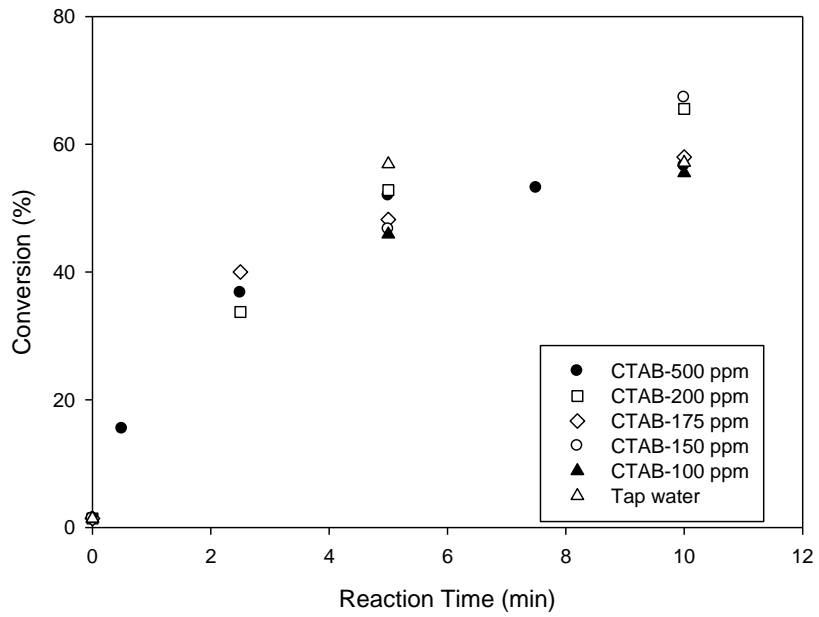
## 4-2-4 Effect of Different Flow Rate, Liquid to Solid and Reaction volume Ratio by Cold-rolling Wastewater

The carbonation conversion for the BOF slag was measured at five different $CO_2$ flow rates of 0.5 L min, 1.0 L/min, 1.5 L/min, 2.0 L/min and 3.0 L/min as shown in Fig. 4-10.

The carbonation conversion was decreased with increasing flow rate above 1 L/min. The channeling effect in the slurry reactor was significant at a high flow rate resulting in a poor gas－liquid mass transfer and causing the decrease of carbonation conversion. The higher conversion was observed when the flow rate was operated between 0.5 L/min and 1 L/min because the media in the reactor mix well under the research velocity.

A slight decrease of carbonation conversion was observed for the flow rate of

3L/min between 20 min and 30 min. It could be explained that the calcium carbonation was converted to calcium bicarbonation when a great amount of $CO_2$ was introduced into the reactor.
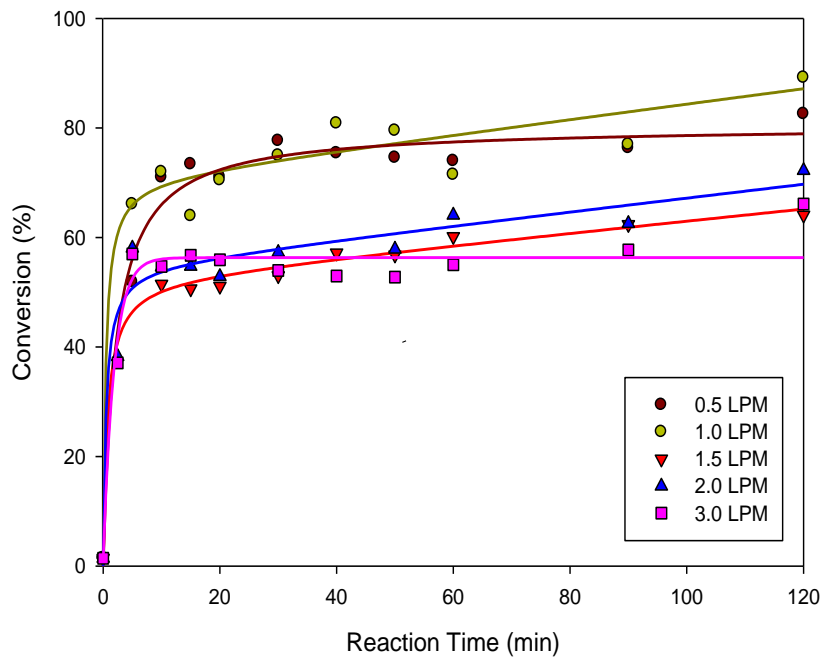


Figure 4-12 Influence of flow rate on the carbonation conversion of the BOF slags (Carbonation conditions: pressure = 14.7 psig $CO_2$; temperature = 25 ℃; particle size < 44 μm; L/S ratio = 20).

The L/S ratio represents the weight ratio of waste water to waste solid of the slurry used in the aqueous carbonation. The aqueous carbonation experiments using the BOF were conducted at L/S ratio ranging from 5 to 50 mL/g with a reaction time of 120 min, as shown in Fig. 4-11. It was found that the conversion was significantly higher for the BOF at the L/S ratio of 20. When the L/S was lower than 20, the slurry couldn't mix well in the reactor resulted in poor solid-liquid mass transfer. When the L/S was higher than 20, there was lower dissolution rate of calcium ion because of fewer BOF slag.

The effect of L/S ratio on the conversion efficiency became insignificant when the reaction time was greater than 40 min. As shown in Figure 4-11, slower conversion

rate was observed for lower L/S ratio slurry when the reaction time was less than 20 min.    The slower conversion rate likely is due to significant amount of foreign ions in the lower L/S ratio slurry resulting in a competitive reaction and lowering the rate of calcium dissolution.
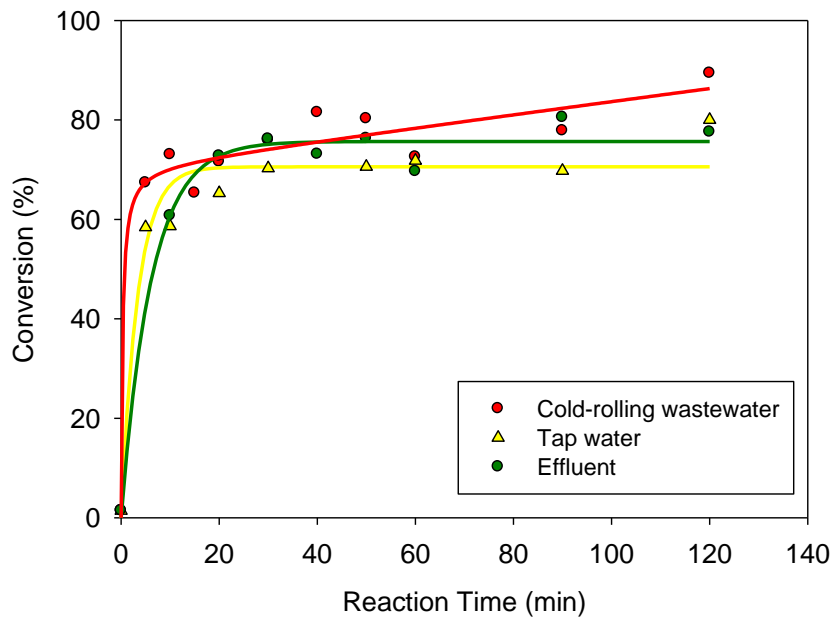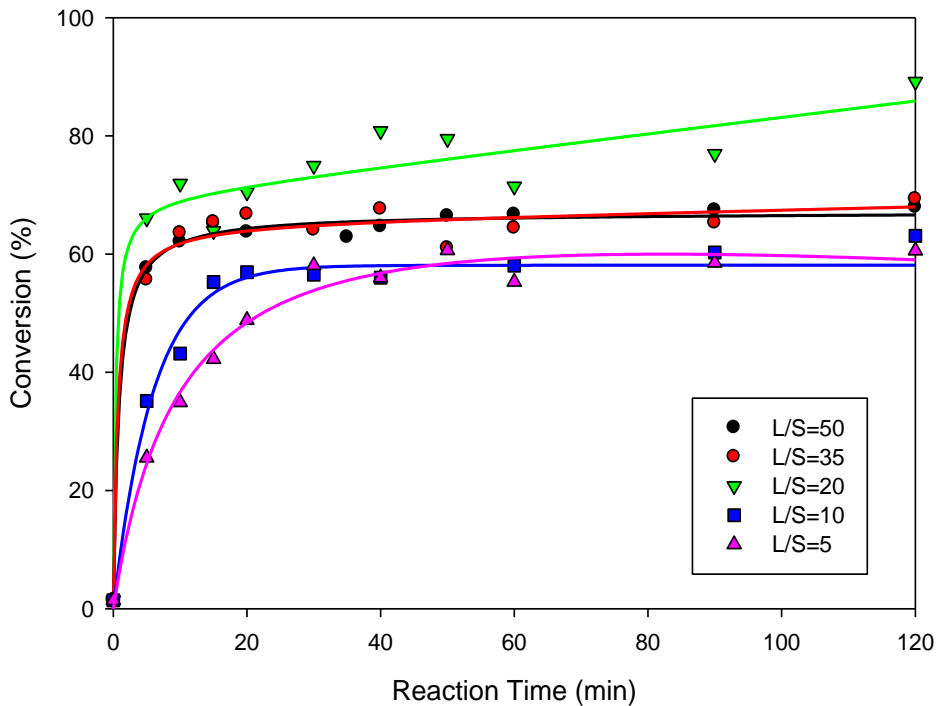


Figure 4-13.    Influence of liquid to solid on the carbonation conversion of the BOF slags (Carbonation conditions: pressure = 14.7 psig $CO_2$; temperature = 25 ℃; particle size < 44 $\mu$m; $CO_2$ flow rate = 1.0 LPM).

Theoretically, the increase of reaction volume would increase the retention time of $CO_2$ resulting in dissolving more gas into the solution.    The conversion would be higher.    The experimental conditions were ambient temperature, atmosphere pressure, L/S of 20 and flow rate of 1 LPM.    The effect of reaction volume on carbonation is shown in Fig. 4-12.

It was found that the conversion was the highest at 350 mL of reaction volume. The conversion was decreased as the increase of reaction volume was increased from 350 mL to 450mL.    The possible explanation of this result may be due to a better

mixing in a smaller reaction volume.
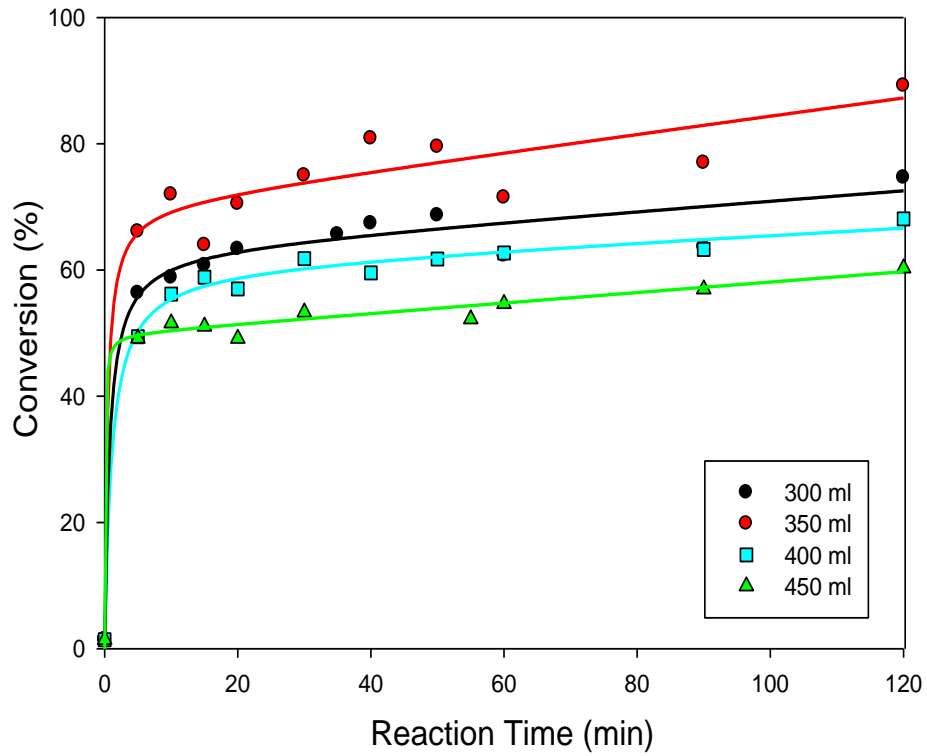


Figure 4-14.    Influence of reaction volume on the carbonation conversion of the BOF slags (Carbonation conditions: pressure = 14. 7 psig $CO_2$; temperature = 25 ℃; particle size < 44 μm; L/S ratio = 20; $CO_2$ flow rate = 1.0 LPM).

**4-2-5 Carbonation by Steelmaking slag**

Figure 4-13 shows the SEM image of the fresh (Fig. 4-13a) and carbonation (Fig 4-13b) slag which were carbonated at L/S ratio of 20, flow rate of 1 L/min, reaction time of 120 minutes in the cold-rolling wastewater. Comparing the feedstock before and after carbonation showed that there were cubic particles on the feedstock after carbonation. The cubic particles were identified as calcium carbonate by XRD.

(a)
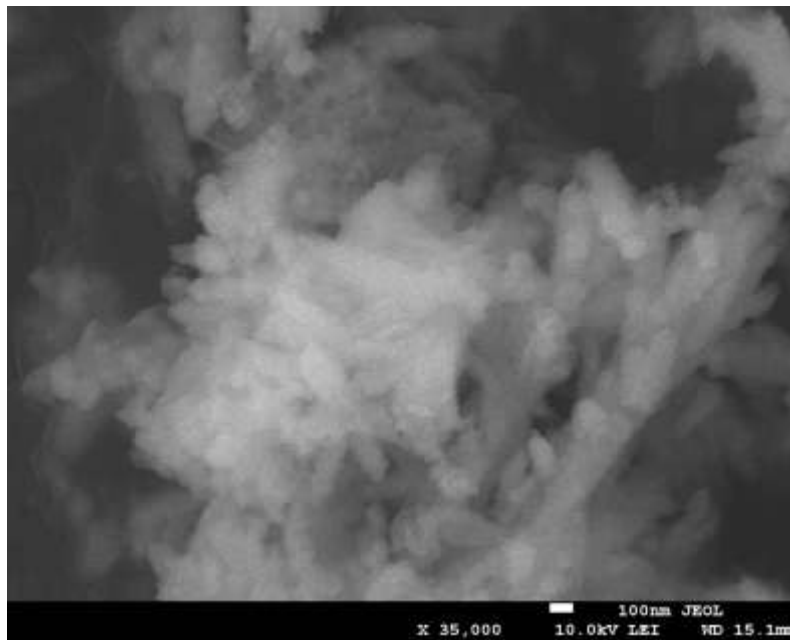


(b)
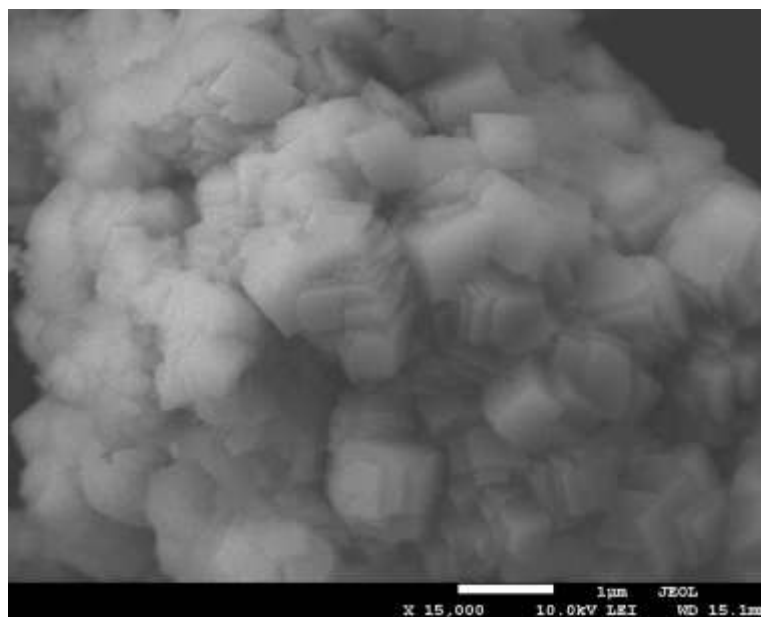


Figure 4-15. Scanning-electron micrographs (SEM) of the steel-making slag: (a) fresh BOF slag (1μm); (b) carbonated BOF slag (1μm)

The slags were examined by XRD. Figure 4-14(a) shows the XRD images of the fresh slags and Figure 4-14 (b) shows the XRD images of carbonated material blended with the BOF slags, which were carbonated at ambient temperature, atmosphere pressure, L/S of 20, flow rate of 1 L/min and reaction volume of 350 mL. The peaks in Figure 4-14(b) appeared at $2\theta = 23.02°$, $29.41°$, $35.97°$, $43.15°$, $47.49°$, $48.50°$, $57.40°$, $60.68°$, and $64.68°$, respectively, which indicate a pure calcite ($CaCO_3$). This suggests that the BOF slags were carbonated with $CO_2$ to form $CaCO_3$. Comparison between the fresh and carbonated BOF, the carbonated BOF became more chemically stability and neutralization.

(a)
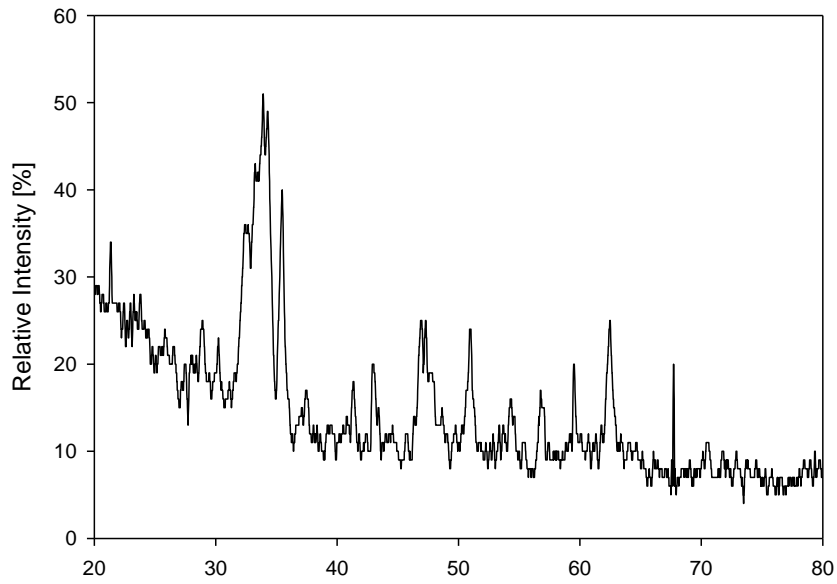


(b)
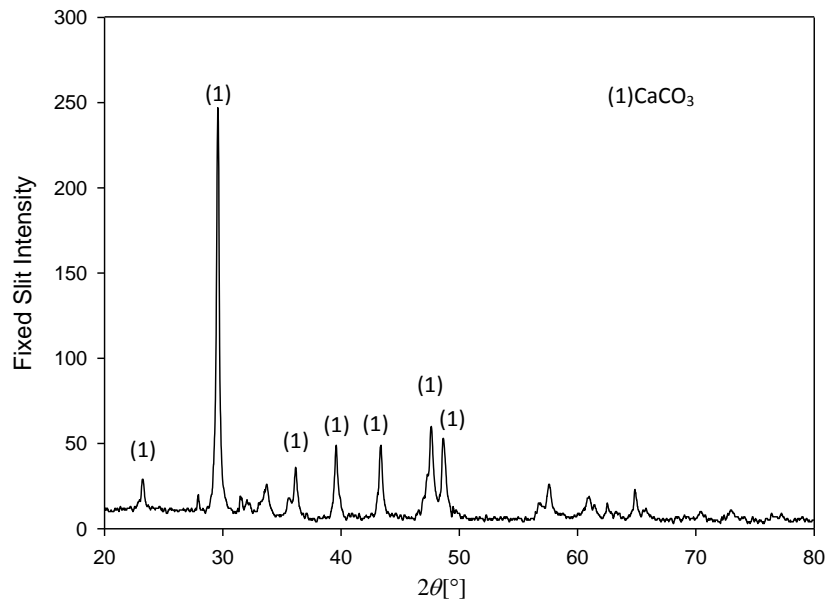


Figure 4-16 XRD spectra of basic oxygen-furnace slag with peak identifications (a) fresh slag (b) carbonated product.

**4-3 Kinetic Modeling**

**4-3-1 Kinetic Modeling of Aqueous Carbonation**

**(a) BOD of Thomas method**

In this study, the experimental data in Figure 4-17 was utilized to fit the Thomas method in spite of the L/S ratio and $CO_2$ flow rate. Figure 4-18 reveals a relating high $R^2$ values ranged from 0.90 to 0.96. The trend of the carbonation conversion was similar to the BOD reaction curve of which the reaction rate decreased as the reaction time elapsed as suggested by Thomas method. The BOD reaction curve utilized in the carbonation model could be expressed as follows:

$$y = L_0\left(1 - e^{(-kt)}\right)$$

Where $t$ is reaction time, $y$ is the conversion, $L_0$ is prediction of ultimate equilibrium conversion and $k$ is the rate constant.

The values of k are estimated by experimental data in the range from 0.056 to 0.0718 and we can predict values of k from the reciprocal of liquid to solid ratio and its $R^2$ value is 0.9671 as shown in Figure 4-19.

(a)
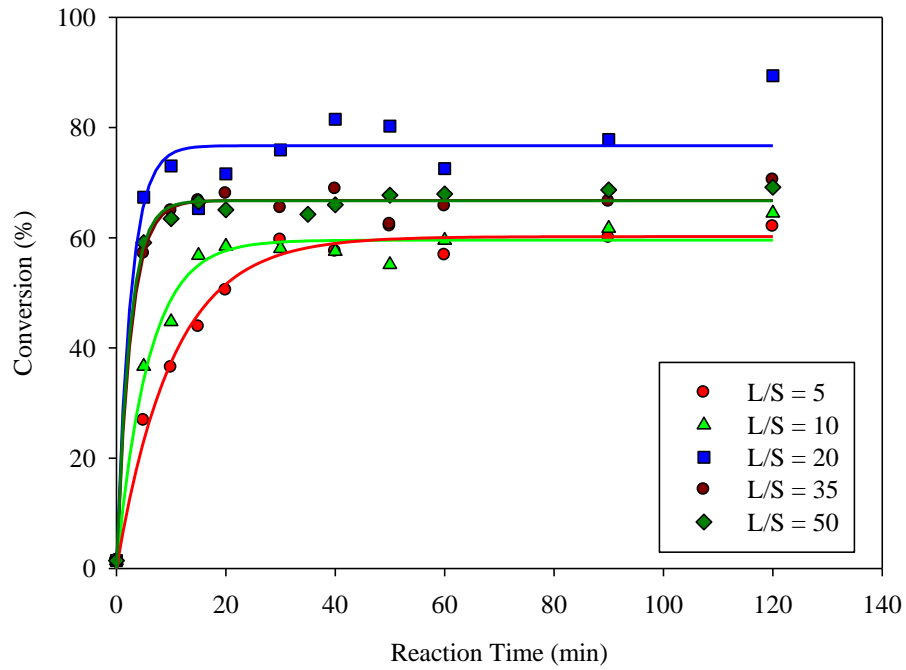


(b)
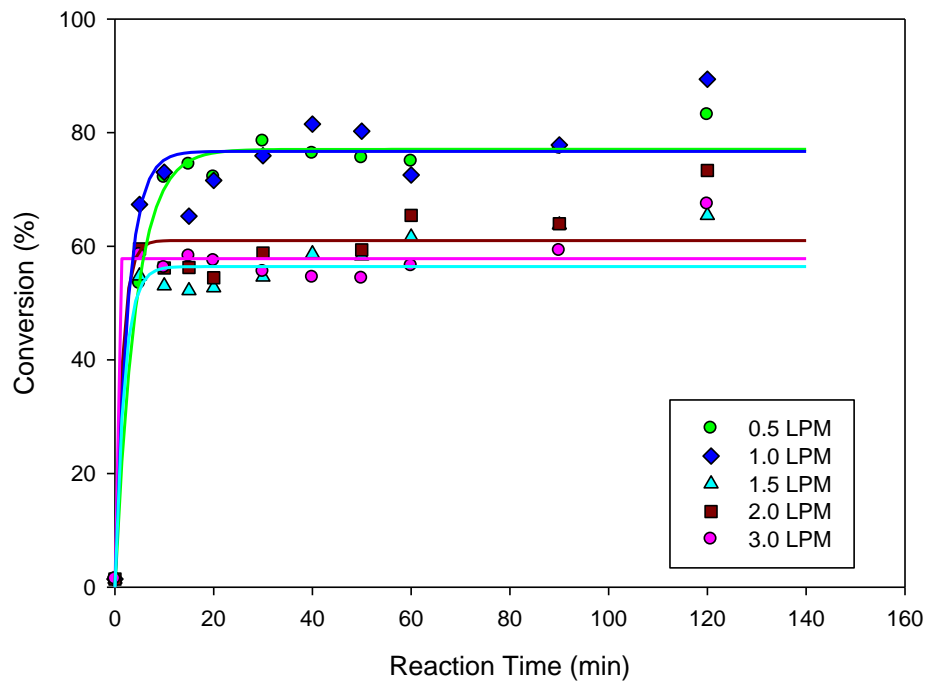


Figure 4-17. Comparison between experimental results and model simulations for the carbonation (a) L/S ratio (b) $CO_2$ flow rate
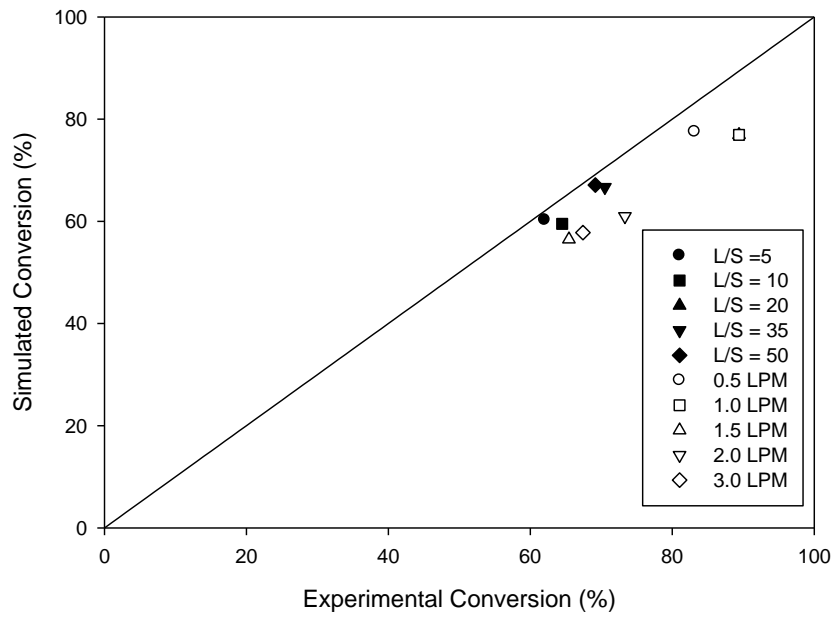
Figure 4-18. Comparison of simulated and experimental conversion value for carbonation
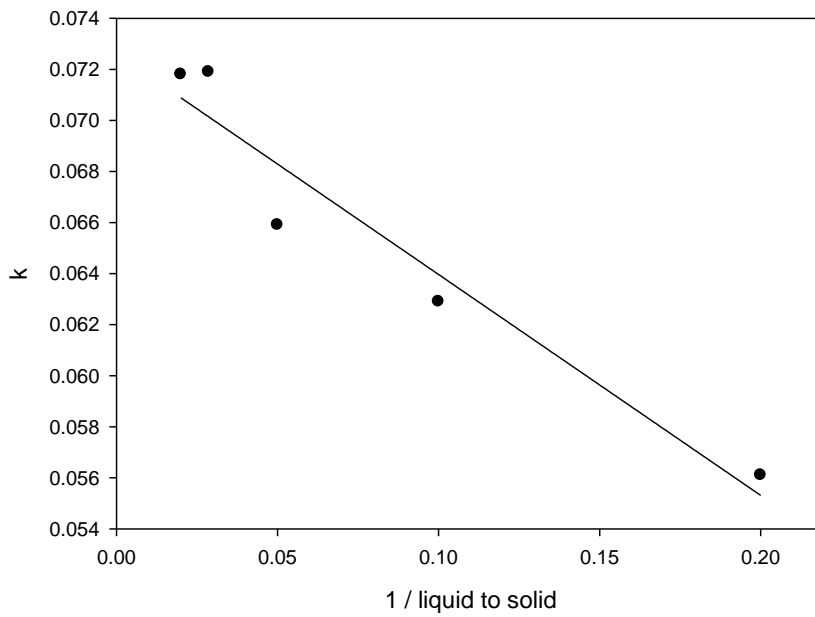


Fig. 4-19 Variation of k with liquid to solid (L/S) for the carbonation conversion of the BOF slag (carbonation conditions: pressure = 14.7 psig $CO_2$; particle size <44μm; $CO_2$ flow rate = 1.0 L/min; reaction volume = 350mL; water source = cold-rolling wastewater).

Table 4-3 Values of parameter for BOD of Thomas Method

| | k | $L_0$ | $R^2$ |
|---|---|---|---|
| Cold-rolling wastewater | 0.066 | 110.2 | 0.91 |
| Tap water | 0.067 | 101.9 | 0.90 |
| Effluent | 0.069 | 93.4 | 0.94 |
| L/S = 5 | 0.057 | 76.5 | 0.96 |
| L/S = 10 | 0.063 | 81.6 | 0.93 |
| L/S = 20 | 0.066 | 110.2 | 0.91 |
| L/S = 35 | 0.073 | 94.2 | 0.92 |
| L/S = 50 | 0.072 | 95.3 | 0.92 |
| 0.5 LPM | 0.068 | 108.3 | 0.93 |
| 1.0 LPM | 0.066 | 110.2 | 0.91 |
| 1.5 LPM | 0.066 | 83.9 | 0.91 |
| 2.0 LPM | 0.066 | 93.3 | 0.90 |
| 3.0 LPM | 0.069 | 83.7 | 0.89 |
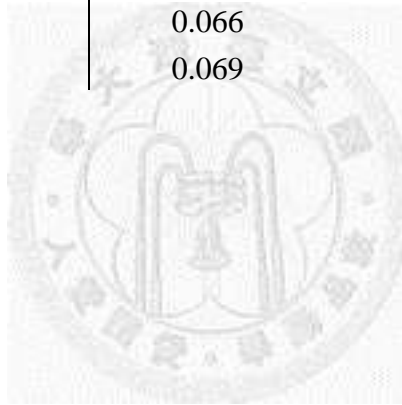
## (b) Surface Coverage Reaction

The kinetic modeling of the carbonation reaction was conducted by only considering surface reaction which only takes place on the surface of the feedstocks (Shih et al., 1999). The reaction rate of per unit surface area can be expressed as

$$r_s = k_s \Phi \qquad (2)$$

where $k_s$ is the rate constant [min$^{-1}$], $\Phi$ is the fraction surface area which is not covered by product.

The rate of conversion $\delta$Ca can be expressed as

$$\frac{d\delta_{Ca}}{dt} = S_g M \cdot r_s = S_g M \cdot k_s \Phi \qquad (3)$$

where $S_g$ [m$^2$/g] is the initial specific surface area of the solid waste, and $M$ [g/mole] is the molecular weight. $\Phi$ [mole/m$^2$] is a function of time and the manner in which the product is deposited on the surface. Hence, $\Phi$ changes with reaction time depended on the reaction rate, and it can be expressed by the following equation:

$$-\frac{d\Phi}{dt} = k_p \cdot r_s = k_p \cdot k_s \Phi \qquad (4)$$

where $k_p$ [1/hr], a function of temperature, concentrations of reacting species, and relative humidity, is a proportional constant reflecting $\Phi$ [mole/m$^2$].

By integrating equation (4), $\Phi$ can be expressed in a function of time shown as equation (5)

$$\Phi = \exp(-k_1 k_2 t) \qquad (5)$$

where $k_1 = k_s S_g M$, and $k_2 = k_p /( S_g M )$.

By substituting equation (5) into equation (3), the integration of equation (3) can obtain the relationship between conversion and reaction time.

$$\delta_{Ca} = [1 - \exp(-k_1 k_2 t)]/ k_2 \qquad (6)$$

Table 4-3 shows the values of ks, kp, k1, and k2 at different water sources, L/S and

flow rate which were determined by non-linear regression which higher correlation coefficient (0.92 to 0.99) based on the experimental data. The results showed that the flow rate of 3L/min had the fastest reaction rate (ks). The conversions of 3 L/min experiment at 5 min and 120 min were 58.5 and 67.4, respectively. It was soon approached the end of conversion at the beginning so that the ks has the largest value. The slowest reaction rate is at L/S of 5. The conversion increased slowly toward the end of the reaction time (26.9 % at the beginning 5 min to 62.0 % at the end) which resulted the smallest value. The slurry couldn't mix well in the reactor at low L/S ratio resulting in poor $Ca^{2+}$ solid-liquid mass transfer rates. Although the conversion was much improved with conversions of 89% for L/S of 20, the reaction rate wasn't the fastest one. Compared with Chang et al., the reaction rate was much higher than this study due to its higher temperature and pressure.

For different water, cold-rolling wastewater had the highest pH resulting in a higher dissolve $CO_2$ into the water consequently, the cold-rolling wastewater exhibited the fastest reaction at the beginning of experiment due to its higher ks in comparison of other feeding water, i.e. tap water and effluent.

The highest kp was observed at the 1.5 LPM flow rate. The reason was likely due to a faster product deposition rate on the surface of the slag. When the product was adhered on the surface of the BOF, the pH value would be decreased. The dominant species is carbon dioxide under acidic condition (pH < 6. 3) and the activity of carbonate ions was not sufficient to react with calcium ions. It was resulting in lower conversion. The lower conversion would result in larger kp.

The comparison between experimental conversion and model predicted conversion between different water sources, L/S ratio and flow rate were shown in Figures 4-20 to 4-22. According to the surface coverage model, the conversion would reach an

equilibrium state at the end of the reaction.   The conversion of the experimental results indicated that most of the experiments had a little increase of conversion at the end of reaction time.   The surfactant would be attached on the surface of the BOF and it may affect the density of the carbonation product.   The product which reacted in the cold-rolling wastewater would be looser than in the tap water because the surfactant would inhibit the product attached on the surface of the BOF.   The loose carbonation product could be dissolved out the calcium ion continuously.   The conversion was slightly increased at the end of reaction.

Figures 4-23 to 4-25 show the comparison of simulated and experimental conversion values for different water sources, L/S and flow rate which indicated that the standard of error (%) for different water sources, L/S and flow rate were about 7%, 3.9 % and 5.4 %, respectively, shown in Table 4-4.
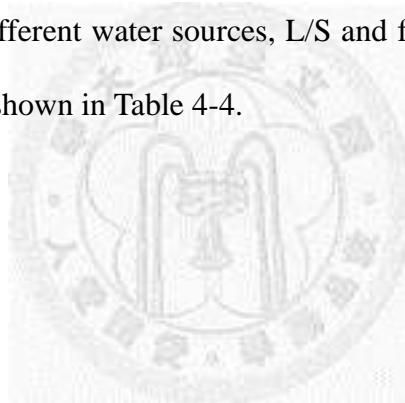
Table 4-4 Values of parameter for surface coverage model

| | $k_s$ (min$^{-1}$) | $k_p$ | $k_1$ (m$^2$/min/mole) | $k_2$ (mole/m$^2$) | $R^2$ | Conversion (%) |
|---|---|---|---|---|---|---|
| Cold-rolling wastewater | 0.11 | 3.62 | 30.27 | 0.0130 | 0.93 | 89.4 |
| Tap water | 0.07 | 3.94 | 20.82 | 0.0142 | 0.95 | 80.0 |
| Effluent | 0.04 | 3.67 | 12.30 | 0.0132 | 0.98 | 77.6 |
| L/S = 5 | 0.02 | 4.62 | 5.85 | 0.0166 | 0.99 | 62.0 |
| L/S = 10 | 0.04 | 4.67 | 10.22 | 0.0168 | 0.97 | 64.5 |
| L/S = 20 | 0.10 | 3.62 | 30.27 | 0.0130 | 0.93 | 89.4 |
| L/S = 35 | 0.08 | 4.62 | 25.73 | 0.0150 | 0.99 | 70.5 |
| L/S = 50 | 0.10 | 4.17 | 28.03 | 0.0149 | 0.99 | 69.2 |
| 0.5 LPM | 0.07 | 3.61 | 18.61 | 0.0129 | 0.99 | 83.1 |
| 1.0 LPM | 0.11 | 3.62 | 30.27 | 0.0130 | 0.93 | 89.4 |
| 1.5 LPM | 0.11 | 4.93 | 30.02 | 0.0177 | 0.93 | 65.4 |
| 2.0 LPM | 0.16 | 4.56 | 43.33 | 0.0164 | 0.92 | 73.3 |
| 3.0 LPM | 1.45 | 4.81 | 404.04 | 0.0173 | 0.96 | 67.4 |
| Chang et al., 2011 (BHC) | 0.45 | 0.12 | 3.28 | 0.0167 | - | 82.0 |

Table 4-5 The standard of error of the experiment

| Parameter | Average standard of error (%) |
|---|---|
| Cold-rolling wastewater | 0.062 |
| Tap water | 0.053 |
| Effluent | 0.094 |
| L/S = 5 | 0.043 |
| L/S = 10 | 0.045 |
| L/S = 20 | 0.062 |
| L/S = 35 | 0.022 |
| L/S = 50 | 0.022 |
| 0.5 LPM | 0.026 |
| 1.0 LPM | 0.062 |
| 1.5 LPM | 0.069 |
| 2.0 LPM | 0.071 |
| 3.0 LPM | 0.041 |
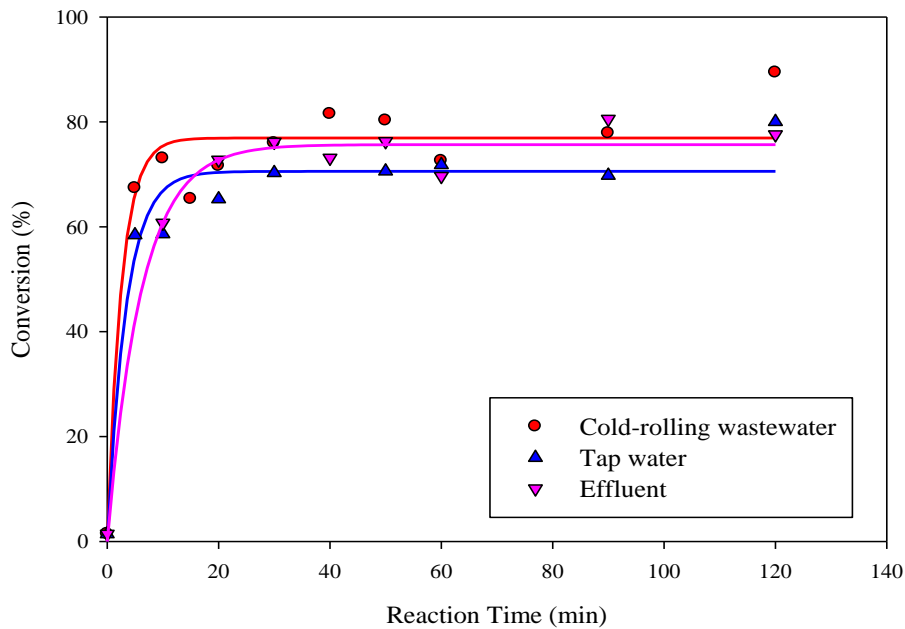


Figure 4-20. Comparison between experimental results and model simulations for the carbonation of the selected three different water source (Carbonation conditions: pressure = 14.7 psig $CO_2$; temperature = 25 ℃; particle size < 44 μm; L/S ratio = 20; $CO_2$ flow rate = 1.0 LPM; reaction volume = 350mL).
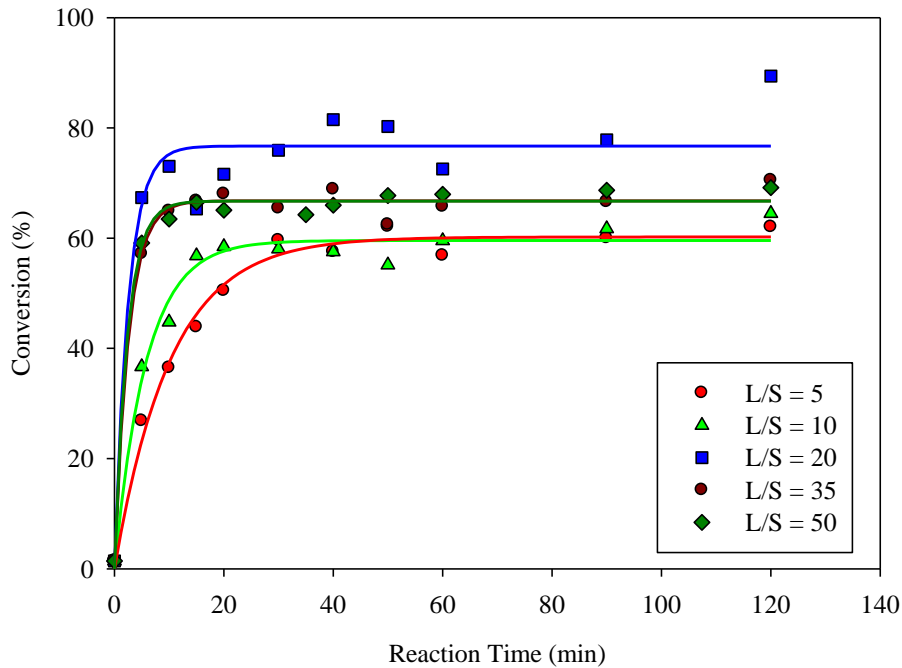
Figure 4-21. Comparison between experimental results and model simulations for the carbonation of different liquid to solid ratio (Carbonation conditions: pressure = 14.7 psig $CO_2$; temperature = 25 ℃; particle size < 44 μm; $CO_2$ flow rate = 1.0 LPM; reaction volume = 350mL; water source = cold-rolling wastewater).
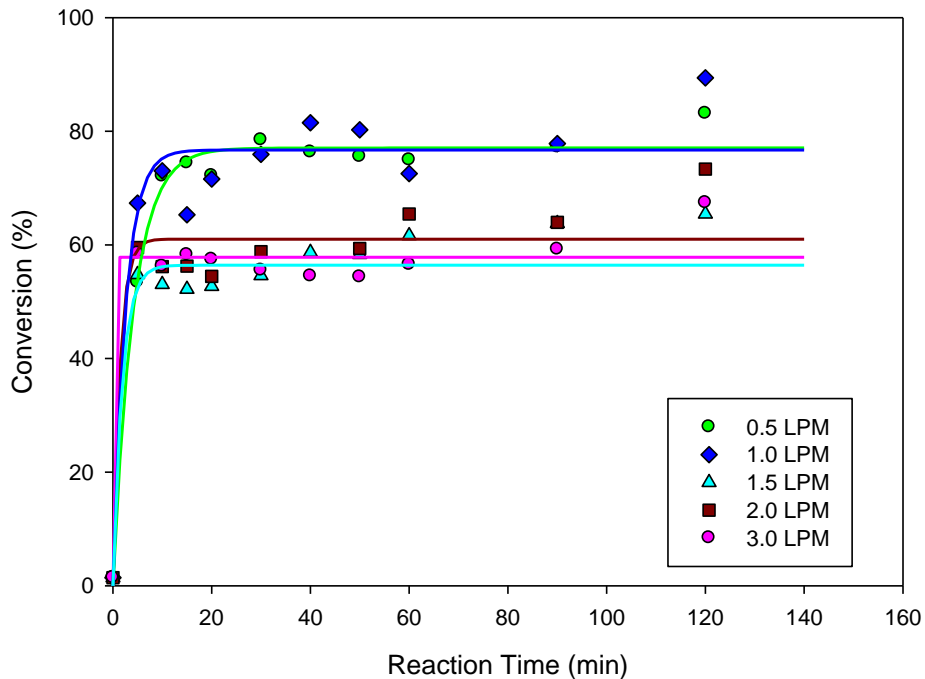


Figure 4-22. Comparison between experimental results and model simulations for the carbonation of different $CO_2$ flow rate (Carbonation conditions: pressure = 14.7 psig $CO_2$; temperature = 25 ℃; particle size < 44 μm; L/S = 20; reaction volume = 350mL; water source = cold-rolling wastewater).
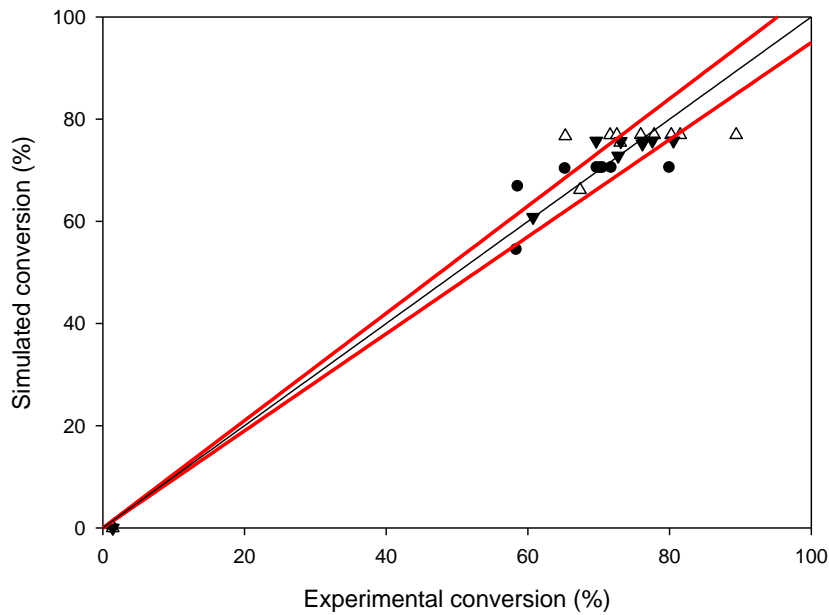
Figure 4-23. Comparison of simulated and experimental conversion value for carbonation of the selected three different water source (Carbonation conditions: pressure = 14.7 psig $CO_2$; temperature = 25 ℃; particle size < 44 μm; L/S ratio = 20; $CO_2$ flow rate = 1.0 LPM; reaction volume = 350mL).
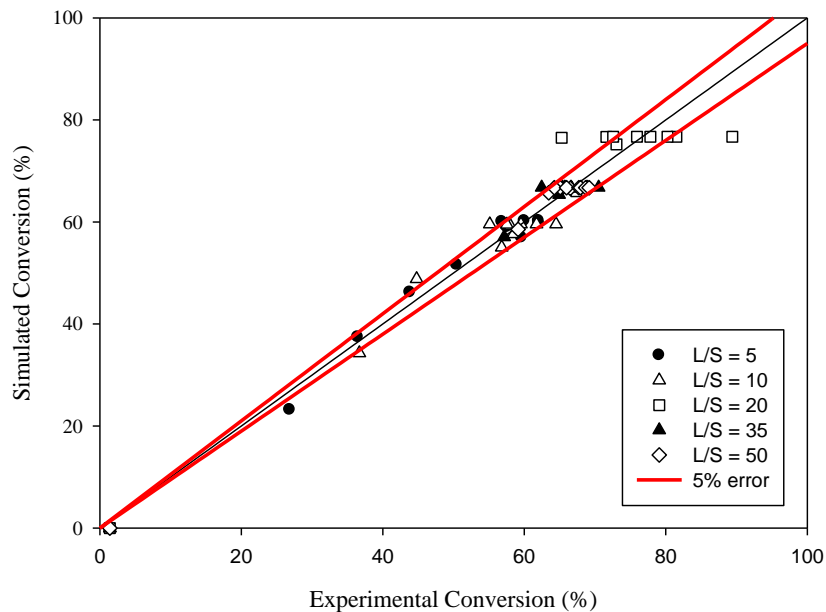


Figure 4-24. Comparison of simulated and experimental conversion value for carbonation of different liquid to solid ratio (Carbonation conditions: pressure = 14.7 psig $CO_2$; temperature = 25 ℃; particle size < 44 μm; $CO_2$ flow rate = 1.0 LPM; reaction volume = 350mL; water source = cold-rolling wastewater).
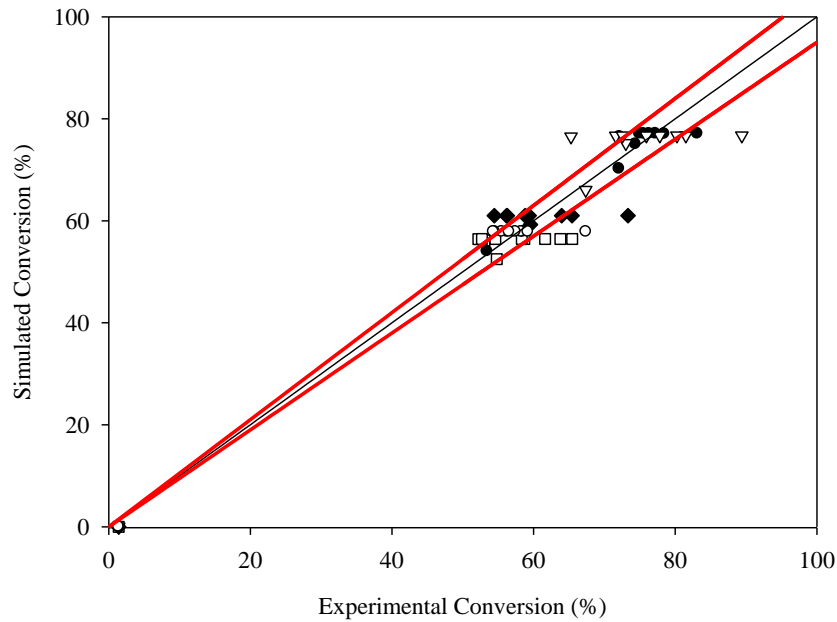
Figure 4-25. Comparison of simulated and experimental conversion value for carbonation of different $CO_2$ flow rate (Carbonation conditions: pressure = 14.7 psig $CO_2$; temperature = 25 ℃; particle size < 44 μm; L/S = 20; reaction volume = 350mL; water source = cold-rolling wastewater).

## 4-3-2 Determination of the optimum operation condition

The factors affected the conversion of carbonation mentioned in the previous section indicate that the conversion was decreased as the $CO_2$ flow rate increased, the liquid to solid decreased and the reaction volume increased. The highest conversion (89%) was achieved at the $CO_2$ flow rate range from 0.5 LPM to 1.0 LPM. as shown in Figure 4-26. It was observed that L/S of 20, $CO_2$ flow rate of 1 LPM and the reaction volume of 350 mL would get the optimum operation condition.
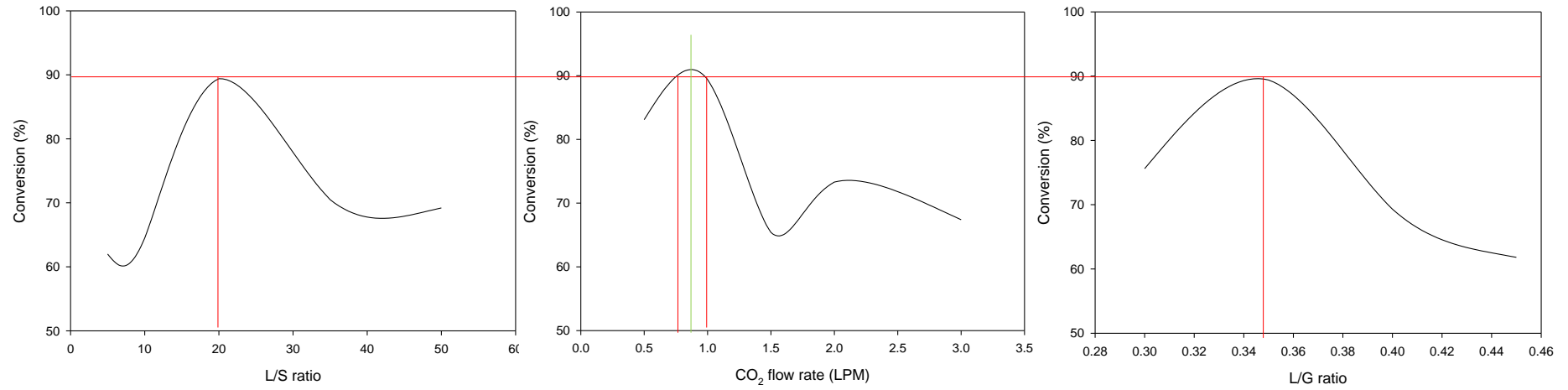
Figure 4-26 The optimum operating condition of basic oxygen furnace slag in cold-rolling wastewater

4-36

## 4-4 Technical assessment

### 4-4-1 Environmental Aspect

The aqueous carbonation is effective in carbon sequestration but this technology may cause other environment effects (IEA GHG, 2006; Khoo and Tan, 2006; Odeh and Cockerill, 2008). This study was focused on GHG reduction and it should assure that there is no extra carbon dioxide produced during the carbonation process. Life cycle assessment was used to track the carbon footprint of every process. The following three tasks were accomplished for conducting the LCA.

1. Comparison of LCA results from other studies and this study

2. Using local electricity data provided by the thermal power plants in Taiwan.

3. Calculating environmental impacts with LCA software – Umberto5. 5.

The material and energy flow network are shown in Figure 4-27. The pretreatment process and aqueous carbonation process were analyzed. The energy consumption and the necessary material for the operation in the boundary were focused and the carbonation product and the pollutant emissions were considered. The function unit is selected by 1 kg $CO_2$ captured, and environmental burdens can be calculated at the same assumptions. The $CO_2$ emission of electricity is 0.637 kg $CO_2$/kWh in Taiwan and the data of fuel consumption and air pollutant emission is given by Tai-power thermal power plants.
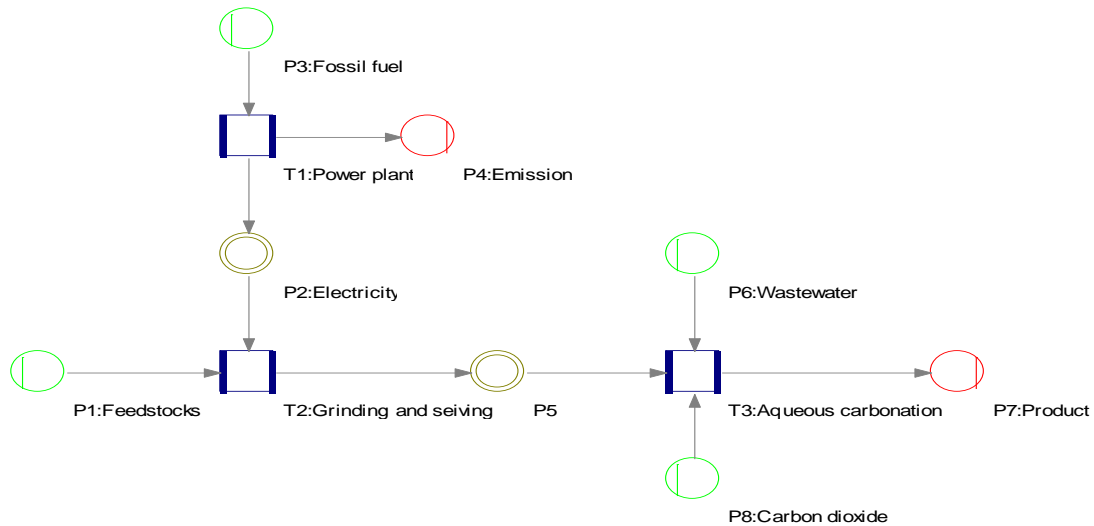
Figure 4-27 Material and energy flow network of laboratory mineral sequestration

**4-4-1-1 $CO_2$ Budget Estimation**

The equivalent $CO_2$ emission during feedstock production was investigated by Lin (2010).   The treatment and recovery of 100,000 tons of the useful BOF requires the following resource including: electricity of 40500 kWh, diesel oil 6700 liters.   The amount of the useful BOF after the recovery process is 94000 tons.   The carbon dioxide emission of diesel is 2.61 kg $CO_2$/L.    The $CO_2$ emission of electricity is 0.637 kg $CO_2$/kWh in Taiwan.    The carbon footprint of the BOF is 0.46 kg $CO_2$/T.

The pre-treatment of the BOF include grinding, sieving and pre-heating.    The energy consumption and $CO_2$ emission of pre-treatment are shown in Table 4-5.    The sum of $CO_2$ emission due to pre-treatment of aqueous carbonation was 3.87439 kg / kg $CO_2$ sequestration.

Table 4-6 $CO_2$ emission of each pre-treatment

|  | (a) Power (kW) | (b) Using time (hr) | (c) Electricity consumption (kW-hr) | (d) CO2 emission (kg) = 0.637 × (c) |
|---|---|---|---|---|
| Grinding | 0.75 | 0.003 | 0.002 | 0.00143 |
| Sieving | 0.18 | 1.000 | 0.180 | 0.11466 |
| Pre-heating | 5.90 | 1.000 | 5.900 | 3.75830 |

**4-4-1-2 Data Collection**

Data collection depends on the system boundary including the associated pollution emission from carbonation process and electricity consumption.   There are three steps of collecting unit processes data:

1.  Collect quantitative data of all relevant inputs and outputs for each of them.

2.  Using data collection forms together with specific flowchart for data documentation.

3.  When collecting specific data, make sure they represent the full operation cycle of the process.

The data for the electricity consumption were calculated from emissions of electricity generated in Taiwan (Tai-power Company).   Table 4-6 showed fuel consumption and air pollutant emission of Tai-power thermal power plants, and the electricity generation of thermal power plants account for over 70% of energy supply system in Taiwan.   Owing to those power plants also are the mainly GHG emission sources; therefore, it is assuming that major electricity were generated by them.

Table 4-7 Fuel consumption and air pollutant emission of Tai-power thermal power plants

|  | Item | Unit | Value |
|---|---|---|---|
| Fuel consumption | Bituminous Coal | Kg/Gwh | $1.15*10^5$ |
|  | Sub-bituminous Coal | Kg/Gwh | $2.84*10^4$ |
|  | Diesel Oil | L/Gwh | $6.50*10^2$ |
|  | Fuel Oil | L/Gwh | $1.42*10^4$ |
|  | LNG | $M^3$/Gwh | $2.94*10^4$ |
| Air pollutant emission | SOx | Kg/Gwh | 493 |
|  | NOx | Kg/Gwh | 446 |
|  | PM10 | Kg/Gwh | 31 |

(Ref: Tai-power Company, 2007)

This study was considered five different scenarios. The first part was three scenarios in this study and the system boundary was shown in Figure 4-28. The scenarios in this study are all slurry reactor, cold-rolling wastewater, ambient temperature, atmosphere pressure and 120 min reaction time. Three scenarios considered at the following condition: (1) System boundary without pre-heating; (2) System boundary; (3) System boundary with consideration to the foot print of slags.
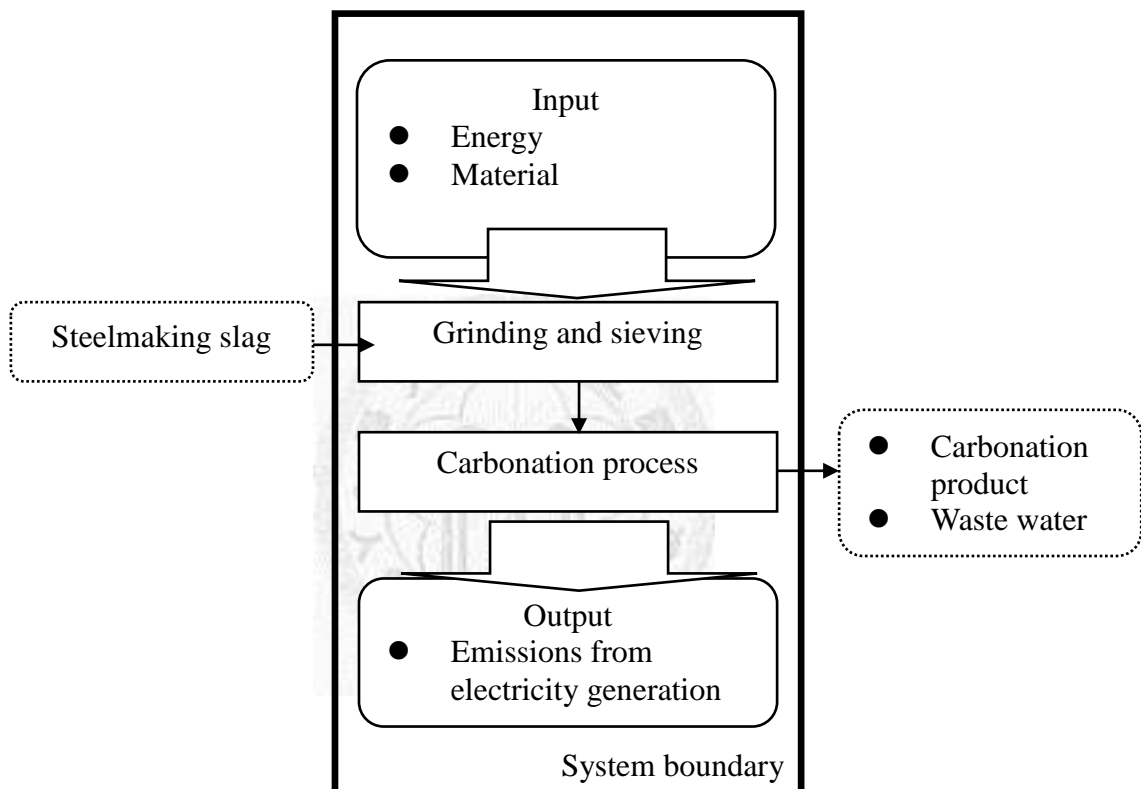


Figure 4-28 System boundary of aqueous carbonation experiment in this study

The second part was the comparison between other literatures. The system boundary was like above and the each scenario operates in performance conditions were expressed as Table 4-7. Scenario 1-3 is aqueous carbonation (direct carbonation) by slurry reactor with cold-rolling wastewater; Scenario 4 is aqueous carbonation (direct carbonation) by slurry reactor with tap water; and Scenario 5 is aqueous carbonation (direct carbonation) by batch reactor.

The data of material usage and electricity consumption is described as Table 4-7, including their parameter, unit and quantity.   All the technique data of emission can be estimated by direct measurement, the calculation of mass balance, use of emission factors, process models or inverse inference from observed ambient concentrations.

Table 4-8 Main operation conditions of mineral sequestration

| Parameter | Unit | Scenario 1 | Scenario 2 | Scenario 3 | Scenario 4 | Scenario 5 |
|---|---|---|---|---|---|---|
| Reactor type | | Slurry | Slurry | Slurry | Slurry | Batch |
| Water source | | Cold-rolling wastewater | Cold-rolling wastewater | Cold-rolling wastewater | Tap water | DI water |
| Feedstock size | μm | < 44 | < 44 | < 44 | < 44 | < 44 |
| Operation time | min | 120 | 120 | 120 | 60 | 60 |
| Operation temperature | ℃ | 25 | 25 | 25 | 60 | 160 |
| Operation pressure | kPa | 101.3 | 101.3 | 101.3 | 101.3 | 4823.8 |
| Conversion | % | 89 – 20* | 89 | 89 | 72 | 58 |

*:The fresh BOF without pre-heating contain about 20% $CaCO_3$, but the end of conversion would be the same like pre-heating.

Table 4-9 Life cycle inventory results for key parameters of laboratory-scale mineral sequestration

| Parameter | Unit | Scenario 1 | Scenario 2 | Scenario 3 | Scenario 4 | Scenario 5 |
|---|---|---|---|---|---|---|
| *Materials* | | | | | | |
| Steelmaking slag | kg | 4.48 | 3.48 | 3.48 | 3.45 | 4.16 |
| Water | kg | 89.6 | 69.5 | 69.5 | 34.5 | 41.6 |
| *Energy* | | | | | | |
| Electricity | kJ | 19683 | 21896 | 21896 | 7235 | 33606 |
| *Wastes and by-product* | | | | | | |
| Waste water | kg | 89.6 | 69.5 | 69.5 | 34.5 | 41.6 |
| Carbonation products | kg | 5.48 | 4.48 | 4.48 | 4.45 | 5.16 |

*Note.   Scenario 4 results was calculated from reference (Chang et al.   , 2011) and scenario 5 was calculated from reference (Chu et al.   , 2007)

**4-4-1-3 Environmental Impact Assessment**

Impact assessment is implemented out in order to identify the environment impacts based on the LCI results.   In theory, impact assessment method converts the pollution results into a set of common impact measures.   To emphasize the effects on different perspectives, choosing different valuation system is necessary.   The impact categories considered in this study are summarized in Table 4-9.   The potential environment impacts of these interventions were quantified by Umberto 5.5 with CML database (The Netherlands, 1997).   These environmental interventions and their potential environmental impacts will be discussed as following in detail.

Table 4-10 Valuation system application on different impact category in this study.

| Impact category | Category indicator | Valuation system | Emission |
|---|---|---|---|
| Global warming | $CO_2$-eq | CML | $CO_2$, $CH_4$, $SF_6$ |
| Acidification | $SO_2$-eq | CML | $SO_x$, $NO_x$, HCl, $NH_3$ |
| Eutrophication | $PO_4$-eq | CML | P, BOD, COD |
| Photo-oxidant formation | Ethen-eq | CML | $NO_x$, NMVOC |
| Cum. Energy demand | MJ | Ecoinvent | Coal, Oil, NG |

**(a) Global warming**

The global warming impact caused by $CO_2$ emission results from this study were assessed by valuation system - IPCC.   Even the laboratory work of this study does not produce $CO_2$ directly but $CO_2$ emission still would be generated from producing energy and material used in this study indirectly.   The global warming potential over a time period of 100 years (GWP100) was used for the analysis.

Figure 4-29 shows that scenario 5 generates the most $CO_2$ among five cases because of the highest operation temperature (160 ℃) and pressure (4823.8 kPa) .   For

scenario 4 and scenario 5, heating to a required temperature in aqueous carbonation process to achieve a maximum conversion was the main contributor (over 90%) of global warming potential in system boundary.   There is pre-heating for scenario 2, 3 and 5, and they are the top 3 highest value among this experiment.   The pre-heating is a intensive energy consumption process.   Scenario 1 without pre-heating was lower value than scenario 2 in this study, although it needs more quantity of the BOF for $CO_2$ sequestration.   The carbon foot print of basic oxygen furnace (BOF) is 0.46 kg $CO_2$/T is much smaller than the energy consumption.   Without pre-heating is a suitable way for $CO_2$ sequestration.
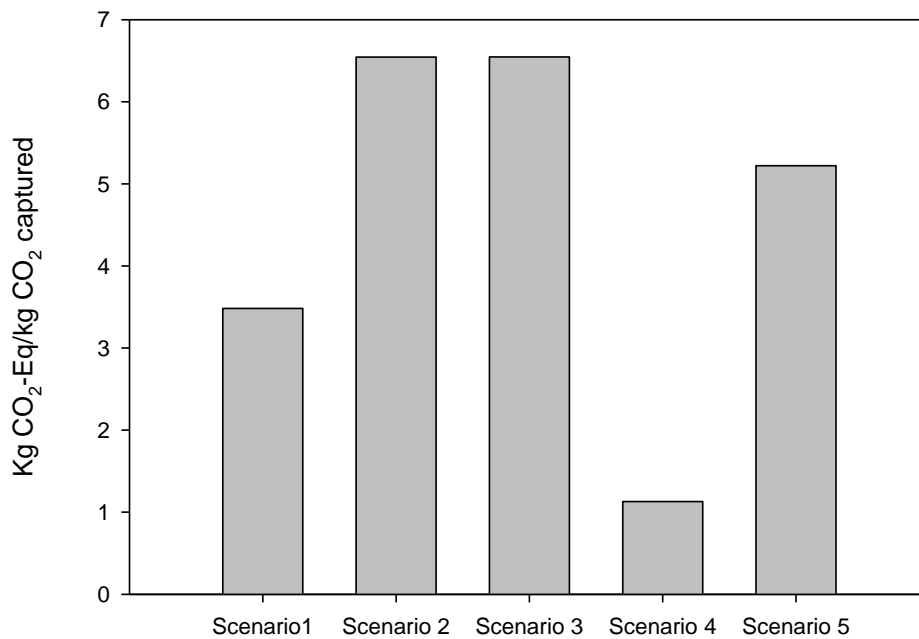


Figure 4-29 Impact results on global warming per kg $CO_2$ captured in second part

**(b) Acidification**

Acidification is due to the emission of acid-forming substances and occurs in terrestrial and aquatic system.   The results (Figure 4-30) of acidification impact category were calculated by valuation system – CML, and produced $SO_2$ equivalent per

unit weight of $CO_2$ capture.   The results are similar to the results of global warming because the electricity consumption is the main contributor.
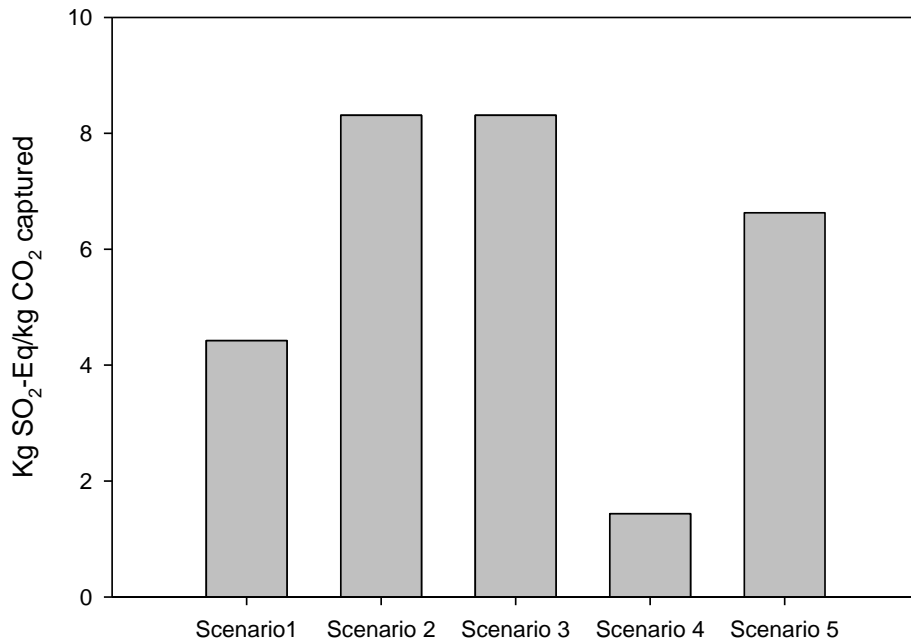


Figure 4-30 Impact results on acidification per kg $CO_2$ captured

**(c) Eutrophication**

Eutrophication means excessive supply of nutrients into surface waters and soils resulting in excessive algae growth.   The results for eutrophication impact category were calculated by the valuation system – CML, and produced an indicator of $PO_4$ equivalent per unit weight of $CO_2$ capture.   These results (Figure 4-31) were similar to the results of global warming because electricity consumption is the main contributor to eutrophication.   In addition, NOx and $NH_3$ emissions from electricity generation were the dominant contributors to this impact category.
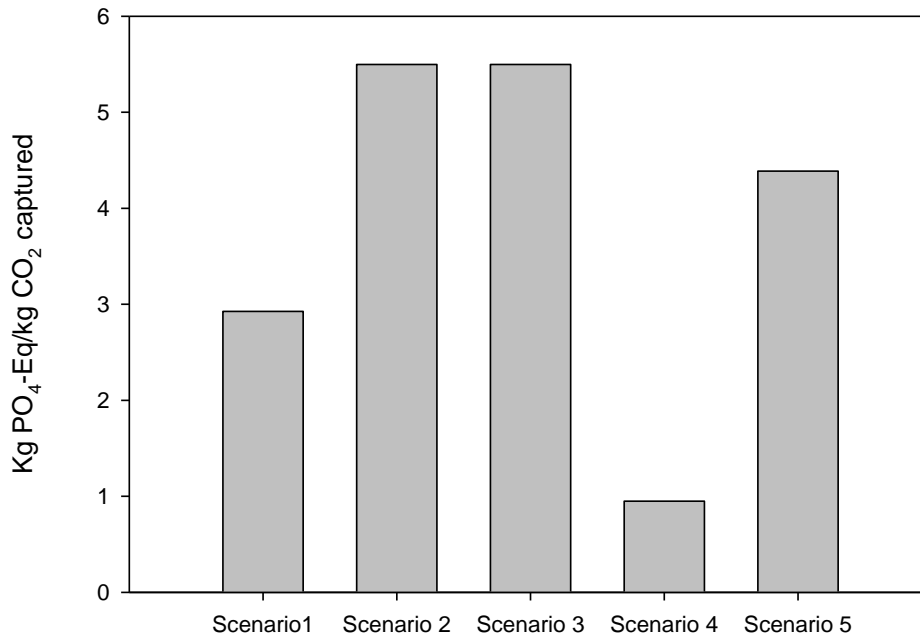
Figure 4-31 Impact results on eutrophication per kg CO$_2$ captured

**(d) Photo-oxidant formation**

The results (Figure 4-32) for photo-oxidant formation impact category were calculated by the valuation system – CML. This method modifies the relationship between VOCs and NOx, and express in ethene equivalents. Figure 4-21 shows that scenario 4 is still the optimal technology among the three scenarios, because aqueous carbonation process could react at low temperature without chemical usage.
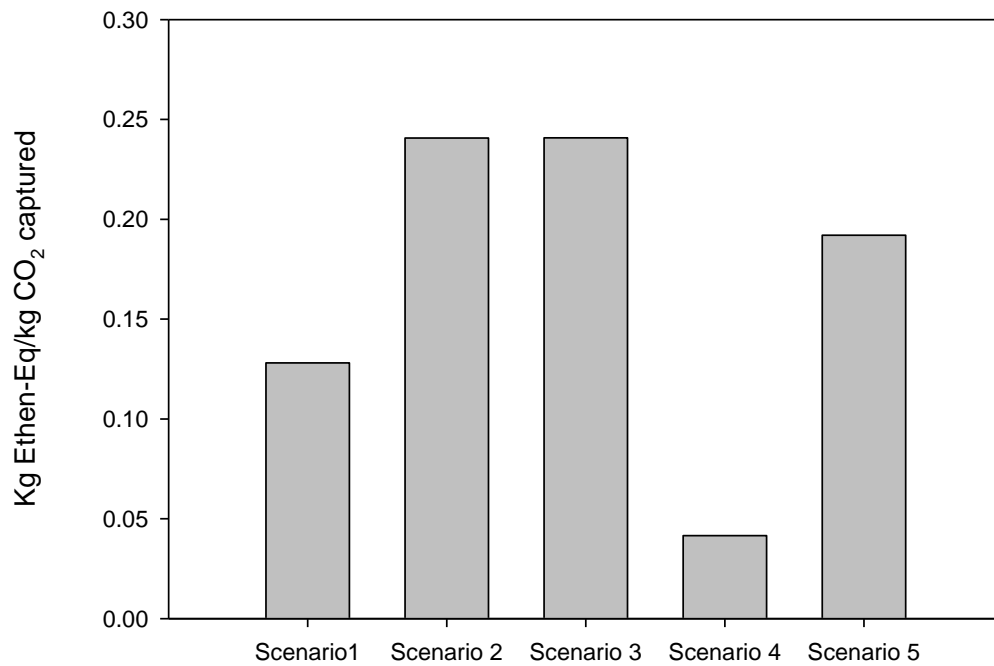
Figure 4-32 Impact results on photo-oxidant formation per kg $CO_2$ captured

**(e) Human toxicity**

The results (Figure 4-33) for human toxicity category were calculated by the valuation system – CML, and produced in 1,4 - DCB equivalent for $CO_2$ capture technology. The human toxicity potential over a time period of 100 years (GWP100) was used for this analysis.
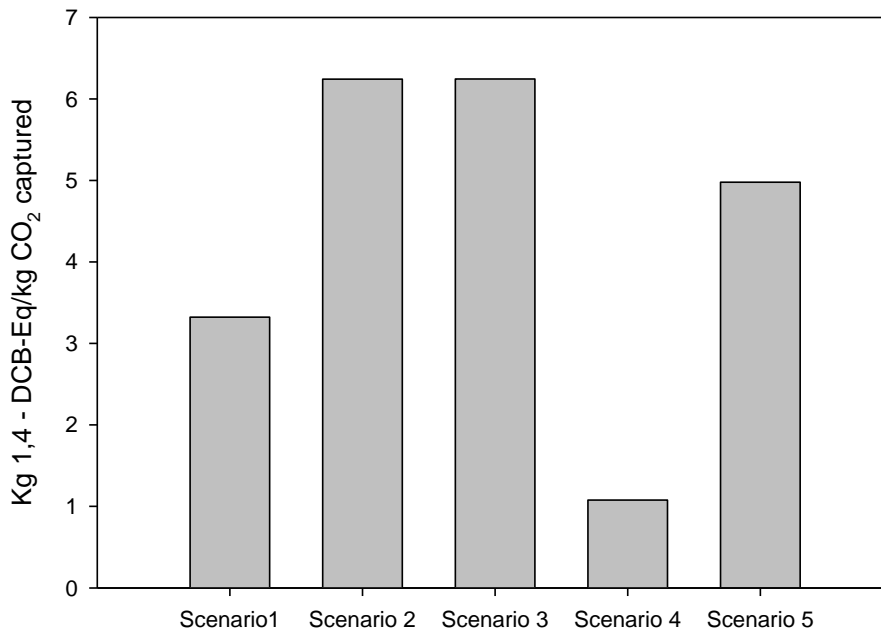
Figure 4-33 Impact results on human toxicity formation per kg $CO_2$ captured

**4-4-2 Engineering Aspect**

Table 4-10 shows the comparison of carbonation conversion by slags between other studies and this study.    There were several different slags and water sources used in various previous studies in the literature.    In the literatures there were many different ways to raise the conversion such as the increase of temperature and pressure or the dose of chemicals.    Nyambura et al.    achieved a higher conversion (86.4%) by applying a higher pressure (580 psig) during the conversion process.    .

This study was operated under ambient temperature and atmosphere pressure. There would be no extra energy consumption in this experiment.    If the carbon dioxide generated during the capturing process is more than it captured, the experiment would be meaningless.    The conversion efficiency by using wastewater as a feedstock was not much higher than that of the tap water.    Using wastewater for feedstock was cost effective because it was near the location of $CO_2$ emission and by-product of

4-49

steelmaking. Using wastewater instead of tap water is a better alternative to sequestrate $CO_2$. Comparing other literatures, this study achieved the highest conversion (89.18%) without extra consumptions of energy and resources.

There are some extra advantages for aqueous carbonation in this study such as $CO_2$ storage, efficiency and $CO_2$ emission reduction.

**(a) $CO_2$ storage**

An alternative to sequester $CO_2$ in mineral form as carbonate can reduce net $CO_2$ emissions to the atmosphere by the chemical processes, which can also produce the valuable carbon containing products. Comparison of different $CO_2$ sequestration methods in storage capacity and storage time, aqueous carbonation of mineral sequestration methods is excellent without the leakage problem (Lackner, 2003). In addition, carbonation products can be transported to the deposit site without $CO_2$ pressurized process.

**(b) Efficiency**

This technology is one of the pipe end treatments which aim at reducing $CO_2$ emission. The operation condition of aqueous carbonation is suitable on IGCC and steelmaking industrials. If the carbonation process is commercialized, this process can be operated at moderate temperature without adding any chemical solvent.

**(c) $CO_2$ emission reduction**

In order to enhance the feasibility of actual operation, $CO_2$ removal is a performance indicator. Unfortunately, even if changing reactor type can increase the carbonation conversion, $CO_2$ emission reduction potential is still inferior to benchmark (85% $CO_2$ removal). According to the calculation of optimal condition in this study, this technology sequesters only 75% $CO_2$ emissions from the source. In conclusion, $CO_2$ emission reduction potential is a critical factor on engineering aspect.

Table 4-11 Compare of experimental results in literature and results in this study

| Feedstock | Water | Reactor | Temperature [℃] | Pressure [psig] | Conversion [%] | Reference |
|---|---|---|---|---|---|---|
| Ground steel slag | ND water* | autoclave reactor | 100 | 275.6 | 74.0 | Huijgen et al. |
| Blended hydraulic-cement slag | DI water | autoclave reactor | 160 | 700 | 58.2 | Chang et al. |
| Basic oxygen-furnace slag | DI water | Slurry | 60 | 14.7 | 72.2 | Chang et al. |
| Blast-furnace slag | Acetic acid solution | CSTR | 30 | 14.7 | 72.5 | Eloneva et al. |
| Converter slag | HCl solution | CSTR | 40 | 1.9 | 72.8 | Kodama et al. |
| Ultrafine slag | HCl solution | autoclave reactor | 40 | 50 | 46.2 | Chang et al. |
| Fly ash | Brine | Slurry | 30 | 580 | 86.4 | Nyambura et al. |
| Basic oxygen-furnace slag | Wastewater | Slurry | 25 | 14.7 | 89.2 | This study |

*ND water: Nanopure-demineralized water

**4-4-3 Economic Aspect**

**Cost**

Costs will vary with the choice of $CO_2$ capture technology and the choice of power system or industrial process that generate the $CO_2$. Some researches revealed that a number of different measures were used to characterize $CO_2$ capture cost. In this study, because there are no power plants in system boundary, the cost of electricity (COE) can't be calculated.

In engineering economic aspect, feedstock for mineralization is the main factor affecting capture cost. Steelmaking slag is one of the solid wastes from iron and steel industries, and those industries usually need to add the chemical reagent to the waste for stabilizing and waste reclamation. Carbonation of steelmaking slag can stabilize the slag without adding chemical reagent; therefore and the reagent saving makes the slag carbonation process a feedback of this technology. In actual, those slags, which were generated from China-steel Company were needed to pay 200 NTD/ton to stabilize. The slag after stabilizing, those slags can use on road construction which sells 600 NTD/ton. The technology developed in this study requires 3.75 tons of slag to sequester 1 ton $CO_2$ with 3000 NTD per ton of $CO_2$ sequestrated.

Table 4-12 Evaluation of $CO_2$ sequestration technology in the study by 3E assessment.

| Aspect | Indicator | This study | Chang et al., 2011 |
|---|---|---|---|
| **Engineering** | $CO_2$ storage (kg-$CO_2$/kg slag) | 0.2878 | 0.2407 |
| | Efficiency | 89 % | 58 % |
| | $CO_2$ emission reduction (kg-$CO_2$ created) | 2.48 | 4.22 |
| **Economic** | Cost (NT) | 24.71 | 46.83 |
| **Environment** | Global warming (kg $CO_2$-Eq/ kg $CO_2$ captured) | 3.48 | 5.22 |
| | Photo-oxidant formation (kg Ethen-Eq/ kg $CO_2$ captured) | 0.13 | 0.19 |
| | Eutrophication (kg $PO_4$Eq/ kg $CO_2$ captured) | 2.93 | 4.39 |
| | Human toxicity (kg 1,4-DCB/ kg $CO_2$ captured) | 3.32 | 4.98 |
| | Acidification (kg $SO_2$-Eq/ kg $CO_2$ captured) | 4.43 | 6.63 |
| | Cum.Energy demand ( MJ/ kg $CO_2$ captured) | 19.7 | 33.6 |

# Chapter 5 Conclusions and Recommendations

## 5-1 Conclusions

$CO_2$ sequestration by basic oxygen slag in a slurry reactor containing effluent from a metalworking wastewater treatment plant and cold-rolling wastewater was investigated in this study.   Two types of metalworking wastewater were used in this study:.   The results indicated that basic oxygen slag in cold-rolling wastewater provided a better carbonation conversion (approximately 89.18%).   It could be explained by the evidence that higher pH values allow more carbon dioxide dissolve in the solution thereby enhancing the carbonation process. However, when the wastewater reacted with $CO_2$ without BOF, the $CaCO_3$ precipitation was not observed due to the absence of $Ca^{2+}$ ion in the wastewater.   It was noted that the surfactant on the surface of BOF slag affected the carbonation conversion.

The carbonation conversion was decreased as the $CO_2$ flow rate increased, the liquid to solid decreased and the reaction volume increased. The reaction time was fixed at 120 min.   In this study, the highest conversion was about 89% when the experiment condition was operated at 1.0 LPM, L/S of 20 and reaction volume of 350mL.

Compared with the study in the literature, this research work exhibits the highest conversion rate with lower energy and resource consumption.   The developed surface coverage model for $CO_2$ sequestration was used in this study to evaluate the carbonation conversion process.

Although many unknown ions were occurred in the cold-rolling wastewater, the conversion of carbonation was approximately held constant.   It was thus concluded that carbonation of BOF slag with metalworking wastewater in a slurry reactor is a

promising alternative for carbon sequestration.

## 5-2 Recommendation

To enhance the performance of carbonation conversion by utilization of BOF slag with metalworking water, the future research works are suggested follows:

1. Improving the sampling and analytical methods for carbon conversion

2. Operating the experiments under high temperature and low concentration of $CO_2$ to validate the carbonation conversion

3. Analyzing the water quality more thoroughly

4. Comparing the performed with HIGEE (high-gravity rotating packed bed)

# References

[1] U. S. department of Commerce National Oceanic & Atmospheric Administration, http://www.esrl.noaa.gov/gmd/ccgg/trends/

[2] Solomon S., Qin D., Manning M., Chen Z., Marquis M., Averyt, K.B., Tignor, M., Miller, H.L., Contribution of working group I to the Fourth Assessment Report of the Intergovernmental Panel on Climate Change, IPCC Fourth Assessment Report (AR4)

**[3]** Huijgen W.J.J., Witkamp, G.J., Comans, R.N.J., Mineral $CO_2$ sequestration in alkaline solid residues. Poster presented at the seventh international conference on greenhouse gas control technologies(GHCT) in Vancouver, BC, Canada, 5-9 September 2004.

[4] Lackner K.S., Wendt C.H., Butt D.P., Joyce E. L., Sharp D. H., Carbon dioxide disposal in carbonate minerals. Los Alamos National Laboratory, LA-UR-97-2094, Los Alamos, NM, USA. 1995

[5] Huijgen W.J.J., Witkamp G.J., Comans R.N.J., Mineral $CO_2$ sequestration by steel slag carbonation, Environmental Science & Technology, Vol. 39, No. 24, 2005.

[6] Lackner K. S., Carbonate chemistry for sequestering fossil carbon. Annu. Rev. Energy Environ. 2002. 27:193–232

[7] Metz B., Davidson O., de Coninck H., Loos M., Meyer L., IPCC Special report on carbon dioxide capture and storage. Prepared by Working Group of the Intergovernmental Panel on Climate Change, Cambridge University press, Cambridge, 2005.

[8] Metzner A. B., Brown L. F., Mass transfer in foam, Ind. Engng Chem. 1956 48,

2040-2045.

[9] Biswas Kumar R., 1981, Mass transfer with chemical reaction in a foam bed contactor. C&m. Engng Sci. 36, 1547-1556.

[10] Alper E., Wichtendahl B., Deckwer W.-D., Gas absorption mechanism in catalytic slurry reactor, Chemical Engineering Science Vol 35, 217-222

[11] Ostergaard K., Gas-liquid-particle operations in chemical reaction engineering, Chem. Eng. J., I, 1970, 71-133

[12] Fauth D. J., Soong Y., White C. M., Carbon sequestration utilizing industrial solid residues, Fuel Chemistry Division Preprints 2002, 47(1), 37

[13] Huijgen W.J.J., Comans R.N.J., Carbon dioxide sequestration by mineral carbonation Literature Review, Energy research Centre of the Netherlands 2003, ECN-C--03-016

[14] Emery J. J., Slag utilization in pavemant construction, Extending aggregate resources 1982, Stp 774

[15] Mahieux P.-Y., Aubert J.-E., Escadeillas G., Utilization of weathered basic oxygen furnace slag in the production of hydraulic road binders, Construction and Building Materials 23, 2009, 742–747

[16] Wang J. W., Integrated analysis of life cycle assessment with eco-efficiency – case studies of Iron and Steel Products, 2005

[17] Seifritz W., $CO_2$ disposal by means of silicates. Nature 1990, 345, 486.

[18] Lackner K. S., A guide to $CO_2$ sequestration, Science, New Series, Vol. 300, No. 5626 (Jun. 13, 2003), pp. 1677-1678

[19] Montes-Hernandez G., Pérez-López R., Renard F., Nieto J.M., Charlet L.,

Mineral sequestration of $CO_2$ by aqueous carbonation of coal combustion fly-ash. J. Hazard. Mater. 2009, vol 161, 1347-1354.

[20] Huijgen W.J.J., Comans R.N.J., Carbon dioxide sequestration by mineral carbonation Literature Review Update 2003-2004, Energy research Centre of the Netherlands 2005, ECN-C--05-022

[21] Lekakh S.N., Rawlins C.H., Robertson D.G.C., Richards V.L., Peaslee K.D., 2008. Kinetic of aqueous leaching and carbonization of steelmaking slag. Metall. Mater. Trans. B 39B, 125-134.

[22] Guinée J.B., Gorrée M., Heijungs R., Huppes G., Kleijn R., De Koning A., van Oers, L., Wegener Sleeswijk, A., Suh, S.,Udo de Haes, H.A., de Bruijn, H., van Duin, R., Huijbregts, M.A.J., 2002. Life cycle assessment. An Operational Guide to the ISO Standards. Centre of Environmental Science, Leiden University, Leiden, The Netherlands.

[23] Hertwicha E. G., Aabergb M., Singha B., Strømman A. H., Life-cycle assessment of carbon dioxide capture for enhanced oil recovery, Chinese Journal of Chemical Engineering Volume 16, Issue 3, June 2008, Pages 343-353

[24] Odeh N. A., Cockerill T. T., Life cycle GHG assessment of fossil fuel power plants with carbon capture and storage, Energy Policy 36 (2008) 367–380

[25] Viebahn P., Nitsch J., Fischedick M., Esken A., Schu wer D., Supersberger, N., Zuberbu¨ hler, U., Edenhofer, O., Comparison of carbon capture and storage with renewable energy technologies regarding structural, economic, and ecological aspects in Germany, international journal of greenhouse gas control 1 (2007) 121 – 133

[26] Koornneef1 J., Faaij A., Turkenburg W., Environmental Impact Assessment of

Carbon Capture & Storage in the Netherlands

[27] Dreybrodtj W., Laucknerl Zaihua, Svensson U., Buhmann. D., The kinetics of the reaction CO2 + Hz0 + H + + HCO, as one of the rate limiting steps for the dissolution of calcite in the system H,O-COz-CaC03, Geochimica et Cosmochimica Acta, Vol. 60, No. IS, pp. 337553381, 1996

[28] Bowers, A.R., Robinson, R., Koussis, A.D., Estimation of BOD parameters by an integral method, Environmental Technology Letters, Vol. 8, pp. 317-326, 1987

[29] Enick, R. M., Beckman, E. J., Shi, C., Xu, J., Remediation of metal-bearing aqueous waste streams via direct carbonation, Energy & Fuels 2001, 15, 256-262

[30] Chang E. E., Chen C. H., Chen Y. H., Pan S. Y., Chiang P. C., Performance evaluation for carbonation of steel-making slags in a slurry reactor, Journal of Hazardous Materials 186 (2011) 558–564

[31] Chu H. W., $CO_2$ sequestration by carbonation of akaline solid waste

[32] Huijgen W. J. J., Janwitkamp G., and Comans R. J., Mineral $CO_2$ sequestration by steel slag carbonation, Environ. Sci. Technol. 2005, 39, 9676-9682

[33] Satoshi Kodamaa, Taiki Nishimotob, Naoki Yamamotoa, Katsunori Yogoa, Koichi Yamada, Development of a new pH-swing $CO_2$ mineralization process with a recyclableReaction solution, Energy 33 (2008) 776－784

[34] Eloneva S., Teir S. , Salminen J. , Fogelholm C.-J., Zevenhoven R. , Fixation of $CO_2$ by carbonating calcium derived from blast furnace slag, Energy 33 (2008) 1461－1467

[35] Nyambura M. G. , Mugera G. W. , Felicia P. L., Gathura N. P., Carbonation of brine impacted fractionated coal fly ash: implications for $CO_2$ sequestration,

Journal of Environmental Management 92 (2011) 655e664

[36] Shih S. M., Ho C. S., Yuen-Sheng Song, and Jyh-Ping Lin, Kinetics of the Reaction of $Ca(OH)_2$ with $CO_2$ at Low Temperature, Ind. Eng. Chem. Res. 1999, 38, 1316-1322

[37] Liu C. F., Shih S. M., Lin R. B., Kinetics of the reaction of $Ca(OH)_2$/fly ash sorbent with $SO_2$ at low temperatures, Chemical Engineering Science 57 (2002) 93–104

[38] Abu-Eishah S. I., Anabtawi M.J.J., Isaac S.L., Upgrading of carbonaceous phosphate rocks by direct carbonation with CO2–water solutions, Chemical Engineering and Processing 43 (2004) 1085–1094

[39] Proctor D. M., Fehling K. A., Shay, Wittenborn E. C. J. L., Green J. J., Avent C., Bigham R. D., Connolly M., Lee B., Shepker T. O. and Zak M. A., Physical and chemical characteristics of Blast Furnace, Basic oxygen furnace, and electric arc furnace steel industry slags, Environ. Sci. Technol. 2000, 34, 1576-1582

[40] 林志忠，公共工程使用再生材料落實節能減碳初步探討, 2010

[41] Uibu M., Uus M. and Kuusik R., $CO_2$ mineral sequestration in oil-shale wastes from Estonian power production, Journal of Environmental Management 90 (2009) 1253－1260

[42] Abanades J. C., Allam R., Lackner K. S., Meunier F., Rubin E., Sanchez J. C., Katsunori Yogo and Ron Zevenhoven, Mineral carbonation and industrial uses of carbon dioxide

[43] Eloneva S., Teir S., Salminen J., Fogelholm C.-J., and Zevenhoven R., Steel converter slag as a raw material for precipitation of pure calcium carbonate, Ind.

Eng. Chem. Res. 2008, 47, 7104–7111

[44] Cho J. S., Kim S. M., Chun H. D., Han G. W., Lee C. H., Carbon Dioxide capture
with accelerated carbonation of industrial combustion waste, International Journal
of Chemical Engineering and Applications, Vol. 2, No. 1, February 2011

[45] Zevenhoven R., Fagerlund J. and Songok J. K., $CO_2$ mineral sequestration:
developments toward large-scale application, Greenhouse Gas Sci Technol.
1:48–57 (2011)

**Appendix**

Table A-1 Experimental conditions and results of basic oxygen furnace slag

| Feedstock | Water source | Dp [μm] | L/S | Flow rate [L/min] | Time [min] | $m_{105℃}$ [mg] | $\Delta m_{CO2}$ [mg] | $CO_2$ [%] | Conversion [%] |
|---|---|---|---|---|---|---|---|---|---|
| BOF slag | Cold-rolling | < 44 | 20 | 1.0 | 0 | 15.85 | 0.090 | 0.568 | 1.422 |
| BOF slag | Cold-rolling | < 44 | 20 | 1.0 | 5 | 15.66 | 2.800 | 17.882 | 67.349 |
| BOF slag | Cold-rolling | < 44 | 20 | 1.0 | 10 | 15.92 | 3.041 | 19.102 | 73.032 |
| BOF slag | Cold-rolling | < 44 | 20 | 1.0 | 15 | 14.38 | 2.506 | 17.429 | 65.286 |
| BOF slag | Cold-rolling | < 44 | 20 | 1.0 | 20 | 15.33 | 2.882 | 18.799 | 71.604 |
| BOF slag | Cold-rolling | < 44 | 20 | 1.0 | 30 | 15.45 | 3.045 | 19.710 | 75.925 |
| BOF slag | Cold-rolling | < 44 | 20 | 1.0 | 40 | 14.17 | 2.955 | 20.857 | 81.506 |
| BOF slag | Cold-rolling | < 44 | 20 | 1.0 | 50 | 15.02 | 3.094 | 20.600 | 80.245 |
| BOF slag | Cold-rolling | < 44 | 20 | 1.0 | 60 | 14.07 | 2.674 | 19.003 | 72.563 |
| BOF slag | Cold-rolling | < 44 | 20 | 1.0 | 90 | 14.34 | 2.882 | 20.104 | 77.825 |
| BOF slag | Cold-rolling | < 44 | 20 | 1.0 | 120 | 14.09 | 3.159 | 22.423 | 89.400 |

Table A-2 Experimental conditions and results of basic oxygen furnace slag

| Feedstock | Water source | Dp [μm] | L/S | Flow rate [L/min] | Time [min] | $m_{105℃}$ [mg] | $\Delta m_{CO2}$ [mg] | $CO_2$ [%] | Conversion [%] |
|---|---|---|---|---|---|---|---|---|---|
| BOF slag | Tap water | < 44 | 20 | 1.0 | 0 | 15.85 | 0.090 | 0.568 | 1.422 |
| BOF slag | Tap water | < 44 | 20 | 1.0 | 5 | 15.80 | 2.510 | 15.889 | 58.426 |
| BOF slag | Tap water | < 44 | 20 | 1.0 | 10 | 15.11 | 2.408 | 15.939 | 58.645 |
| BOF slag | Tap water | < 44 | 20 | 1.0 | 20 | 13.91 | 2.425 | 17.431 | 65.295 |
| BOF slag | Tap water | < 44 | 20 | 1.0 | 30 | 15.87 | 2.939 | 18.520 | 70.298 |
| BOF slag | Tap water | < 44 | 20 | 1.0 | 50 | 15.11 | 2.808 | 18.586 | 70.610 |
| BOF slag | Tap water | < 44 | 20 | 1.0 | 60 | 17.11 | 3.225 | 18.847 | 71.831 |
| BOF slag | Tap water | < 44 | 20 | 1.0 | 90 | 15.21 | 2.800 | 18.410 | 69.791 |
| BOF slag | Tap water | < 44 | 20 | 1.0 | 120 | 15.05 | 3.094 | 20.559 | 80.044 |

Table A-3 Experimental conditions and results of basic oxygen furnace slag

| Feedstock | Water source | Dp [μm] | L/S | Flow rate [L/min] | Time [min] | $m_{105℃}$ [mg] | $\Delta m_{CO2}$ [mg] | $CO_2$ [%] | Conversion [%] |
|---|---|---|---|---|---|---|---|---|---|
| BOF slag | Effluent | < 44 | 20 | 1.0 | 0 | 15.85 | 0.090 | 0.568 | 1.422 |
| BOF slag | Effluent | < 44 | 20 | 1.0 | 10 | 15.12 | 2.482 | 16.414 | 60.738 |
| BOF slag | Effluent | < 44 | 20 | 1.0 | 20 | 17.15 | 3.266 | 19.041 | 72.745 |
| BOF slag | Effluent | < 44 | 20 | 1.0 | 30 | 14.75 | 2.915 | 19.760 | 76.164 |
| BOF slag | Effluent | < 44 | 20 | 1.0 | 40 | 15.63 | 2.988 | 19.117 | 73.103 |
| BOF slag | Effluent | < 44 | 20 | 1.0 | 50 | 14.78 | 2.923 | 19.781 | 76.269 |
| BOF slag | Effluent | < 44 | 20 | 1.0 | 60 | 20.83 | 3.829 | 18.382 | 69.657 |
| BOF slag | Effluent | < 44 | 20 | 1.0 | 90 | 16.99 | 3.511 | 20.662 | 80.550 |
| BOF slag | Effluent | < 44 | 20 | 1.0 | 120 | 16.61 | 3.331 | 20.054 | 77.582 |

c